# PREPARATION OF ACTIVATED CLAY FROM RATCHABURI BENTONITE FOR PYROLYSIS OIL DECOLORIZATION

Miss Woranan Koedsang

A Thesis Submitted in Partial Fulfillment of the Requirements
for the Degree of Master of Science in Petrochemistry and Polymer
Science
Field of Study of Petrochemistry and Polymer Science
FACULTY OF SCIENCE
Chulalongkorn University
Academic Year 2020
Copyright of Chulalongkorn University

การเตรียมดินกัมมันต์จากเบนโทไนต์ราชบุรีสำหรับการฟอกสีน้ำมันไพโรไลซิส

น.ส.วรฉัน เกิดสังข์

| Thesis Title | PREPARATION OF ACTIVATED CLAY FROM RATCHABURI BENTONITE FOR PYROLYSIS OIL DECOLORIZATION |
|---|---|
| By | Miss Woranan Koedsang |
| Field of Study | Petrochemistry and Polymer Science |
| Thesis Advisor | Professor THARAPONG VITIDSANT, Ph.D. |

Accepted by the FACULTY OF SCIENCE, Chulalongkorn University in Partial Fulfillment of the Requirement for the Master of Science

.......................................................... Dean of the FACULTY OF SCIENCE
(Professor POLKIT SANGVANICH, Ph.D.)

THESIS COMMITTEE

.......................................................... Chairman
(Professor Chawalit Ngamcharussrivichai, Ph.D.)

.......................................................... Thesis Advisor
(Professor THARAPONG VITIDSANT, Ph.D.)

.......................................................... Examiner
(Assistant Professor Duangamol Tungasmita, Ph.D.)

.......................................................... External Examiner
(Associate Professor Witchakorn Charusiri, Ph.D.)

วรฉัน เกิดสังข์ : การเตรียมดินกัมมันต์จากเบนโทไนต์ราชบุรีสำหรับการฟอกสีน้ำมันไพโรไลซิส. ( PREPARATION OF ACTIVATED CLAY FROM RATCHABURI BENTONITE FOR PYROLYSIS OIL DECOLORIZATION) อ.ที่ปรึกษาหลัก : ศ. ดร.ธราพงษ์ วิทิตศานต์

เบนโทไนต์เป็นดินชนิดหนึ่งที่มีการนำมาใช้งานในหลายๆ ด้าน อาทิเช่น ใช้เป็นสารฟอกสีในอุตสาหกรรมกลั่นน้ำมัน ใช้เป็นสารหล่อลื่นในการขุดเจาะสำหรับงานโยธา ใช้เป็นสารตัวเติมและสารเติมแต่ง ตลอดจนใช้ดูดซับกลิ่นจากของเสีย ซึ่งจะเห็นได้ว่าเบนโทไนต์มีประโยชน์อย่างมากและมีการนำไปใช้งานอย่างกว้างขวางในหลายอุตสาหกรรม งานวิจัยนี้มีวัตถุประสงค์เพื่อศึกษาการเตรียมดินกัมมันต์จากเบนโทไนต์ราชบุรีสำหรับการฟอกสีน้ำมันไพโรไลซิส โดยนำเบนโทไนต์มาผ่านกระบวนการปรับปรุงคุณภาพด้วยการทำปฏิกิริยากระตุ้นกับกรดซัลฟิวริก, กรดไฮโดรคลอริก, โซเดียมไฮดรอกด์ และโพแทสเซียมไฮดรอกไซด์ ที่อัตราส่วนระหว่างเบนโทไนต์ต่อปริมาณกรดและเบส 1:1, 1:2 และ 1:3 และเวลาในการกระตุ้น 30, 60 และ 120 นาที ที่อุณหภูมิ 100 องศาเซลเซียส จากนั้นนำดินกัมมันต์ที่ได้ไปฟอกสีน้ำมันไพโรไลซิสที่ปริมาณดินกัมมันต์ 10, 30, 50 และ 70 กรัมต่อน้ำมันไพโรไลซิส 100 มิลลิลิตร ที่อุณหภูมิ 30, 60, 80, 100 และ 120 องศาเซลเซียส แล้วเปรียบเทียบสีของน้ำมันไพโรไลซิสที่ฟอกแล้วกับน้ำมันดีเซลทางการค้า และทำการฟื้นฟูสภาพกากดินกัมมันต์โดยผ่านกระบวนการฟื้นฟูสภาพด้วยความร้อนที่อุณหภูมิ 400, 500 และ 800 องศาเซลเซียส จากนั้นวิเคราะห์องค์ประกอบทางเคมีของดินกัมมันต์ด้วยเครื่องวิเคราะห์การเรืองรังสีเอกซ์, วิเคราะห์องค์ประกอบแร่ด้วยเครื่องวิเคราะห์การเลี้ยวเบนรังสีเอ็กซ์, วิเคราะห์พื้นที่ผิวและความพรุนด้วยเครื่องวิเคราะห์การดูดซับไนโตรเจน และวิเคราะห์สัณฐานวิทยาด้วยกล้องจุลทรรศน์อิเล็กตรอนแบบส่องกราด พบว่า ดินกัมมันต์ที่ได้จากเบนโทไนต์ราชบุรีมีพื้นที่ผิวและความพรุนเพิ่มขึ้น และมีประสิทธิภาพในการฟอกสีน้ำมันไพโรไลซิสมีสีใกล้เคียงกับน้ำมันดีเซลทางการค้า

จุฬาลงกรณ์มหาวิทยาลัย
CHULALONGKORN UNIVERSITY

| | | |
|---|---|---|
| สาขาวิชา | ปิโตรเคมีและวิทยาศาสตร์พอลิเมอร์ | ลายมือชื่อนิสิต ................................................ |
| ปีการศึกษา | 2563 | ลายมือชื่อ อ.ที่ปรึกษาหลัก ............................. |

# # 6072409623 : MAJOR PETROCHEMISTRY AND POLYMER SCIENCE

KEYWOR
D:
Bentonite, Activated clay, Acid-activation, Alkali-activation, Decolorization

Woranan Koedsang : PREPARATION OF ACTIVATED CLAY FROM RATCHABURI BENTONITE FOR PYROLYSIS OIL DECOLORIZATION. Advisor: Prof. THARAPONG VITIDSANT, Ph.D.

Bentonite is a clay mineral which widely used in considerable applications, such as bleaching agent in the oil refining process, lubricant in drilling for civil works, filler and additive as well as used to absorb odors from the waste. It can be achieved that bentonite is very tremendously advantageous and employ in many industries. The aims of this research were carried out to study the preparation of activated clay from bentonite Ratchaburi for pyrolysis oil decolorization. The bentonite was processed by activation with sulfuric acid ($H_2SO_4$), hydrochloric acid (HCl). sodium hydroxide (NaOH) and potassium hydroxide (KOH), various the ratio of bentonite to activation agents of 1:1, 1:2 and 1:3 and soaking time of 30, 60 and 120 min at a temperature of 100 °C. The activated clays were investigated decolorize pyrolysis oil with various activated clay dosages of 10, 30, 50 and 70 g per 100 ml of pyrolysis oil and temperatures of 30, 60, 80, 100 and 120°C then comparable the color of bleached pyrolysis oil with commercial diesel. Regeneration of spent activated clay was carried out by thermal regeneration processes at temperatures of 400, 500 and 800°C. The chemical composition and mineralogical composition of activated clays were determined by X-ray fluorescence analyzer (XRF) and X-ray diffraction analyzer (XRD) respectively. Specific surface area and porosity were analyzed by nitrogen adsorption analyzer (BET) and morphological analysis using scanning electron microscopy (SEM). The results have shown that activated clays from Ratchaburi bentonite were increased surface area and porosity and effective in decolorize pyrolysis oil with obtaining the color of pyrolysis oil is similar to commercial diesel.

จุฬาลงกรณ์มหาวิทยาลัย
CHULALONGKORN UNIVERSITY

| | | |
|---|---|---|
| Field of Study: | Petrochemistry and Polymer Science | Student's Signature ............................. |
| Academic Year: | 2020 | Advisor's Signature ............................. |

# ACKNOWLEDGEMENTS

# TABLE OF CONTENTS

# LIST OF TABLES

จุฬาลงกรณ์มหาวิทยาลัย

CHULALONGKORN UNIVERSITY

# LIST OF FIGURES

จุฬาลงกรณ์มหาวิทยาลัย

CHULALONGKORN UNIVERSITY

# LIST OF ABBREVIATIONS

$H_2SO_4$      :   Sulfuric acid

HCl      :   Hydrochloric acid

NaOH      :   Sodium hydroxide

KOH      :   Potassium hydroxide

XRF      :   X-ray Fluorescence

XRD      :   X-ray Diffraction

SEM      :   Scanning electron microscope

CEC      :   Cation exchange capacity

BET      :   Brunauer-Emmett-Teller

pH      :   Potential hydrogen

IS      :   Indian standard

ASTM      :   American society for testing and materials

min      :   Minimum

$^{o}C$      :   Degree Celsius

g      :   Gram

h      :   Hours

ml      :   Milliliter

nm      :   Nanometer

**CHAPTER I**

**INTRODUCTION**

## 1.1    Background and Signification of the Research

Energy is one of the most important in the world which leads to constantly increase in global energy consumption. Both household energy and fuel energy are considerably used to accommodate the rising population and manufacturing industry developments. Generally, most of the energy is derived from crude oil, coal and natural gas which are all considered fossil fuels and its reserves of fossil fuels remaining in the world are limited. However, if the amounts of fossil fuels have been using as persistently as the present, it will be the cause of fossil fuel sources are available only for 50 to 100 years hence it is imperative to explore alternative energy sources for substituting fossil fuel exhaustion. The pyrolysis is a thermal decomposition process to break down the long chain molecules of organic materials such as plastics into fuels without the presence of oxygen [1]. The pyrolysis process is a suitable technique for the conversion of waste plastics into liquid fuels and gas fuels with an efficiency of 60 to 90 percent and it is effective in eliminating waste plastics. Pyrolysis oil is a major product that manufactures from the pyrolysis of waste plastics at a temperature around 450°C which is a feedstock for the production of liquid fuels including diesel, benzene, kerosene and so on [1]. Pyrolysis oil is a complex blends of hydrocarbon molecules cause the physical appearance of pyrolysis oil is black or dark brown liquid. For this reason, one of the qualities of pyrolysis oil that need to be improved before using in several applications is oil color thus the decolorization process is mostly preferred to encourage its color improvement.

Decolorization process is one of the oil refining process, it is the most influential stage since it helps to enhance the appearance of the final oil products. The decolorization process is an adsorption process that is carried out using an adsorbent such as bleaching earth, activated clay, activated carbon and silica-based, to adsorb color bodies and other impurities in the oil to achieve high-quality oil standards for various applications [2]. Activated clay is commonly used as an absorbent in the oil

decolorization process which is mostly produced from bentonite clay by activation process because it is high cation exchange capacity and high specific surface area with high adsorption performance for reducing color bodies in the oil without changing the chemical properties of the oil, causes an appearance of final oil product is changed to a lighter shade. Bentonite clay is not only inexpensive and environmentally friendly adsorbent but also available to find in many countries. Moreover, Thailand also has a good source of bentonite clay that can develop into activated clay. In order to enhance the properties of bentonite clay, the activation process is desired, there are many methods for the activation process and one of the activation methods which is widely used is acid-activation. Acid-activation is a chemical treatment for bentonite clay modification which is a technique that uses an acidic substance to perform activated clay and the most widely uses in the industry due to it is uncomplicated to implement and it also has a lot of research support [3]. Furthermore, there have been more studies about alkali-activation by using an alkaline substance to perform activated clay to investigate the potential of alkali-activated clay for the oil decolorization process [4].

In this research, the purpose of this work was carried out to modify the local bentonite clay from Ratchaburi province into activated clay by using an activation process for pyrolysis oil decolorization with benchmarking between acid-activation clay and alkali-activation clay. Sulfuric acid ($H_2SO_4$) and hydrochloric acid (HCl) substances are used to perform acid-activation while sodium hydroxide (NaOH) and potassium hydroxide (KOH) substances are used to perform alkali-activation and optimize conditions for pyrolysis oil decolorization as the color similar to commercial diesel oil.

### 1.2    Objectives of the Research

The objectives of this research are as follow:

1.  To optimize conditions and preparation of activated clays from Ratchaburi bentonite by acid activation and alkali activation process for pyrolysis oil decolorization.
2.  To regenerate spent activated clays by the direct heat-treatment process.

### 1.3    Scope of the Research

The activated clays from Ratchaburi bentonite to investigate are as follow:

1.  Preparation of two acid-activated clays by activated with sulfuric acid ($H_2SO_4$) and hydrochloric acid (HCl) solution for acid-activation at $100\pm5°C$ with constant stirring, various weight ratios of bentonite clay to activation agent of 1:1, 1:2 and 1:3 (by mass) and various soaking time of 30, 60 and 120 min.
2.  Preparation of two alkali-activated clays by activated with sodium hydroxide (NaOH) and potassium hydroxide (KOH) solution for alkali-activation at $100\pm5°C$ with constant stirring, various weight ratios of bentonite clay to activation agent of 1:1, 1:2 and 1:3 (by mass) and various soaking time of 30, 60 and 120 min.
3.  Characterization of the Ratchaburi bentonite and activated clays by X-ray fluorescence spectrometer (XRF), X-ray diffraction spectrometer (XRD), $N_2$ physisorption measurement (BET), Cation exchange capacity (CEC) and Scanning electron microscope (SEM).
4.  Investigate the pyrolysis oil decolorization by using the activated clay to remove color bodies from pyrolysis oil with various activated clay dosages of 10, 30, 50 and 70 g (g/100ml Oil) and various temperatures of 30, 60, 80, 100 and $120\pm5°C$ for 2 h with constant stirring. The decolorization efficiency for pyrolysis oil decolorization process was determined by using UV-VIS spectrophotometer at a wavelength of 450 nm.

5. Regeneration of spent activated clay by the direct heat-treatment process with various temperatures of 400, 500 and 800°C.

## 1.4  Expected Benefits of the Research

The Ratchaburi bentonite was modified and improved into activated clay, which was the development of local clay as effective as commercial activated clay and could be able to use as an adsorbent for pyrolysis oil decolorization. It could be to promote an alternative source of adsorbent in the oil industry and also increases the value of Thai bentonite clay.

# CHAPTER II

# THEORY AND LITERATURE REVIEWS

## 2.1    Bentonite Clay

### 2.1.1 Definitions of bentonite clay

Bentonite is a relatively soft stone, formed over the geological age by the natural alteration of volcanic tuffs with acid or alkaline rain. Bentonite is a kind of clay whose main constituent is Montmorillonite that belongs to the smectite group and contains impurities such as quartz, feldspar, and other minerals. Smectites are a group of clay minerals belong to the phyllosilicate family which was classified as the aluminosilicate group that expand upon contact with water or interlayer organic matter and exhibit cation exchange properties. The major minerals are montmorillonite, beidellite, and nontronite, which are di-octahedral smectites and saponite, hectorite and sauconite which are tri-octahedral smectites as shown in Figure 2.1 [1].

Montmorillonite has been identified in France by Mr. Damour and Mr. Salvetat in 1847 on a small mine nearby Montmorillon city. The first industrial exploitation at the beginning of the 20th century started at a mine located near Fort Benton in Wyoming province, USA. This explains the origin of the term "Bentonite" which was first a trading name. It has a crystal structure type of 2:1 phyllosilicate which was called T-O-T structure, explain that it is composed of three layers of small plates with an alumina octahedral sheet sandwiched between two layers of silica tetrahedral sheet where some aluminum atoms are replaced by magnesium atoms or iron atoms, resulting in the generation of negative charges on the base plane of the silica molecule and the equilibrium is achieved by exchanging positive ions with adjacent plates. The crystal structural of montmorillonite is shown in Figure 2.2 [1].
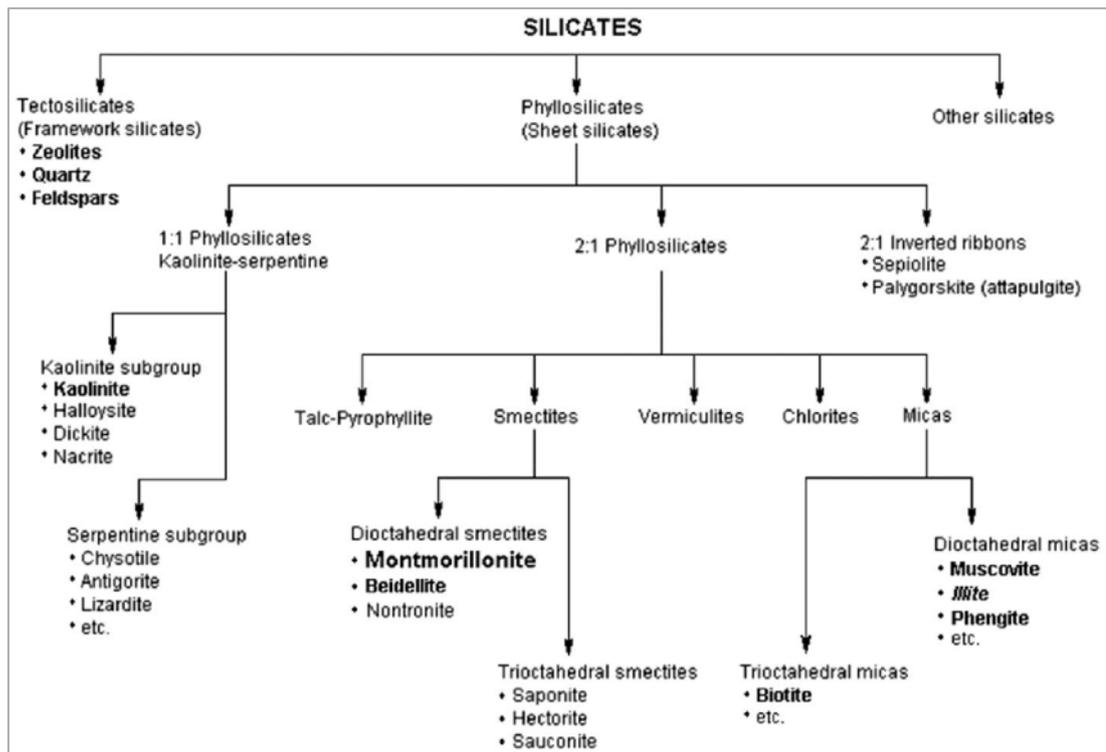
Figure 2.1 Clay minerals classifications
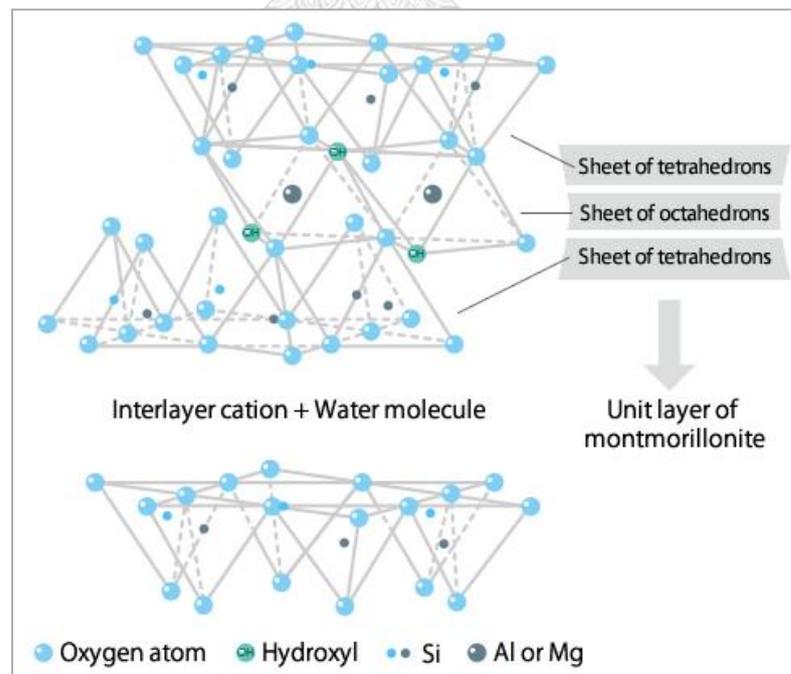


Figure 2.2 The crystal structural of montmorillonite [2]

### 2.1.2 Bentonite clay classification

In general, bentonite clays are divided into two main categories: the first is highly water absorption properties with shown swelling and can be remain suspended in water for a long time including sodium bentonite or swelling bentonite with the chemical formula is $Na_{0.3}(Al,Mg)_2Si_4O_{10}(OH)_2$. The second includes bentonite clay that exhibits neither swelling characteristic nor suspended in aqueous distribution which is known as calcium bentonite or non-swelling bentonite with the chemical formula is $Ca_{0.2}(Al,Mg)_2Si_4O_{10}(OH)_2$. Moreover, bentonite clay is also divided into different five types in commercial-grade by the European bentonite association (EUBA) based on application consist of natural sodium bentonite which is widely known as Wyoming bentonite, calcium bentonite or non-activated bentonite, activated bentonite or alkali-activation bentonite, acid-activated bentonite or bleaching earth and organophilic bentonite or organoclays [3].

### 2.1.3 Bentonite clay properties

Bentonite clay has a crystalline structure in the monoclinic system. There are very small particles and fine particles texture. Dry bentonites have color range from cream to olive green. Specific gravity of dry bentonites is between 2.4 and 2.8 [3]. An important physical property is very high toughness and can highly expand from 5 to 10. The primary specific surface area is between 50 and 200 $m^2$/g. and secondary specific surface area up to 840 $m^2$/g. It has high suspension stability and excellent ion exchange capability. Normally, the surface of bentonite clay is negatively charged, its resulting in bentonite clay having good adsorption properties and possible ion exchangeable where $Mg^{2+}$ ion replaces $Al^{3+}$ ion in the octahedral layer and the surface become surplus of electron cause by the surface is negatively charged, it is able to absorb cations such as $Na^+$, $K^+$, $Ca^{2+}$ ions and so on. The mechanism of surface charge of bentonite clay is in Figure 2.3 [4].
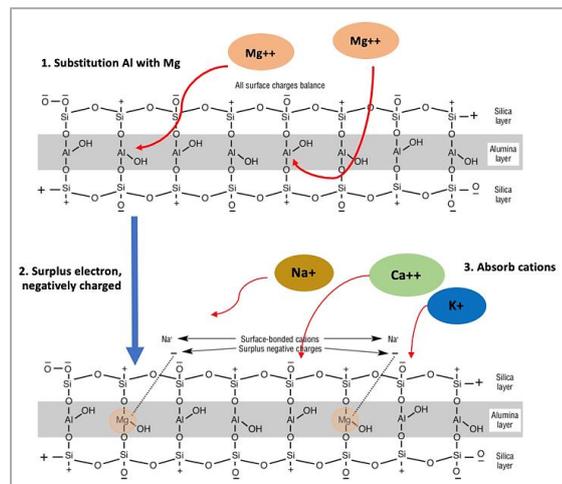
Figure 2.3 Mechanism of cation exchange on bentonite clay

2.1.4 Industrial uses of bentonite clay

Bentonite clay is widely used in many industries due to its unique properties. In particular, both its ion exchangeable properties and it is high surface area which the implementation consists of;

a) Decolorization; alkali or acid-activated bentonite is used for adsorption of impurities of oils and fats.

b) Foundry; sodium bentonite is used as a binder of the mold for iron mass foundries using the green sand process.

c) Civil works; drilling, calcium but mostly sodium bentonites are used to make a mud that allows the drilling through the soils. Soil sealing, calcium or sodium bentonites are blended with the soil and compacted in order to prepare a waterproof layer. It is used for storing waste, waterproofing lakes and dykes.

d) Ceramics; sodium bentonite is used for stabilizing the viscosity of the slurries, giving strength to the bodies and increasing the elasticity and fragility limit of ceramics.

e) Paper; sodium bentonite is used for the viscosity of the pulp, giving more strength to the paper or cardboard and adsorption of stickies.

f) Detergents; sodium bentonite is used for soft effect for washes.

g) Stockfeed; usually sodium bentonite is used for binding animal feed, reducing the pH of animals and toxins adsorption.

h) Paints and coatings; both sodium and organophilic bentonites are used for reducing flows and drops of paints and coatings.

i) Wine and fruit juices; sodium bentonite is used for adsorption of long-chain proteins

j) Other applications; many other uses of bentonite such as fire-retardant panel, Iron ore palletization, pet litter, pharmaceutical, cosmetics, waste water treatment and so on.

## 2.2    Activation Techniques

### 2.2.1 Acid activation process

The acid activation process is one of the most chemical modifications of clay to involves reacting bentonite with an acid substance at temperatures between 60 and 100°C which is more effective on calcium bentonite than sodium bentonite. This is because sodium bentonite has a swelling property, causing the cations to be pushed away from the soil surface. Therefore, the property is not suitable for use as an adsorbent. The acid activation process consists of the dissolution of impurities such as calcite, leaching of $Fe^{2+}$, $Fe^{3+}$, $Al^{3+}$ and $Mg^{2+}$ ions and replacement of exchangeable cations such as $Na^+$ or $Ca^{2+}$ ions with $H^+$ ion. The physical changes that occur due to acid activation cause erosion along the edges surrounding the bentonite sheet causing the edge of the slit to break while the inside still adheres. In addition, the pore and clay surface erosion caused the pore size to widen. More than 80% of the total surface area is formed by porosity, which has a diameter in the range of 20 to 60 Å. The changes in the crystal structure cause bentonite clay to increase the specific surface area and porosity, so large cations and pigments can be absorbed from the oil and lipids inside under the right conditions which are known to be able to decolorize or remove the color bodies from the oil [5]. Structural of acid activation is shown in Figure 2.4. There are many types of acids used for acid activation for example sulfuric acid, hydrochloric acid, nitric acid and organic acids such as acetic acid, citric acid,

oxalic acid and lactic acids. Sulfuric acid and hydrochloric acid are the most widely used in stimulation processes because they show beneficial results in specific surface area, porosity and adsorption capacity [6].
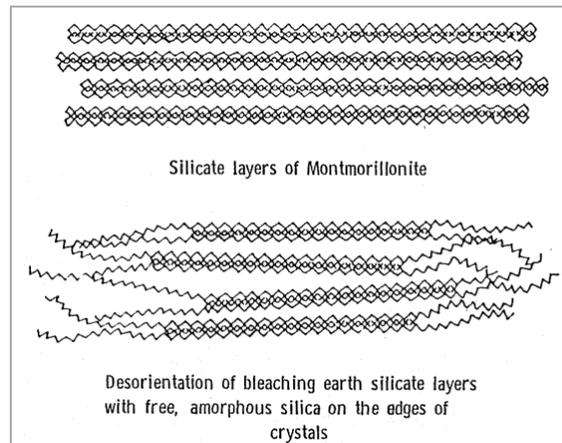


Figure 2.4 Structural of acid activation [7]

2.2.2 Alkali activation process

The alkali activation process is a chemical modification to involves reacting bentonite with an alkali substance such as sodium hydroxide, potassium hydroxide and so on for increasing specific surface area and porosity of bentonite clay like acid activation. While acid activation removes alkaline metals but alkali activation brings about the dissolution of the silica lattice and promotes adsorption [8]. There are still many studies investigating the effect of alkali activation on the oil decolorization process, which has a good bleaching performance and is promising as an alternative to the activation process.

2.2.3 Pillaring process

The Pillaring process is one of the activation techniques that combine both chemical modification and physical modification for clay mineral modification. Pillared clays are produced by calcination at a temperature around 400 to 500°C of the exchangeable oxacations for use as adsorbents or catalysts [9].

2.2.4 Thermal activation process

Thermal activation is a physical modification to modify the surface of bentonite clay by calcination at high temperatures. The physical properties such as cation exchange capacity, specific surface area and pore structure, adsorptive properties and so on can be changed [10].

2.2.5 Microwave activation process

Microwave activation is a physical modification by using microwave radiation to cause increasing specific surface area, micropore and mesopore with increasing irradiation time that can be used to modify the adsorption properties of the bentonite clay [6].

## 2.3    Pyrolysis Technique

Pyrolysis is a thermochemical process that transforms biomass, plastics and used rubber into higher calorific fuels such as charcoal, bio-oil and non-condensable gas by heating at a medium temperature of 500 to 800°C in the absence of oxygen. The proportion of products from the pyrolysis process depends on several factors, including reaction conditions, characteristics of raw materials used as reactants, type of reactor, etc. Pyrolysis process It is divided into two types consist of slow pyrolysis and fast pyrolysis [11]. The flow diagram of pyrolysis is shown in Figure 2.5.

2.3.1 Slow pyrolysis

Slow pyrolysis is a process that reacts at temperatures between 400 and 600°C with a heating rate of less than 10°C/min. The diameter of the reaction raw materials is larger than 2 mm. The slow pyrolysis products amount liquid for 30 to 50% and 25 to 35% for charcoal and produces a small fraction of the oil. Therefore, most of the oil is used as fuel in the combustion process. However, some chemicals can be separated from the polar or soluble portions of the oil. The chemicals that can be extracted from this oil are acetone, ketone, methanol, formic acid and acetic acid [11].

2.3.2 Fast pyrolysis

Fast pyrolysis is a process that produce oil as the main product. It reacts at medium temperatures between 400 and 650°C with a heating rate of more than 1,000°C/sec. The diameter of the raw material is less than 2 mm. Approximately obtained 60 to 75% for bio-oil, 15 to 25% for solids and 10 to 15% for non-condensing gas together with 10 to 30% water content in bio-oil which depending on the moisture content in the initial biomass thus the fast pyrolysis processes can improve quality in many types of fuels and chemicals [11].
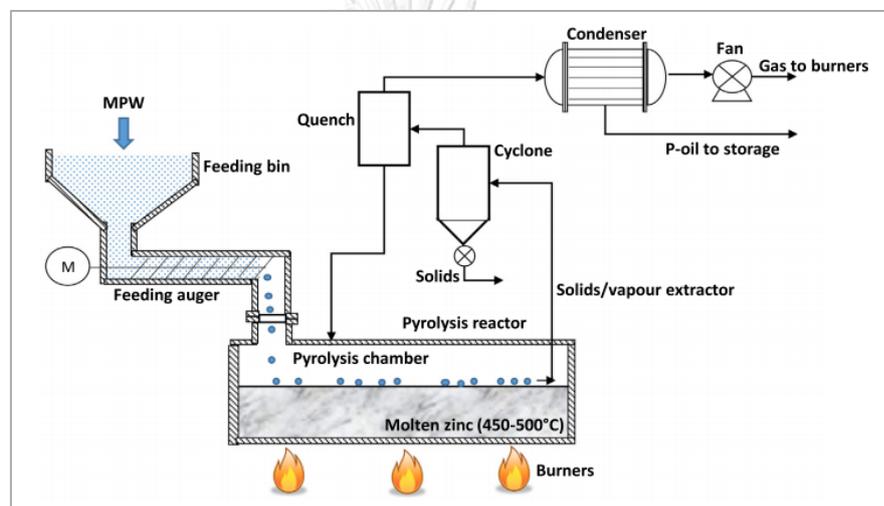


Figure 2.5 Pyrolysis process diagram [12]

## 2.4 Decolorization Process

Decolorization or bleaching is one of the key process in oil refining that designed to remove the color bodies in the oil. It is an adsorption process with mostly uses bleaching earth or activated clay as an adsorbent and another adsorbent such as activated carbon and silica to adsorb color bodies and impurities from the oil that makes the color of the oil is clear. Decolorization is the physical and chemical interaction of an oil or fat with adsorbent to improve its quality.

### 2.4.1 Dry bleaching

The oil is heated before mixed with bleaching earth or activated clay, activated carbon or a mixture of these two. This is done under vacuum to prevent oxidation and in the presence of sparging steam then separated spent bleaching agent [13].

### 2.4.2 Wet bleaching

Wet bleaching is a bleaching process in which water is added to the oil while it is in contact with the bleaching agent in the bleaching reactor. The water present during wet bleaching is introduced in the form of a citric acid solution, or by taking wet oil from the separation line. The oil therefore has to be dried before filtration [13].

### 2.4.3 Two-stage bleaching

The two-stage bleaching process is essentially a combination of wet and dry bleaching. At the second stage fresh bleaching agent is then added to the treated oil until a new state of equilibrium is reached. This oil then passes through a second filtration stage [13].

## 2.5 Adsorption Process

The adsorption process occurs when atoms or molecules move against the surface of a solid and there is an attraction between the surface of the solid and those particles. The solid acts as an adsorbent and the particles are called adsorbate. The adsorption process can be divided into two types according to the mutual attraction between the solid surface and the particles, which consist of two main types, there are physisorption and chemisorption. The interaction between adsorbent and adsorbate is shown in Figure 2.6.

### 2.5.1 Physisorption

The physisorption physical adsorption is multilayer adsorption on the adsorbent surface between the adsorbent and adsorbate. This is weak adsorption and is not chemically bonded but is attracted by Van-der Waal's forces. It usually occurs under low-temperature conditions and low adsorption energy. In addition, reversal of adsorption can occur depending on the strength of attraction between the adsorbent and the adsorbate.

2.5.2 Chemisorption

The chemisorption or chemical adsorption is a process that does not change the arrangement of the solid structure. It is monolayer adsorption, whereby this adsorption is a strong adsorption chemical bond between the adsorbent and the adsorbate with specificity depending on the type of adsorbent and the surface of the adsorbent.
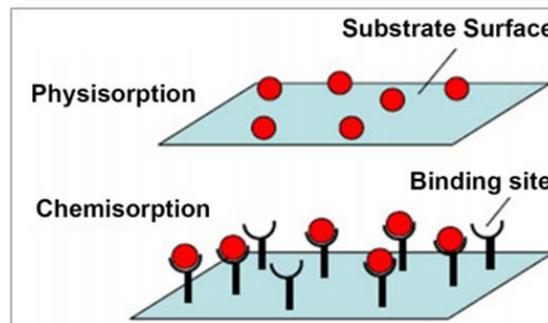


Figure 2.6 Interaction of adsorption [14]

2.5.3 Adsorption equilibrium

Base on at equilibrium of adsorption which is the relationship between the intensity of the adsorbate in the solid phase and the intensity of the adsorbate in the liquid phase, the isotherm was performed to describe the distribution of adsorbate in the solid and liquid phases. The adsorption process continuously adsorbs adsorbate on the adsorbent surface together with desorption until it reaches the adsorption equilibrium at the rate of adsorption and desorption is equivalent. Isotherm shape depends on physicochemical conditions and solid porous texture. According to IUPAC isotherm classification as shown in Figure 2.7, there are six types consist of [15];

a) Type I isotherm; this is characteristic of either a chemisorption isotherm or physisorption on microporous solids with monolayer adsorption.

b) Type II isotherm; this is characteristic of nonporous or macroporous solids and has a high energy of adsorption.

c)  Type III isotherm; this is characteristic of nonporous or macroporous solids and has a low energy of adsorption.

d)  Type IV isotherm; this is characteristic of mesoporous solids and has a high energy of adsorption with contain hysteresis loop in the isotherm due to capillary condensation.

e)  Type V isotherm; this is characteristic of mesoporous solids and has a low energy of adsorption with contain hysteresis loop in the isotherm due to capillary condensation.

f)  Type VI isotherm; this isotherm can be assigned as stepwise multilayer adsorption and presents in the sample surface contains different types of adsorption sites.
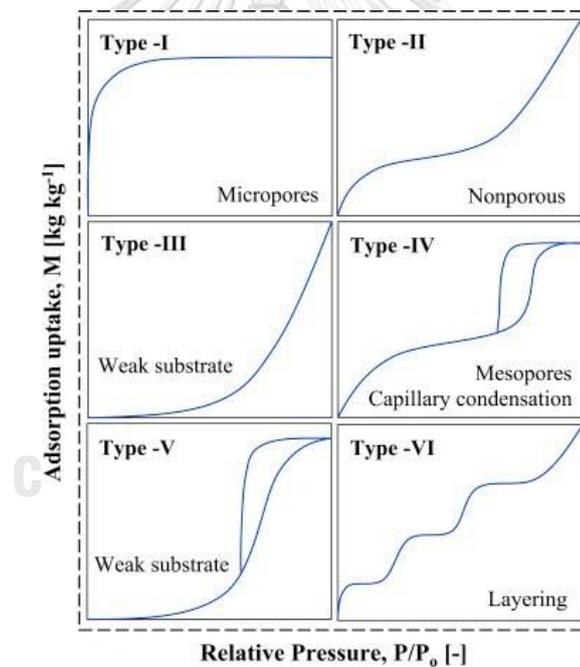


Figure 2.7 IUPAC adsorption isotherm classification

2.5.4 Hysteresis loops

The hysteresis loop appears in the physisorption absorption isotherm of mesoporous structures. Hysteresis loop can describe the pore characteristic of the adsorbent which classified into four categories by IUPAC committee as shown is Figure 2.8. Type H1 appears characteristic in cylinder-shaped pore, Type H2 appears

characteristic in bottle-neck pore, Type H3 appears characteristic in wedged-shaped pore and Type H4 appears characteristic in slit-shaped pore.
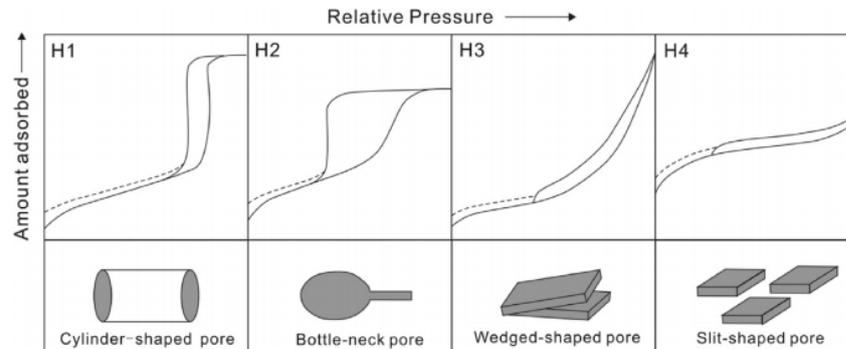


Figure 2.8 IUPAC hysteresis loop classification [16]

## 2.6    Adsorption Isotherm

Adsorption isotherm describes the relationship between the equilibrium concentration and the amount of adsorbate at a constant temperature. There are several types of absorption isotherms, while the most popular ones are Langmuir and Freundlich theories.

### 2.6.1 Langmuir adsorption isotherm

The Langmuir isotherm was proposed by Irving Langmuir, a British chemist, who describes that the entire surface on the adsorbent has homogenous adsorption surface and adsorption mechanism. It is monolayer adsorption where the adsorbates are arranged in a monolayer on the adsorbent and the adsorption energy is the same across all areas of the adsorbent. From the hypothesis, it can be expressed as the Langmuir equation as follows [17]:

$$\frac{C_e}{q_e} = \frac{1}{q_m K_L} + \frac{C_e}{q_m}$$

Where $C_e$ = concentration of adsorbate at equilibrium (mg/g) and

$K_L$ = Langmuir constant related to adsorption capacity (mg/g)

$q_m$ = maximum adsorption capacity (mg/g)

2.6.2 Freundlich adsorption isotherm

The Freundlich isotherm was proposed by Herbert Max Finlay Freundlich, a German physicist, who describes that is suitable for the adsorption on heterogenous surface and it is multiple layer adsorption. From the hypothesis, it can be expressed as the Freundlich equation as follows [17]:

$$\log q_e = \log K_F + \frac{1}{n} \log C_e$$

Where $K_F$ = adsorption capacity (L/mg) and

1/n = adsorption intensity

## 2.7 Regeneration Technique

2.7.1 Thermal treatment

Thermal treatment technique such as pyrolysis is the direct heat treatment process for spent bleaching clay regeneration by directly apply heat to extract residual oil under inert atmosphere.

2.7.2 Solvent extraction

Solvent extraction is a common strategy to regenerate spent bleaching clay by removing the residual oil using the organic solvents for example acetone, methyl ethyl ketone, perchloroethylene, methylene chloride, isopropyl alcohol, and chloroform as polar solvents such as petroleum ether, petroleum benzene, xylene, toluene, and hexane were utilized to extract the polar components, while nonpolar solvents were applied to extract nonpolar components [18].

2.7.3 Chemical treatment

Chemical treatment including acid treatment, base treatment and salt treatment are used to recovery spent bleaching clay by directly using the inorganic substance to extract residual oil.

2.7.4 Combining of various methods

The combination of regeneration techniques at low cost and high efficiency will certainly offer the optimum spent bleaching clay regeneration alternative. For example, solvent extraction followed by thermal process, acid activation followed by thermal process, salt activation followed by thermal and acid treatment, salt activation followed by thermal and acid treatment and so on [18].

## 2.8    Literature Reviews

Aziz et al. [19] studied the improvement and the bleaching capacity of individual clays in the Iraqi Kurdistan region by reacting with HCl, $H_2SO_4$ and $H_3PO_4$ solution at concentrations between 0.2 and 4 N. The clay to acid ratio was 1:15 under the temperature condition of 70±1°C for 0.5 and reaction time of 24 h. The oil bleaching analysis was carried out under the temperature conditions of 150, 200, 250, 300, 350 and 400°C for 3 h that was found to be the reaction conditions at a concentration of 2 N HCl at a temperature of 70°C with the reaction time of 2 h was the optimum condition for the best bleaching ability. They also found that the color adsorption isotherms were consistent with the Freundlich adsorption model. The results are shown in Figure 2.9.
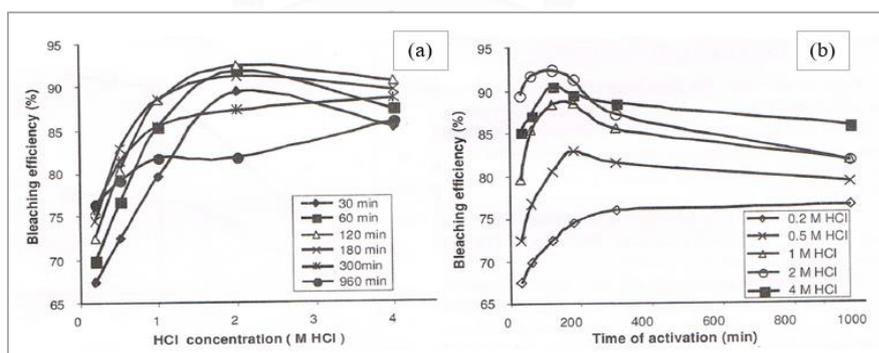


Figure 2.9 Bleaching efficiency

(a) different acid concentration, (b) different activation time

Ajemba and Onukwuli [20] studied the effects on structure and adsorption efficiency of Nteje clay which is activated by using HCl solution. The activation was performed at a temperature of 90°C for 2.5 h. The clay to acid ratio was 1:10 and the acid concentrations of 1 to 5 M were used. The adsorption efficiency was investigated by bleaching palm oil at a temperature of 80°C for 30 min. The exchange ions of $Al^{3+}$, $Fe^{3+}$ and $Mg^{2+}$ with $H^+$ resulted in a change in the crystal structure and surface area of the clay, making the clay is a highly absorbent capacity when bleaching palm oil. At acid strange of 3 M concentration provides the best adsorption efficiency.

Ajemba and Onukwuli [21] studied the influence of HCl leaching on structural changes and the bleaching performance of Nigerian clay from UDI. The acid leaching was investigated with various acid strange of 2 to 7 M concentration, reacting time of 30 to 150 min and temperatures of 70 to 120°C. In the term of adsorption, the experiment was proceeding at a temperature of 80°C with a contact time of 30 min for decolorizing palm oil. The specific surface area, Si/[Al+Fe+Mg] ratio and adsorption capacity were found to be increased when increasing in acid concentration together with rising in reacting time with bleaching efficiency increased from 29.8 to 66.7%. The results are shown in Figure 2.10
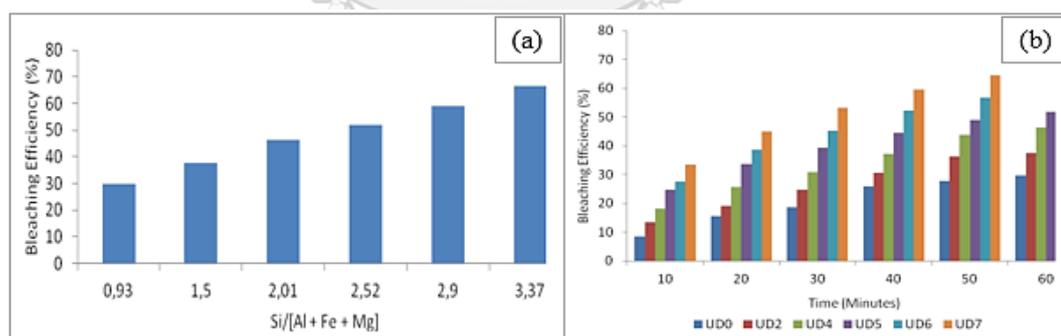


Figure 2.10 Bleaching efficiency

(a) with Si/[Al+Fe+Mg], (b) the natural and acid-activated clay

Zhansheng et al. [22] studied the improvement and bleaching efficacy of bentonite from Xinjiang by reacting with $H_2SO_4$ solution at concentrations of 15%, 20%, 25%, 30%, 40%. and 45% using clay to acid ratio of 1:2 under the temperatures of 96 to 98°C for 4 h, and then the oil bleaching was investigated under the temperatures of 96 to 98°C for 25 min. The reaction conditions at a 25% $H_2SO_4$ concentration are the ideal conditions for the best bleaching ability.

Okwara and Osaka [8] studied the bleaching of palm oil using clays enhanced by alkali-activation. Kaolin and bentonite clay were reacted with NaOH solution at alkali strange of 1, 2, 3 and 4 M concentration under temperatures of 80 to 85°C for 35 to 40 min. At the temperature of 150°C for 20 min, alkali -activated kaolin had the best bleaching efficiency of 76.38% at 3 M concentration of NaOH, while bentonite was effective in bleaching oil is 78.66% at 1 M concentration of NaOH.

Akinwande et al. [23] studied edible oil bleaching with Nigeria clay that improved quality by the alkali-activation process. The clay was reacted with NaOH and KOH solution at a temperature of 90°C. Then, the oil bleaching test at a temperature of 100°C for 20 min. The results were found that the activation of Nigeria clay which is mainly composed of muscovite resulted in structural modifications to increase the bleaching efficiency when activated with NaOH showed high bleaching efficiency at a low concentration of 0.5 M, while activation with KOH showed high bleaching efficiency at a high concentration of 5 M.

Wafti [24] studied the regeneration of spent bleaching clay for use in oil bleaching by using two heat recovery methods consist of solvent extraction together with heat treatment (DHRSBC) and direct heat treatment (HRSBC). The spent bleaching clay was heated in furnaces at temperatures of 400, 500 and 800°C. The direct heat treatment higher yield and specific surface area than solvent extraction together with heat treatment and uncleanness were eliminated. It was found that the temperature of 500°C gave the best efficiency in the regeneration of spent activated clay. The results are shown in Figure 2.11.
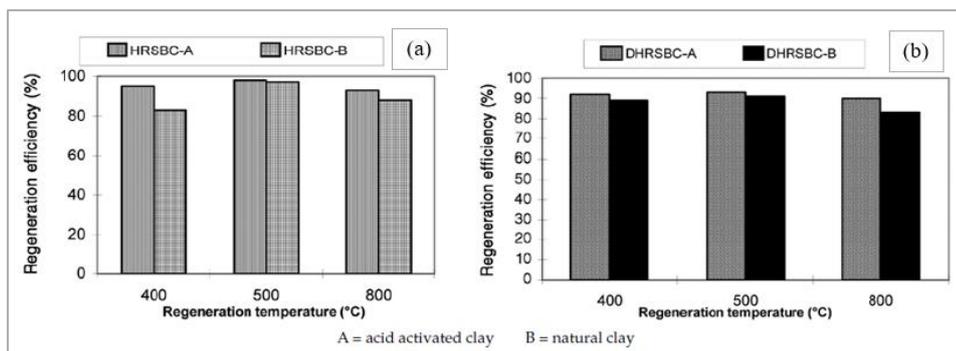
Figure 2.11 Regeneration efficiency; (a) HRSBC, (b) DHRSBC

Majid and Mat [25] studied the feasibility of reusing spent bleaching clay through acid and heat treatment for decolorization and reduction of biological oxygen demand (BOD). The acid treatment was carried out by impregnating the de-oil bleached earth (DSBE) with 1 M concentration of $H_2SO_4$ and stirred for 5 h at 200 rpm. The clay was then washed with distilled water, dried at a temperature of 500°C for 2 h. The results were found regenerated spent bleaching earth (RDSBE-AH) has a maximum surface area and pore volume of 122.3 m2/g and 68 cm3/g when compared to spent bleaching earth (SBE), de-oil bleached earth (DSBE) and new bleaching earth (NBE). In terms of decolorization, RDSBE-AH has a maximum efficiency of 68.3% and 46.4% of BOD reduction. It was shown that regenerated spent bleaching earth which is produced through combined acid and heat treatment has the potential to change adsorb color bodies and reduce BOD.

Balci [26] studied structural property improvements of bentonite from Middle Anatolia by thevacid-activation process using $H_2SO_4$ as an activation agent. The characterization results demonstrated that the acid activation caused increases in the surface area and pore volumes by changing the morphology and surface properties. The increase of the acid strength resulted in enhancement in the specific surface area up to 2 M concentration with a value of 131.15 m$^2$/g.

# CHAPTER III

# RESEARCH METHODOLOGY

## 3.1    Materials

All of the required materials and chemicals were used in this research are shown in Table 3.1.

Table 3.1 List of materials and chemicals

| Materials / Chemicals | Producer / Source | Function |
|---|---|---|
| Ratchaburi bentonite | Ratchaburi province | Raw bentonite clay |
| Pyrolysis oil | Center of Fuels and Energy from Biomass, Chulalongkorn University | Crude pyrolysis oil |
| Esso Hi Diesel | Esso (Thailand) Public Co., Ltd. | Commercial diesel oil |
| Supreme Plus Diesel | Bangchak Corporation Public Co., Ltd. | Commercial diesel oil |
| PTT Diesel B7 | PTT Public Co., Ltd. | Commercial diesel oil |
| Susco Diesel B7 | Susco Public Co., Ltd. | Commercial diesel oil |
| Sulfuric acid ($H_2SO_4$) 98 %w/v | QRec Co., Ltd. | Activation agent |
| Hydrochloric acid (HCl) 37 %w/v | QRec Co., Ltd. | Activation agent |
| Sodium hydroxide (NaOH) | QRec Co., Ltd. | Activation agent |
| Potassium hydroxide (KOH) | QRec Co., Ltd. | Activation agent |
| X-ray flux type 12:22 | Multibusiness Co., Ltd. | X-ray flux |
| Methylene blue | Carlo erba Co., Ltd. | CEC analysis |
| Tetra-sodium pyrophosphate | Sigmaaldrich Co., Ltd. | CEC analysis |

## 3.2    Instruments

All of the required instruments and equipment were used in this research are shown in Table 3.2.

Table 3.2 List of Instruments and equipment

| Instrument / Equipment | Brand / Model |
| --- | --- |
| X-ray fluorescence spectrometer (XRF) | Panalytical / Axios mineral |
| X-ray diffraction spectrometer (XRD) | Bruker / D8 Advance |
| $N_2$ physisorption measurement (BET) | Micromeritic / TriStar 3000 |
| Scanning electron microscope (SEM) | JEOL / JSM-6510LV |
| UV-VIS spectrophotometer | Spectronic / 20 Genesys |
| Fusion instrument | Claiese / TheOx Advance |
| Sample degas system | Micromeritic / FlowPrep 060 |
| Sputter coater | Quorum / Q150R S |
| Tube furnace | Carbolite / Gero |
| Muffle furnace | Vecstar / MRF1 |
| Drying oven | Memmert / UFB500 |
| Hotplate magnetic stirrer and magnetic bar | IKA / C-MAG HS7 |
| Overhead stirrer | Wisestir / HS-100D |
| Auto titration | Hirschann / DE-M 16 |
| pH meter | Sartorius / Docu-pH+ |
| Balance | Sartorius / BSA224S-CW |
| Digital thermometer | Traceable / 15-078J |
| Ultrasonic bath cleaner | GT Sonic / VGT-1200 |
| Vacuum filter and Buchner funnel | Fasco / D304X |
| Sieve 200 mesh | Endecotts / ASTM E11 |
| Platinum crucible and mould | XRF Scientific |
| Porcelain crucible | JIPO |
| Glass beaker | Pyrex |
| Filter paper | Whatman No.5 |
| Desiccator | Pyrex |
| Porcelain mortar and pestle | |

### 3.3    Activation of Ratchaburi Bentonite

3.3.1 Purification of Ratchaburi bentonite

The Ratchaburi bentonite was purified before use to activated clay preparation in the activation process for impurities elimination by washing with deionized water. The procedure was performed by weigh approximately 500 g of Ratchaburi bentonite placed into a plastic bucket. Added 2000 ml of deionized water and then Ratchaburi bentonite was soaked in deionized water for 30 min. Stirred by using overhead stirrer until the Ratchaburi bentonite was dispersed to suspension then sieved with 200 mesh (75 µm). The fine particles smaller than 200 mesh were dried at a temperature of 105°C overnight and ground to powder by porcelain mortar and pestle. The purification setup of bentonite clay is shown in Figure 3.1.



Figure 3.12 Purification setup process; (a) Mixing, (b) Sieve

3.3.2 Acid-activation process

Acid-activation was investigated by mixing the Ratchaburi bentonite, which was eliminated impurities with activation agents include sulfuric acid ($H_2SO_4$) or acid hydrochloric (HCl) solution in a glass beaker to prepare acid-activated clay with various weight ratios of bentonite clay to activation agent of 1:1, 1:2 and 1:3 (by mass). The suspension was heated on a hotplate magnetic stirrer and stir continuously at a temperature of 100±5°C until it was dried as follow an impregnation technique. After it was dried, various soaking times of 30, 60 and 120 min. The acid-activated clay was washed several times with deionized water and filtered under vacuum via a

Buchner funnel using Whatman No.5 filter paper until the pH of filtrate water became neutral. The filtered acid-activated clay was dried at a temperature of 105°C overnight and ground to powder by porcelain mortar and pestle. The setup of the activation process is shown in Figure 3.2.

### 3.3.3 Alkali-activation process

Alkali-activation was carried out by mixing the Ratchaburi bentonite, which was eliminated impurities with activation agents include sodium hydroxide (NaOH) or potassium hydroxide (KOH) solution in a glass beaker to prepare alkali-activated clay with various weight ratios of bentonite clay to activation agent of 1:1, 1:2 and 1:3 (by mass). The suspension was heated on a hotplate magnetic stirrer and stir continuously at a temperature of 100±5°C until it was dried as follow an impregnation technique. After it was dried, various soaking times of 30, 60 and 120 min. The alkali-activated clay was washed several times with deionized water and filtered under vacuum via a Buchner funnel using Whatman No.5 filter paper until the pH value of filtrate water became neutral. The filtered alkali-activated clay was dried at a temperature of 105°C overnight and ground to powder by porcelain mortar and pestle. The setup of the activation process is shown in Figure 3.2.
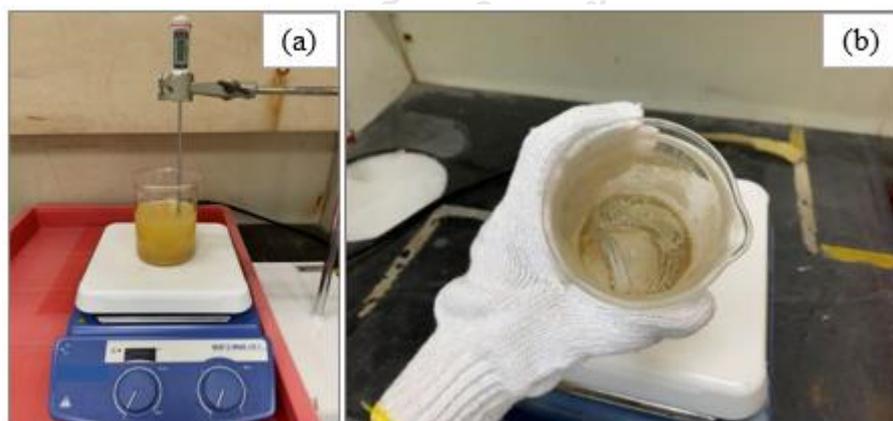


Figure 3.13 Setup of the activation process

(a) Activation setup process, (b) Impregnation technique

**3.4    Clays Characterization**

In this research, the Ratchaburi bentonite and all of activated clays were characterized are as follow:

3.4.1 Moisture content

The test method for moisture content is based on the Indian standard (IS 6186-1986). Weigh approximately 10.0 g of sample powder (M1) into a porcelain crucible. Dried in an oven at a temperature of 105°C for 2 h as shown in Figure 3.3 and transferred to cooling in a desiccator and weighed (M2). Moisture content was calculated by the equation below:

$$\% \text{ Moisture content} = \frac{(M1 - M2) \times 100}{M1}$$

Where M1 = mass in g of undried sample and

M2 = mass in g of sample dried to constant mass



Figure 3.14 Moisture content analysis

3.4.2 pH value

The test method for pH value is based on the Indian standard (IS 6186-1986). Weigh approximately 2.0 g of dried sample powder into a glass beaker, added 100 ml of deionized water and mixed by using a magnetic stirrer and magnetic bar with mixing time for 10 min. The pH value was determined by a pH meter (Sartorius, Docu-pH+) using glass electrodes as shown in Figure 3.4.



Figure 3.15 pH value analysis

3.4.3 $N_2$ physisorption measurement

Specific surface area, total pore volume and pore size distribution were determined by using $N_2$ physisorption measurement (Micromeritic, TriStar 3000) to measure $N_2$ adsorption-desorption at liquid nitrogen temperature of -195.7°C which based on the American society for testing and materials (ASTM C1069-86) as shown in Figure 3.5. The procedure was performed by weighing approximately 0.3 g of dried sample powder to degassed at a temperature of 105°C for 3 h and cooling before adsorption measurement by using FlowPrep 060. Transferred degassed sample to $N_2$ physisorption analyzer. The Brunauer-Emmett-Teller (BET) method was used to evaluated the specific surface area and total pore volume in the range of relative pressure from 0.05 to 0.30 while pore size distribution was evaluated by Barret-Joyner-Halenda (BJH) method.

Figure 3.16 $N_2$ physisorption measurement

3.4.4 Cation exchange capacity

Cation exchange capacity was determined by the methylene blue adsorption method, which is based on German institute for standardization (DIN standard VDG P69). The procedure was weighed accurately 0.5 g of dried sample powder into a glass beaker, added 50 ml of tetra-sodium pyrophosphate solution with a concentration of 2 %w/v. The suspension was stirred by using a magnetic stirrer and magnetic bar for 10 min, transferred to ultrasonic bath cleaner and started to vibrate for 5 min. After vibration, 10 ml of 1 N sulfuric acid was added to the suspension and stirred for 1 min and immediately filled 1 ml of methylene blue solution to the suspension with continuously stirred for 2 min. The mixed solution was dropped on Whatman No.5 filter paper to verify the light blue halo. Initially, a circle of the drop was formed which is dark blue, more methylene blue solution was added until the light blue halo has appeared around the dark blue drop. At this point, continuously stirred again for 2 min to confirm the existence of the light blue halo. Cation exchange capacity analysis is shown in Figure 3.6.
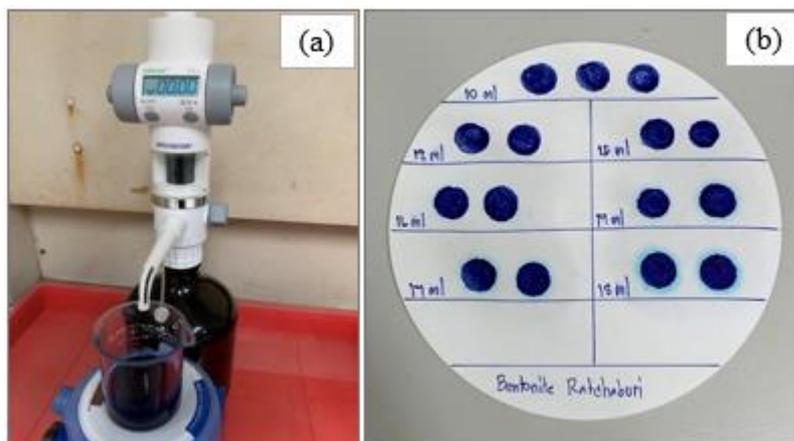
Figure 3.17 Cation exchange capacity analysis

(a) Methylene blue titration, (b) The light blue halo

### 3.4.5 Chemical composition

The chemical composition of clays was investigated by an X-ray fluorescence spectrometer (Panalytical, Axios mineral) as shown in Figure 3.7. Weigh accurately 1.7 g of dried sample powder mixed with 8.5 g of X-ray flux type 12:22 (lithium tetraborate 35.3%: lithium metaborate 64.7%) plus 0.5% release agent of lithium bromide (LiBr) and the mixture was fused in a platinum ware at a temperature of 1050°C into a glass bead. As an X-ray fluorescence determination, loss on ignition (L.O.I.) was required which based on the American society for testing and materials (ASTM C323-56) by weighing accurately 2.0 g of dried sample powder into a porcelain crucible. Ignited at a temperature of 1000°C for 1 h and transferred to cooling in a desiccator and weighed. Loss on ignition was calculated by the equation below:

$$\% \text{ Loss on ignition (L.O.I)} = \frac{[B-(C-A)]\times100}{B}$$

Where A = mass in g of sample and

B = initial mass in g of sample and crucible

C = final mass in g of sample and crucible

Figure 3.18 X-ray fluorescence spectrometer

3.4.6 Mineralogical composition

The mineralogical composition of clays was investigated by using X-ray diffraction spectrometer (Bruker, D8 Advance) as shown in Figure 3.8. The sample was prepared to pressed powder. The X-ray diffraction spectrometer condition include step size of 0.01°, time/step of 1, Cu tube voltage of 40kv, current of 40mA and Cu-Ka (l = 1.5418 Å) radiation with operating in between 5 to 80 2-theta degrees.



Figure 3.19 X-ray diffraction spectrometer

3.4.7 Morphological characteristic

Morphological characteristic of samples was obtained using a scanning electron microscope (JEOL, JSM-6510LV) with operating at 20 kV to the comparison of the structural changes after the activation at a magnification of 2000 and 5000. The samples were coated with gold before analysis and morphology analysis as shown in Figure 3.9
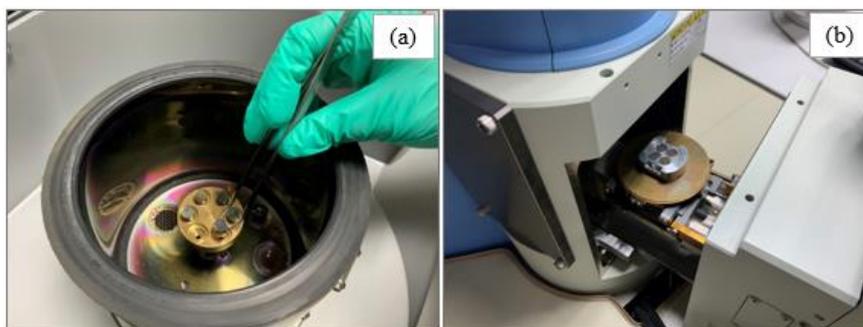


Figure 3.20 Scanning electron microscope

(a) Coating with conductive material, (b) Morphology analysis

## 3.5    Decolorization of Pyrolysis Oil

All the activated clays, which were produced from the activation process were carried out to pyrolysis oil decolorization following by mixing in grams of clay with 100 ml oil. The procedure was performed 100 ml of crude pyrolysis oil mixed with an activated clay dosage of 10 g in a glass beaker to remove color bodies in the pyrolysis oil at a temperature of $100\pm5°C$ on a hotplate magnetic stirrer with constant stirring for 2 h of reaction time. The decolorization setup process is shown in Figure 3.10. Bleached pyrolysis oil was filtered under vacuum via a Buchner funnel using Whatman No.5 filter paper for separate spent activated clay. Bleaching efficiency for the decolorization process of the activated clay was determined by using a UV-Vis spectrophotometer (Spectronic, 20 Genesys) to measure the absorbance of bleached pyrolysis oil as shown in Figure 3.11 with a wavelength of 450 nm as according to reference [9]. Activated clays of each activation agent that effective to bleach pyrolysis oil at dosages of 10 g were taken to continuously bleach pyrolysis oil with

various activated clay dosages of 30, 50 and 70 g and various temperatures of 30, 60, 80, 100 and 120±5°C until the color of bleached pyrolysis oil was comparable to commercial diesel. Decolorization efficiency was calculated by the equation below:

$$\% \text{ Decolorization efficiency} = \frac{(A_0 - A) \times 100}{A_0}$$

Where $A_0$ = absorbance of crude pyrolysis oil and

A = absorbance of bleached pyrolysis oil
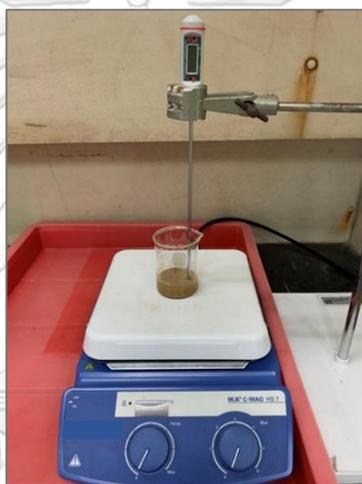


Figure 3.21 Decolorization setup process



Figure 3.22 UV-Vis Spectrophotometer

The nomenclature of each activated clay sample is divided into four names as according to Table 3.3

Table 3.3 The sample name of activated clays

| Activation process | Activated clays | Sample name |
| --- | --- | --- |
| Acid-activation | $H_2SO_4$ activated clay | AC-$H_2SO_4$ |
| Acid-activation | HCl activated clay | AC-HCl |
| Alkali-activation | NaOH activated clay | AC-NaOH |
| Alkali-activation | KOH activated clay | AC-KOH |

## 3.6    Regeneration of Spent Activated Clay

The spent activated clays obtained from pyrolysis oil decolorization were regenerated by the direct heat-treatment process to remove residual oil as according to reference [24] for reusing in the oil decolorization process. Weight approximately 30 g of spent activated clay was placed into a reactor tube and transferred to a tube furnace. Pre-heated at a temperature of $100\pm5°C$ for 30 min then heat to heat-treatment temperature, various heat-treatment temperatures of 400, 500 and $800\pm5°C$ and soaking time of 1 h with a heating rate of $10°C/min$ under nitrogen gas atmosphere with a constant flow rate of 200 $cm^3/min$ [27]. Characterization and determine bleaching efficiency for the decolorization process of the regenerated spent activated clay by using a UV-Vis spectrophotometer (Spectronic, 20 Genesys) at a wavelength of 450 nm. After that, the regenerated spent activated clays which were obtained at optimum temperature continue to replicate in the regeneration and decolorization five times. Regeneration of the spent activated clay setup process is shown in Figure 3.12.

Figure 3.23 Regeneration setup process

The nomenclature of each spent activated clay sample is divided into four names according to Table 3.4.

Table 3.4 The sample name of spent activated clay

| Spent activated clay | Sample name | |
| --- | --- | --- |
| | Spent clay | Regenerated clay |
| $H_2SO_4$ activated clay | SC-$H_2SO_4$ | RC-$H_2SO_4$ |
| HCl activated clay | SC-HCl | RC-HCl |
| NaOH activated clay | SC-NaOH | RC-NaOH |
| KOH activated clay | SC-KOH | RC-KOH |

## CHAPTER IV

## RESULTS AND DISCUSSIONS

### 4.1    Activated Clay from Ratchaburi Bentonite

The Ratchaburi bentonite was used as feedstock for activated clay production include acid-activated clays and alkali-activated clays by acid-activation using sulfuric acid ($H_2SO_4$) or hydrochloric acid (HCl) and alkali-activation using sodium hydroxide (NaOH) or potassium hydroxide (KOH). In general, the mechanism of the acid-activation process consists of the substitution of the exchangeable cations by protons and the metal ions, such as Al, Fe and Mg ions are removed from the octahedral layer while alkali-activation brings about to dissolution of the silica lattice. Simultaneously, a gradual transformation of the tetrahedral sheets into a three-dimensional framework proceeds resulting in a solid product contains unaltered layers and amorphous silica causes activated bentonite exhibits high specific surface area and large porosity what makes it an excellent absorbent [28].

After purification and activation of the as a received Ratchaburi bentonite, its physical appearance is changed. It was found that the activated clays are lightweight because it is a lower density than initial bentonite clay due to the activation increased space in the clay [29]. Moreover, its modification which significant to the difference from original bentonite clay is clay color as clearly shows in Figure 4.1. The appearance color of acid-activated clays is changed from drab to cream while alkali-activated clays are faded drab as shown in Figure 4.2.

Figure 4.24 Acid-activated clay

(a) Ratchaburi bentonite, (b) AC-$H_2SO_4$, (c) AC-HCl
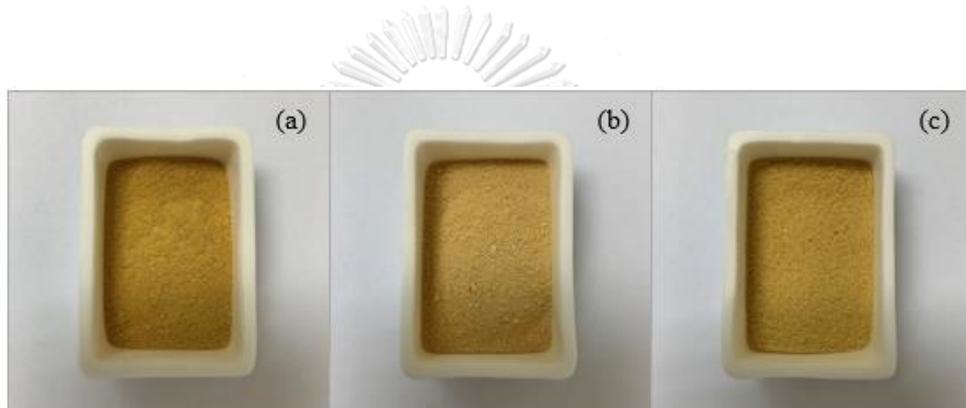


Figure 4.25 Alkali-activated clay

(a) Ratchaburi bentonite, (b) AC-NaOH, (c) AC-KOH

Table 4.1 shows the yield of activated clays preparation which was produce from the Ratchaburi bentonite. The results show that the yield after activation of AC-$H_2SO_4$, AC-HCl, AC-NaOH, AC-KOH are 73.20%, 73.80%, 74.00% and 73.40% respectively as according to previous research [29] which explained that activated clay is a lower density than initial bentonite clay due to the activation increased space in the clay.

Table 4.5 Yield of activated clays preparation

| Activated clay | Yield (%) |
|----------------|-----------|
| AC-H$_2$SO$_4$ | 73.20 |
| AC-HCl | 73.80 |
| AC-NaOH | 74.00 |
| AC-KOH | 73.40 |

## 4.2 Activated Clays Characterization

4.2.1 Physical characterization of Ratchaburi bentonite

The as a received Ratchaburi bentonite was characterized before use as material feedstock for the activation process. Its physical properties are shown in Table 4.2. The results show BET specific surface area of 41 m$^2$/g with total pore volume of 0.077 cm³/g and cation exchange capacity of 133 mg/g. It indicated that is characteristics of bentonite clay mineral.

Table 4.6 Ratchaburi bentonite characterization

| Characterization | Ratchaburi bentonite |
|------------------|----------------------|
| Moisture content (%) | 4.32 |
| pH value | 8.80 |
| BET surface area (m$^2$/g) | 41 |
| Pore volume (cm³/g) | 0.077 |
| Average pore size (nm) | 7.60 |
| Cation Exchange Capacity (mg/g) | 133 |

4.2.1 Moisture content and pH value analysis

In this research, the results show that the overall moisture content of activated clays is in the range of 1.84% to 4.86%, which was in the range of requirement for commercial activated clay specification as according to Indian standard (IS 1965-1972) with a maximum value of 10%. The trend of moisture content of acid-activated

clay is quite lower than alkali-activated clay because acid attacks motivate the hydrogen ions to remove the metal ions from the crystal lattice and the formation of silanol groups and amorphous silicic acid [30] cause increasing in amorphous silica. The pH value of activated clays, which were prepared at neutral condition is in the range of 6.76 to 7.89, it is confirms that the neutral activated clay. The moisture content and pH value are shown in Table 4.3

Table 4.7 Moisture content and pH value analysis

| Sample Name | Moisture content % | pH value |
|---|---|---|
| AC-H$_2$SO$_4$ (1:1/30min) | 2.89 | 6.97 |
| AC-H$_2$SO$_4$ (1:1/60min) | 2.29 | 6.89 |
| AC-H$_2$SO$_4$ (1:1/120min) | 2.84 | 7.26 |
| AC-H$_2$SO$_4$ (1:2/30min) | 2.52 | 7.31 |
| AC-H$_2$SO$_4$ (1:2/60min) | 2.34 | 7.23 |
| AC-H$_2$SO$_4$ (1:2/120min) | 2.84 | 7.21 |
| AC-H$_2$SO$_4$ (1:3/30min) | 3.67 | 6.77 |
| AC-H$_2$SO$_4$ (1:3/60min) | 2.65 | 7.16 |
| AC-H$_2$SO$_4$ (1:3/120min) | 3.87 | 7.28 |
| AC-HCl (1:1/30min) | 2.77 | 7.07 |
| AC-HCl (1:1/60min) | 2.56 | 7.24 |
| AC-HCl (1:1/120min) | 2.37 | 7.41 |
| AC-HCl (1:2/30min) | 2.26 | 7.29 |
| AC-HCl (1:2/60min) | 2.39 | 7.28 |
| AC-HCl (1:2/120min) | 2.35 | 7.23 |
| AC-HCl (1:3/30min) | 2.32 | 7.39 |
| AC-HCl (1:3/60min) | 2.57 | 7.42 |
| AC-HCl (1:3/120min) | 2.78 | 7.40 |

Table 4.8 Moisture content and pH value analysis (continuous)

| Sample Name | Moisture content % | pH value |
|---|---|---|
| AC-NaOH (1:1/30min) | 3.43 | 7.03 |
| AC-NaOH (1:1/60min) | 2.27 | 6.93 |
| AC-NaOH (1:1/120min) | 3.93 | 6.80 |
| AC-NaOH (1:2/30min) | 4.77 | 6.88 |
| AC-NaOH (1:2/60min) | 4.37 | 6.79 |
| AC-NaOH (1:2/120min) | 3.85 | 6.76 |
| AC-NaOH (1:3/30min) | 4.86 | 6.94 |
| AC-NaOH (1:3/60min) | 4.33 | 7.07 |
| AC-NaOH (1:3/120min) | 4.40 | 7.10 |
| AC-KOH (1:1/30min) | 2.14 | 7.10 |
| AC-KOH (1:1/60min) | 1.84 | 6.97 |
| AC-KOH (1:1/120min) | 2.32 | 7.08 |
| AC-KOH (1:2/30min) | 2.85 | 7.89 |
| AC-KOH (1:2/60min) | 3.66 | 7.08 |
| AC-KOH (1:2/120min) | 3.54 | 7.12 |
| AC-KOH (1:3/30min) | 4.37 | 7.09 |
| AC-KOH (1:3/60min) | 4.17 | 7.24 |
| AC-KOH (1:3/120min) | 4.27 | 7.31 |

CHULALONGKORN UNIVERSITY

4.2.2 $N_2$ physisorption and cation exchange capacity analysis

From $N_2$ physisorption and cation exchange capacity analysis, the results of acid-activated clay after activated with $H_2SO_4$ are shown in Table 4.4 and Figure 4.3, the preparation of AC-$H_2SO_4$, at the activation conditions of 1:2 (bentonite/$H_2SO_4$) ratio with soaking time of 30 min was found to be the highest BET specific surface area about 182 $m^2$/g together with a total pore volume of 0.423 $cm^3$/g and average pore size of 8.02 nm. Its trend can be indicated that the BET specific surface area and total pore volume increase with increasing in bentonite clay to $H_2SO_4$ ratio up to 1:2 then dropped while average pore size is still increase caused by the destruction of the clay structure by the excess acid [31] and when considering the soaking time, it was

found that the soaking time up to 120 min tends to decrease in specific surface area but it affects less than the bentonite clay to $H_2SO_4$ ratio.

The term of cation exchange capacity was decrease increasing bentonite clay to $H_2SO_4$ ratio because excess acid resulting in more remove exchangeable cation from clay structure.

Table 4.9 $N_2$ physisorption and CEC analysis of AC-$H_2SO_4$

| Sample Name | BET m²/g | Pore Volume cm³/g | Average Pore Size nm | CEC mg/g |
|---|---|---|---|---|
| AC-$H_2SO_4$ (1:1/30min) | 161 | 0.269 | 6.04 | 50 |
| AC-$H_2SO_4$ (1:1/60min) | 158 | 0.460 | 9.72 | 35 |
| AC-$H_2SO_4$ (1:1/120min) | 148 | 0.407 | 8.98 | 35 |
| AC-$H_2SO_4$ (1:2/30min) | 182 | 0.423 | 8.02 | 32 |
| AC-$H_2SO_4$ (1:2/60min) | 160 | 0.443 | 9.56 | 38 |
| AC-$H_2SO_4$ (1:2/120min) | 148 | 0.452 | 10.70 | 15 |
| AC-$H_2SO_4$ (1:3/30min) | 154 | 0.547 | 12.23 | 23 |
| AC-$H_2SO_4$ (1:3/60min) | 115 | 0.517 | 15.49 | 17 |
| AC-$H_2SO_4$ (1:3/120min) | 134 | 0.488 | 12.39 | 31 |
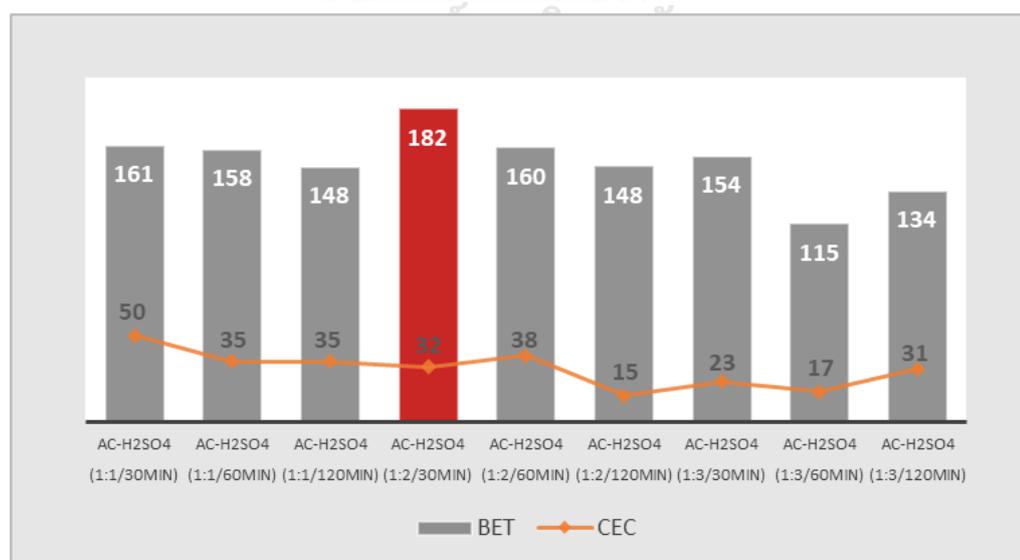


Figure 4.26 BET and CEC analysis of AC-$H_2SO_4$

Table 4.5 and Figure 4.4 shown $N_2$ physisorption and cation exchange capacity analysis of acid-activated clay after activated with HCl, the preparation of AC-HCl shows the highest BET specific surface area about 144 $m^2$/g with a total pore volume of 0.324 $cm^3$/g and average pore size of 7.98 nm that achieved at a bentonite clay to HCl ratio of 1:1 with a soaking time of 30 min. Its trend can be indicated that the BET specific surface area and total pore volume decrease with increasing bentonite clay to HCl ratio while average pore size is also increase caused by the destruction of the clay structure by the excess acid [31] and when considering the soaking time, it was found that the soaking time up to 120 min tends to decrease in specific surface area but it affects less than the bentonite clay to HCl ratio.

The term of cation exchange capacity was decreased increasing bentonite clay to HCl ratio because excess acid resulting in more remove exchangeable cation from clay structure.

Table 4.10 $N_2$ physisorption and CEC analysis of AC-HCl

| Sample Name | BET | Pore Volume | Average Pore Size | CEC |
|---|---|---|---|---|
| | $m^2$/g | $cm^3$/g | nm | mg/g |
| AC-HCl (1:1/30min) | 144 | 0.324 | 7.98 | 42 |
| AC-HCl (1:1/60min) | 140 | 0.283 | 6.94 | 43 |
| AC-HCl (1:1/120min) | 140 | 0.310 | 7.63 | 45 |
| AC-HCl (1:2/30min) | 134 | 0.305 | 8.05 | 30 |
| AC-HCl (1:2/60min) | 132 | 0.255 | 6.91 | 30 |
| AC-HCl (1:2/120min) | 136 | 0.342 | 9.04 | 28 |
| AC-HCl (1:3/30min) | 131 | 0.344 | 9.37 | 29 |
| AC-HCl (1:3/60min) | 131 | 0.352 | 9.63 | 30 |
| AC-HCl (1:3/120min) | 127 | 0.311 | 8.88 | 36 |
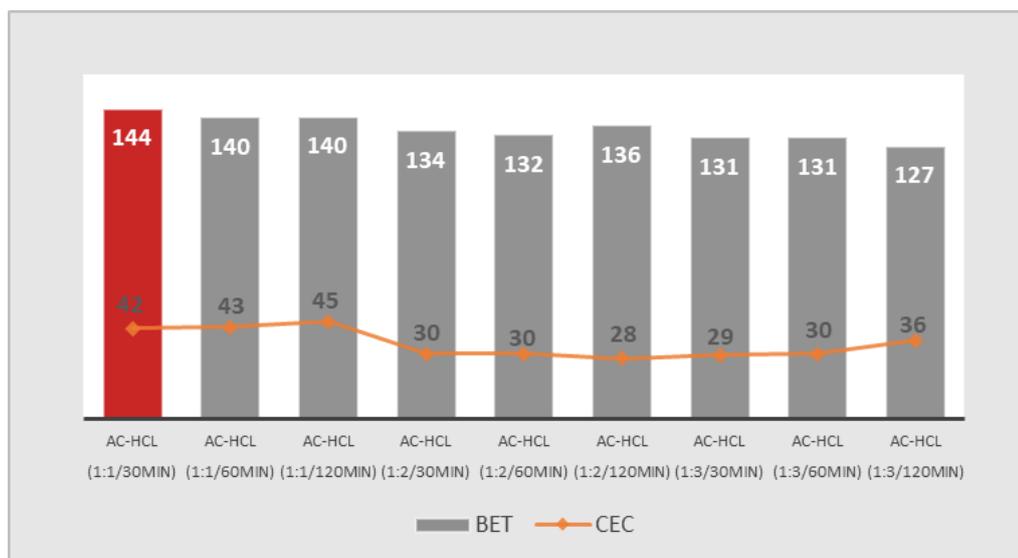
Table 4.11 BET and CEC analysis of AC-HCl

On the whole, the textural changes of acid-activated clays both AC-$H_2SO_4$ and AC-HCl which are determined by $N_2$ physisorption and cation exchange capacity analysis. It can be seen that the increase in bentonite clay to acid ratio, which means an increase in acid concentration resulting in decreased the specific surface area and total pore volume together with reducing in cation exchange capacity. For this result, the octahedral sheet of bentonite clay structure was destroyed by cations into the solution at high concentrations and generates large silica by the tetrahedral sheet remains in the solids which are deposited at the mouth of the pores, it could be described by the passivation process [32]. In addition, it was also found that AC-$H_2SO_4$ has a higher specific surface area, total pore volume and average pore size than AC-HCl because $H_2SO_4$ is a diprotic acid, it has several exchange cations of diacid and also found that the $H_2SO_4$ was used in the activation in a larger proportion than the HCl due to $H_2SO_4$ lower acid strength, which identified by $K_a$ value than HCl resulting in obtained the bentonite clay to an acid ratio in the activation condition at the highest specific surface area of 1:2 for activating with $H_2SO_4$ and 1:1 for activating with HCl.

Table 4.6 and Figure 4.5, the preparation of AC-NaOH shows the highest BET specific surface area of AC-NaOH about 119 $m^2$/g with a total pore volume of 0.286 $cm^3$/g and average pore size of 8.49 nm, it is achieved at a bentonite clay to NaOH

ratio of 1:1 and soaking time of 30 min. Its trend can be indicated that the BET specific surface area decreases with increasing bentonite clay to NaOH ratio while the total pore volume and average pore size are still increase caused by the destruction of the clay structure by the excess alkali and when considering the soaking time, it was found that the soaking time up to 120 min seems to increase in specific surface area but it affects less than the bentonite clay to NaOH ratio.

The term of cation exchange capacity was increased increasing bentonite clay to NaOH ratio because excess alkali resulting in more $Na^+$ exchangeable cation in clay structure. The cation exchange capacity is preferred by the exist of interlayer sodium cations because it is more easily exchangeable, since its greatest power of hydration and lower valence reduce its bond strength with the clay mineral surface [32].

Table 4.12 $N_2$ physisorption and CEC analysis of AC-NaOH

| Sample Name | BET $m^2/g$ | Pore Volume $cm^3/g$ | Average Pore Size nm | CEC mg/g |
|---|---|---|---|---|
| AC-NaOH (1:1/30min) | 119 | 0.286 | 8.49 | 74 |
| AC-NaOH (1:1/60min) | 69 | 0.194 | 11.90 | 57 |
| AC-NaOH (1:1/120min) | 96 | 0.445 | 16.06 | 67 |
| AC-NaOH (1:2/30min) | 97 | 0.392 | 14.05 | 108 |
| AC-NaOH (1:2/60min) | 108 | 0.370 | 13.07 | 153 |
| AC-NaOH (1:2/120min) | 111 | 0.393 | 12.57 | 76 |
| AC-NaOH (1:3/30min) | 110 | 0.473 | 16.33 | 118 |
| AC-NaOH (1:3/60min) | 87 | 0.330 | 14.48 | 63 |
| AC-NaOH (1:3/120min) | 107 | 0.406 | 14.22 | 138 |
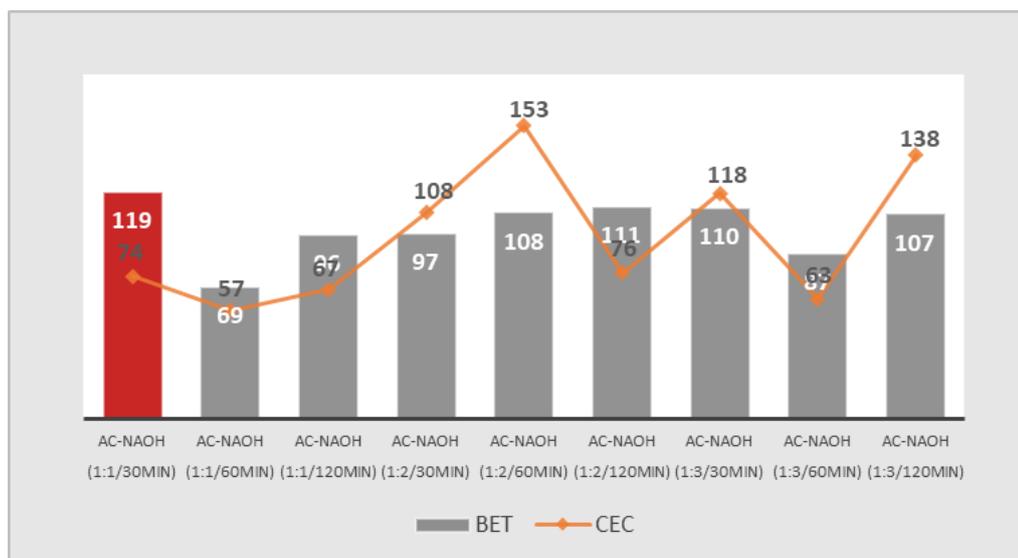
Figure 4.27 BET and CEC analysis of AC-NaOH

Table 4.7 and Figure 4.6, the preparation of AC-KOH shows the highest BET specific surface area of AC-KOH about 150 $m^2$/g with a total pore volume of 0.397 $cm^3$/g and average pore size of 7.79 nm, it is achieved at a bentonite clay to KOH ratio of 1:3 and soaking time of 60 min. Its trend can be indicated that the BET specific surface area is increased with increasing bentonite clay to KOH ratio while the total pore volume and average pore size are also increased caused by the destruction of the clay structure by the excess alkali and when considering the soaking time, it was found that the soaking time up to 120 min seems to increase in specific surface area but it affects less than the bentonite clay to KOH ratio.

The term of cation exchange capacity seemed to lightly decrease increasing bentonite clay to KOH ratio because excess alkali resulting in more $K^+$ exchangeable cation in clay structure.

Table 4.13 $N_2$ physisorption and CEC analysis of AC-KOH

| Sample Name | BET m²/g | Pore Volume cm³/g | Average Pore Size nm | CEC mg/g |
|---|---|---|---|---|
| AC-KOH (1:1/30min) | 82 | 0.265 | 11.06 | 29 |
| AC-KOH (1:1/60min) | 64 | 0.138 | 7.53 | 21 |
| AC-KOH (1:1/120min) | 98 | 0.283 | 10.59 | 29 |
| AC-KOH (1:2/30min) | 110 | 0.344 | 11.19 | 15 |
| AC-KOH (1:2/60min) | 102 | 0.313 | 9.74 | 15 |
| AC-KOH (1:2/120min) | 121 | 0.330 | 7.97 | 45 |
| AC-KOH (1:3/30min) | 125 | 0.329 | 7.68 | 10 |
| AC-KOH (1:3/60min) | 150 | 0.397 | 7.79 | 16 |
| AC-KOH (1:3/120min) | 103 | 0.572 | 19.38 | 46 |
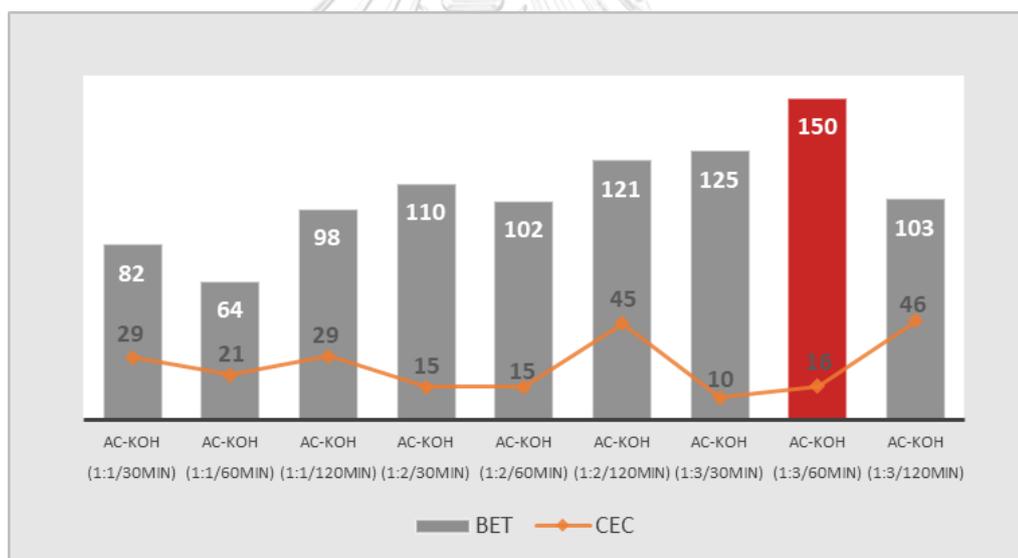


Figure 4.28 BET and CEC analysis of AC-KOH

The textural changes of the alkali-activated clays after activation, which determined by $N_2$ physisorption and cation exchange capacity analysis can be summarized that increase in an alkali concentration by the rise in bentonite clay to alkali ratio effect on the decrease in specific surface area and total pore volume for AC-NaOH while cation exchange capacity trend to increase due to activating with

NaOH whereas activating with KOH was found increasing in specific surface area and total pore volume due to activating with NaOH is changed of $SiO_2$ content in the activated clay because some of the silica is bonded with NaOH during the activation process, forming sodium-aluminum-silicate ($NaAlSiO_8$) [34] resulting in KOH has the $OH^-$ concentration together with KOH is high alkali strength more than NaOH, it significant to dissolve of montmorillonite causes the AC-KOH has a higher specific surface area and porosity than AC-HCl.

Figure 4.7 shows the overall BET specific surface area and cation exchange capacity analysis of activated clays in comparison to initial Ratchaburi bentonite. The results are clearly shown that the activation process is a significant effect on textural characteristic modification of bentonite clay, it is resulting in increased specific surface area, total pore volume and average pore size due to the destruction of clay structure by the activated agent with concluding the highest BET specific surface area can be increased from 41 $m^2$/g to 182, 144, 119 and 150 $m^2$/g with increased total pore volume from 0.077 $cm^3$/g to 0.423, 0324, 0.286 and 0.397 $cm^3$/g and increased average pore size from 7.60 nm to 8.02, 7.98, 8.49 and 7.79 nm together with the cation exchange capacity decreased from 133 mg/g to 32, 42, 74 and 16 mg/g for AC-$H_2SO_4$, AC-HCl, AC-NaOH, AC-KOH respectively. It can be described that both activation process acid-activation and alkali-activation can be modified bentonite structure to increase in specific surface area together with reduce cation exchange capacity from original bentonite clay, which is a consequence of the bentonite structure destruction mechanism in the activation process. Certainly, acid-activation which activating with $H_2SO_4$ provide the activated clay with the highest specific surface area while activating with NaOH shown lowest specific surface area due to some part of sodium forming as sodium-aluminum-silicate ($NaAlSiO_8$) and also found that the KOH was used in the activation in a larger proportion than the $H_2SO_4$ and HCl due to acid substance higher leaching performance than alkali.
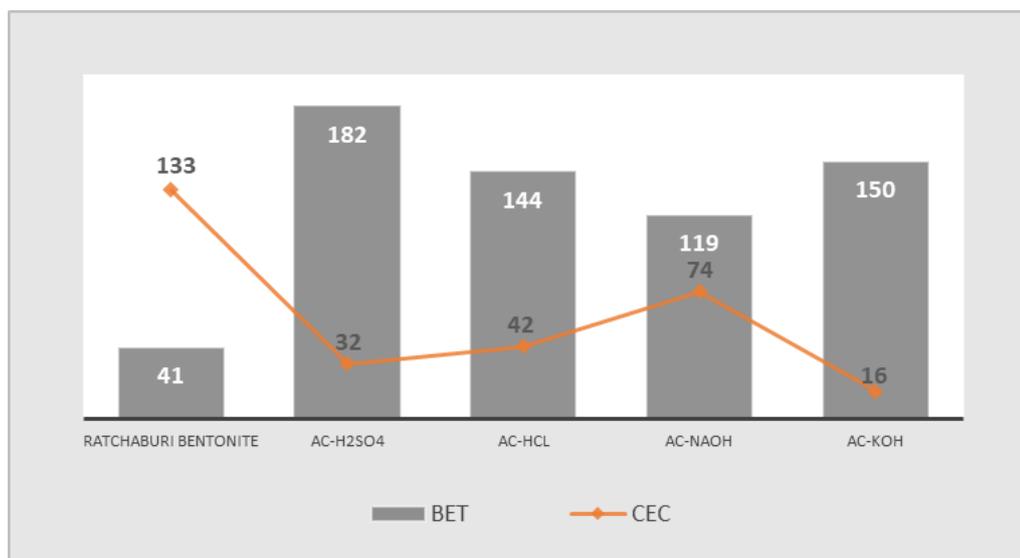
Figure 4.29 Overall BET and CEC analysis

Eventually, it is available to obtain the outcome of the $N_2$ adsorption isotherm of Ratchaburi bentonite and activated clays as shown in Figure 4.8. The adsorption isotherm of all clays is present in type IV which is divided by an IUPAC committee it indicated that the classification of clays is mesopore. The mechanism of adsorption in mesoporous materials is recognized to start with the formation of a monolayer on the surface and then continue with multilayer formation and finally capillary condensation [33]. Furthermore, when considering the hysteresis loop shape, it was found to be type H3 for as a received Ratchaburi bentonite and AC-NaOH, it shows wedge-shaped pore and capillary condensation in mesopores, possibly due to the multilayer formation. For AC-$H_2SO_4$ and AC-HCl are shown hysteresis loop shape seems to combine between H1 and H3, it shows cylinder-shaped with wedge-shaped pore while AC-KOH was to be evident in hysteresis loop shape type H1, it shows cylinder-shaped pore [34].
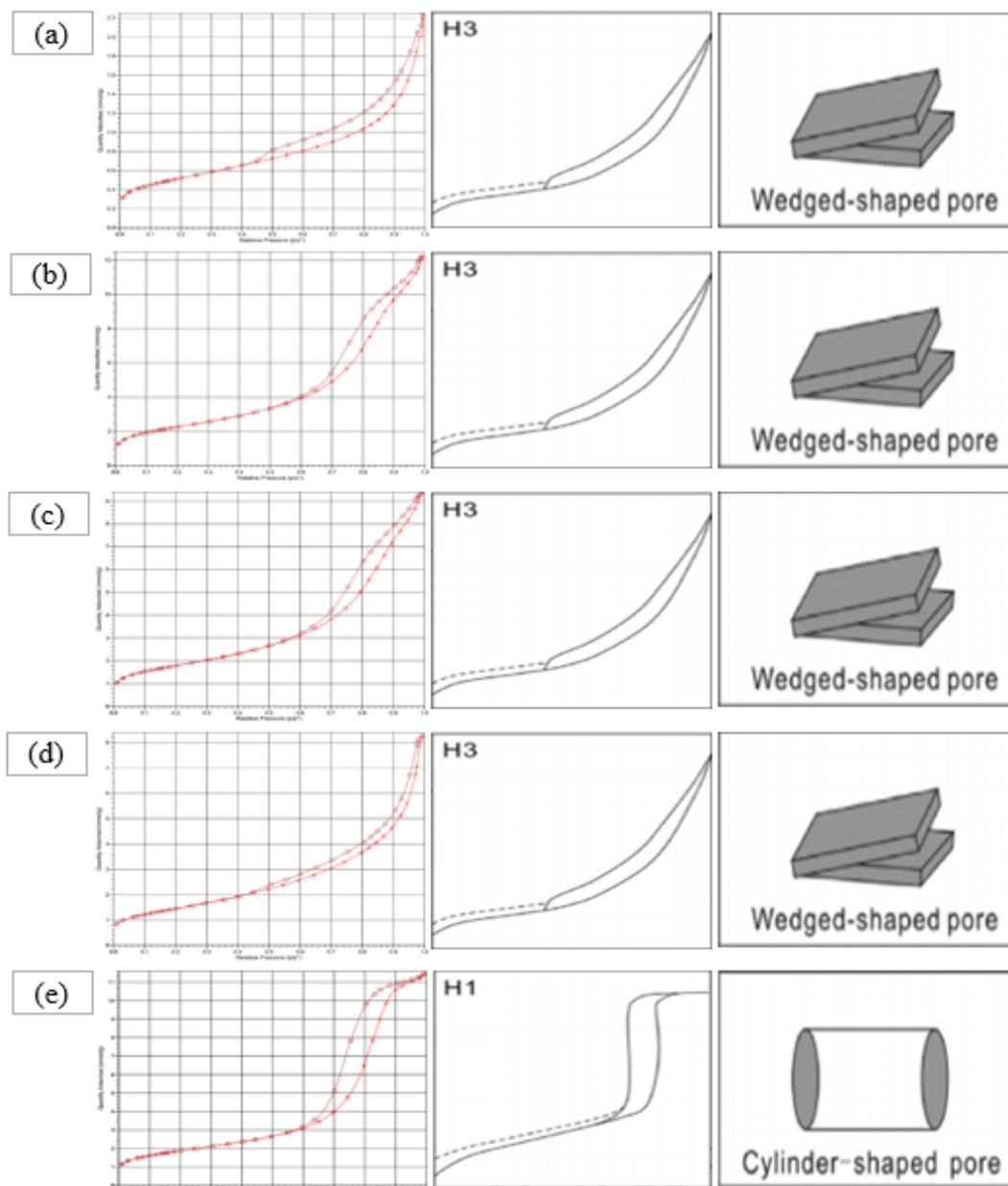
Figure 4.30 N$_2$ adsorption isotherm of activated clays

(a) Ratchaburi bentonite, (b) AC-H$_2$SO$_4$, (c) AC-HCl, (d) AC-NaOH, (e) AC-KOH

### 4.2.3 Chemical composition analysis

The chemical compositions of the Ratchaburi bentonite and activated clays are shown in Table 4.8. The results show that the ratio of Na$_2$O to CaO is 0.04 for as a received Ratchaburi bentonite which is less than 1, it revealed that the presence of calcium bentonite also known as non-swelling bentonite. After activation, the

chemical compositions have been changed from original bentonite clay because it is modified the structure of bentonite chemistry. The chemical compositions of acid-activated clays both of AC-$H_2SO_4$ and AC-HCl are changed evidently with greater $SiO_2$ contents which increased in an amount from 60.93% to 86.73% and 74.84% respectively and decreased intenseness of the metal oxide include $Al_2O_3$, $Fe_2O_3$, MgO, CaO and $K_2O$ because of acid leaching cause the hydrogen ions attack the metallic ions. For alkali-activated clays, the chemical compositions of AC-NaOH are increased in $Na_2O$ apparently with an amount from 0.04% to 8.43% and an increasing amount of $K_2O$ from 1.05% to 13.72% for AC-KOH where it appears that the alkali-activation is not substituted the exchangeable cations that can be observed in the CaO content does not decrease but dissolves the silica in the structure.

Table 4.14 Chemical composition analysis

| Chemical compositions | Ratchaburi bentonite | AC-$H_2SO_4$ | AC-HCl | AC-NaOH | AC-KOH |
|---|---|---|---|---|---|
| $SiO_2$ (%) | 60.93 | 86.73 | 74.84 | 53.16 | 50.40 |
| $TiO_2$ (%) | 0.716 | 0.853 | 0.870 | 0.725 | 0.553 |
| $Al_2O_3$ (%) | 16.52 | 6.67 | 14.75 | 16.06 | 16.46 |
| $Fe_2O_3$ (%) | 7.31 | 0.631 | 1.453 | 7.47 | 5.478 |
| CaO (%) | 1.10 | 0.18 | 0.30 | 2.54 | 2.61 |
| MgO (%) | 0.99 | 0.18 | 0.31 | 1.34 | 1.45 |
| $K_2O$ (%) | 1.05 | 0.58 | 0.98 | 0.53 | 13.72 |
| $Na_2O$ (%) | 0.04 | 0.07 | 0.04 | 8.43 | 0.61 |
| MnO (%) | 0.033 | 0.002 | 0.003 | 0.035 | 0.027 |
| $P_2O_5$ (%) | 0.043 | 0.035 | 0.042 | 0.007 | 0.003 |
| $SO_3$ (%) | 0.029 | 0.104 | 0.021 | 0.031 | 0.019 |
| L.O.I. (%) | 11.24 | 3.97 | 6.39 | 9.67 | 8.68 |

In addition, Figure 4.9 is described that the acid-activated clays are changed in major composition, it increasing in $SiO_2$ content and decreasing in $Al_2O_3$ due to the acid treatment resulted in a gradual increase in the amount of $SiO_2$ in the bentonite clay at the expense of the octahedral cations and tetrahedral Al from the smectite

structure. The majority of the exchangeable cations and most of the Fe, Mg, and Al atoms in the octahedral sheet of the bentonite clay were removed [35]. On the other hand, alkali-activated clays have slightly decreased the content of $SiO_2$ due to dissolution of silica in tetrahedral sheet while the content of $Al_2O_3$ is almost unchanged maybe cause by alkali-activation does not remove the $Al^{3+}$ from the structure. Figure 4.10 is shown about the $Fe_2O_3$ levels, the results show that the $Fe_2O_3$ levels greatly reduced for acid-activated clays and hardly changed for alkali-activated clays that indicate acid-activation can be removed $Fe_2O_3$ better than alkali-activation. In the clay minerals, the $Fe_2O_3$ contents are an important effect on the clay color, if the clay consists of a high of $Fe_2O_3$ levels it will be dark color or yellow. For this reason, it made the appearance color of acid-activated clays is light and alkali-activated clays are yellow.



Figure 4.31 The $SiO_2$ and $Al_2O_3$ Levels
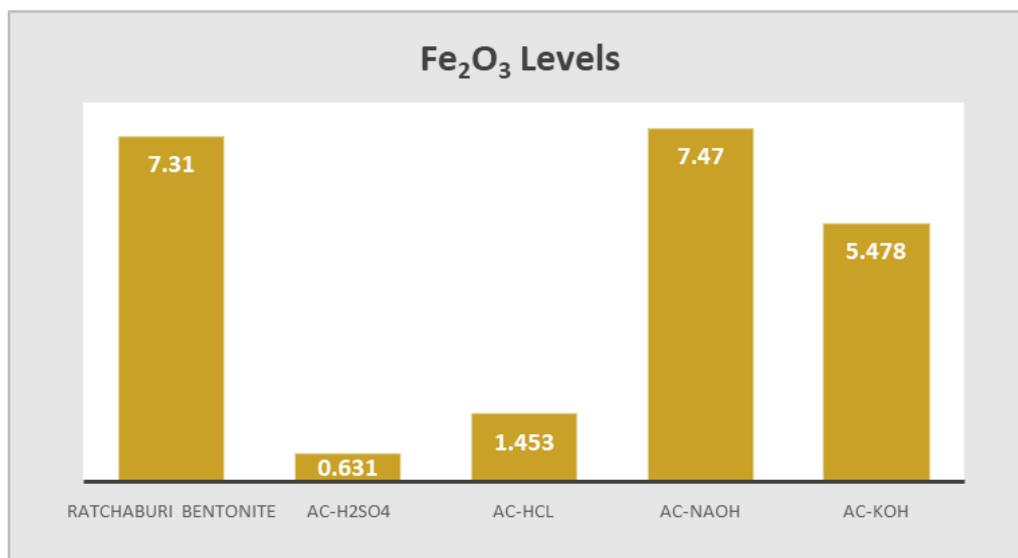
Figure 4.32 The $Fe_2O_3$ Levels

4.2.4 Mineralogical composition

The mineralogical composition of the Ratchaburi bentonite and activated clays are shown in Figure 4.11. The results from XRD patterns are indicated that the Ratchaburi bentonite is generally comprised of montmorillonite and consequential amounts of quartz and kaolinite impurities. After activation, the montmorillonite of both activated clays, acid-activated clays and alkali-activated clays, is reduced and the montmorillonite peak is disappeared at a 2-theta degree of 6.08, 29.42 and 62.41 due to the montmorillonite structure was destroyed. Moreover, the alkali-activation by using sodium hydroxide as an activation agent shows the peaks of plagioclase as observe in AC-NaOH due to some part of sodium forming plagioclase as sodium-aluminum-silicate ($NaAlSiO_8$) and the amorphous silica phase is presented in all activated clay according to activation mechanism that produce a large of amorphous silica, it can be clearly observed in AC-KOH.
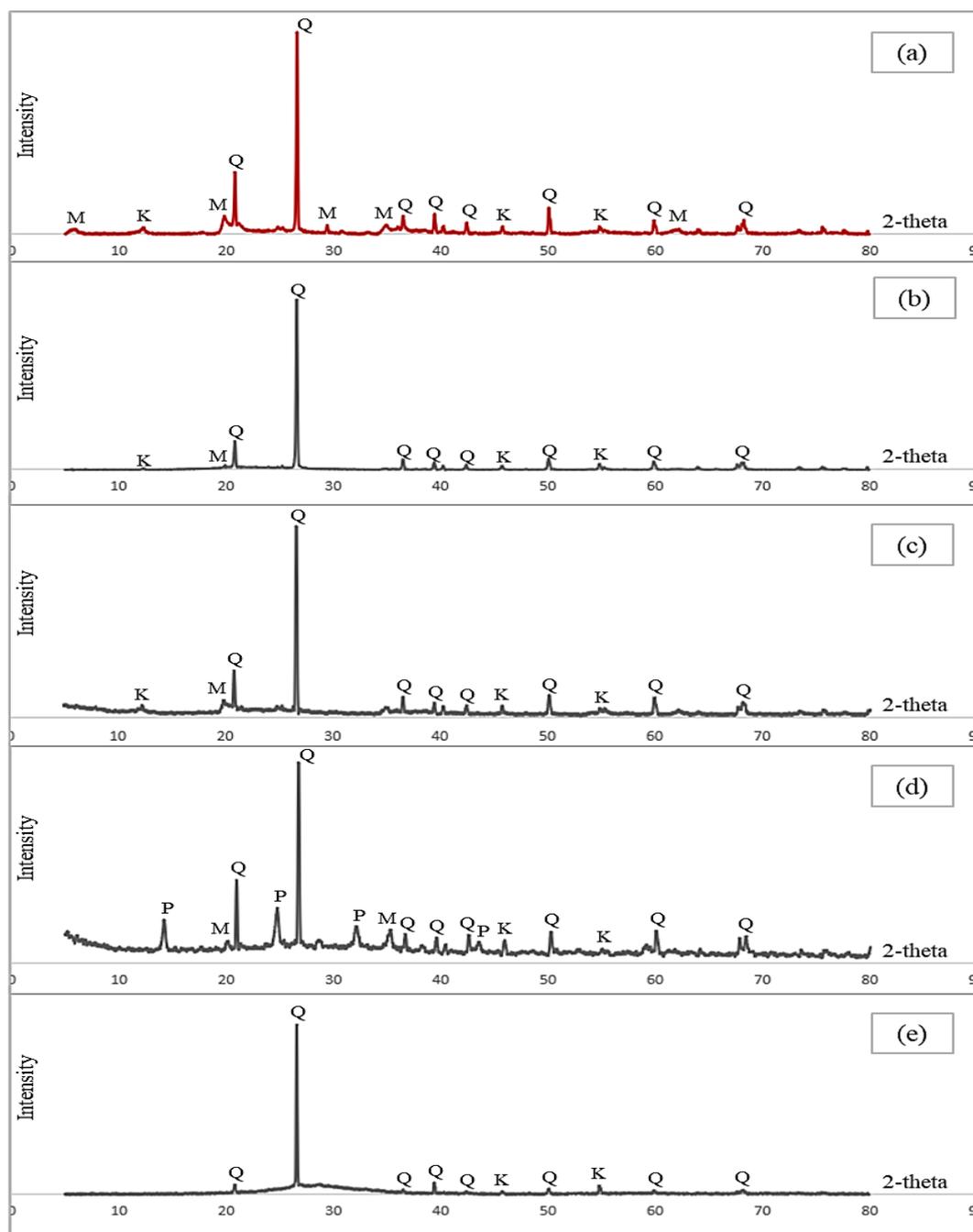
Figure 4.33 XRD patterns of activated clays

(a) Ratchaburi bentonite, (b) AC-$H_2SO_4$, (c) AC-HCl, (d) AC-NaOH, (e) AC-KOH,

M: montmorillonite, K: kaolinite, Q: quartz, P: plagioclase

4.2.5 Morphological characteristic

Scanning electron microscopy is one method used to investigate the physical structure. It will provide information as a 3D image showing the characteristics of the sample as well as the characteristics of the surface. From scanning electron microscopy images are shown in Figure 4.12, the differences in the shape of the surface of the Ratchaburi bentonite before and after improvement by the activation process can be seen at the same magnification. The Ratchaburi bentonite before quality improvement has a rough surface and a sheet structure when applied to improve quality with the activation agent, the appearance of the surface has been changed is more porous so the surface area is more increasing.
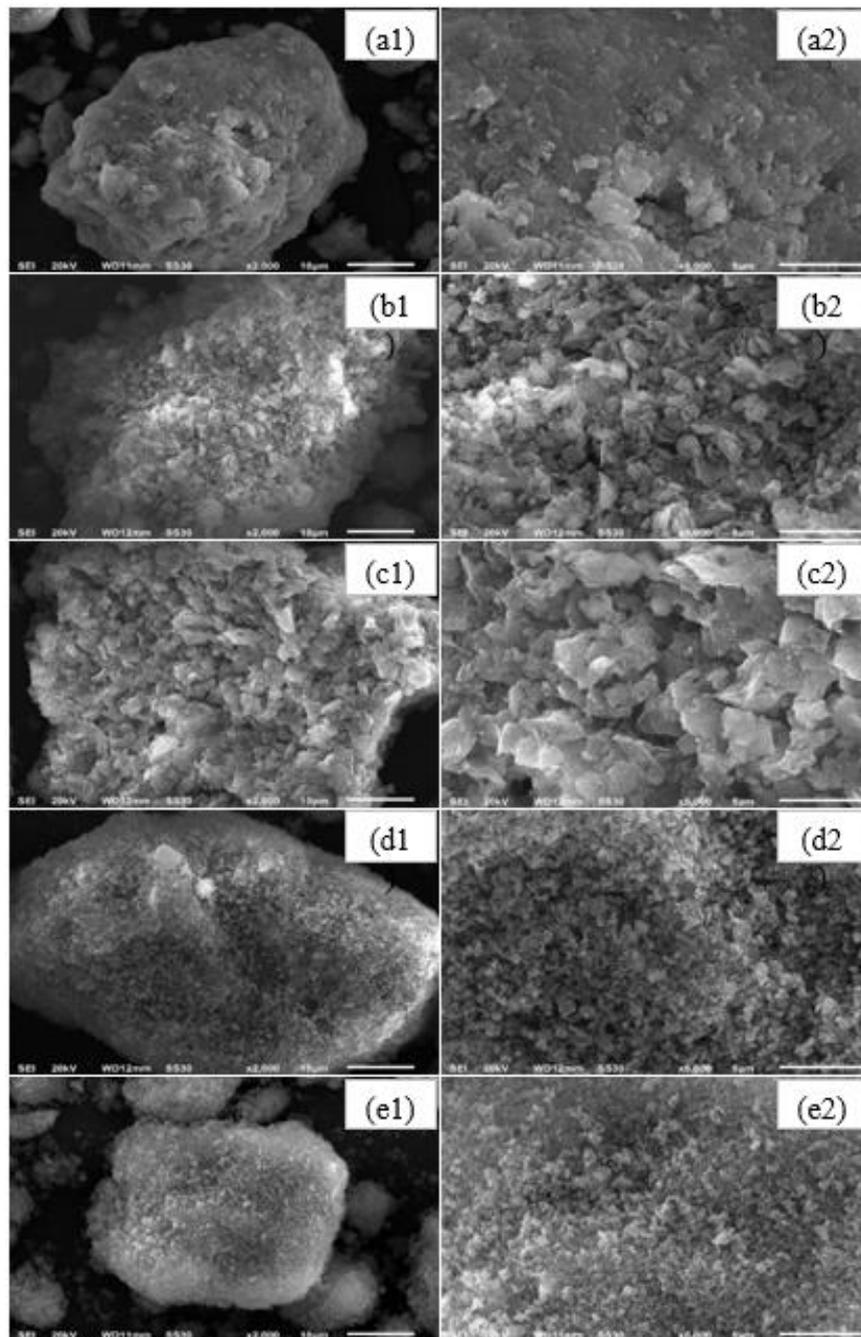
Figure 4.34 Scanning electron micrographs of activated clay

(a1) Ratchaburi bentonite x2000, (a2) Ratchaburi bentonite x5000, (b1) AC-$H_2SO_4$ x2000, (b1) AC-$H_2SO_4$ x5000, (c1) AC-HCl x2000, (c2) AC-HCl x5000, (d1) AC-NaOH x2000, (d2) AC-NaOH x5000, (e1) AC-KOH x2000, (e2) AC-KOH x5000

### 4.3 Decolorization of Pyrolysis Oil

4.3.1 Pyrolysis oil decolorization at 10 g of activated clay dosages

The mechanism of decolorization of pyrolysis oils occurs when the organic matter, which is the coloring body that contaminates in pyrolysis oil, is attracted on activated clay surface by van der Waals forces and chemisorbed by electrochemical bonding to the surface together with trap these contaminants inside the pores by molecular sieves.

Table 4.9 and Figure 4.13 show decolorization at 10 g of AC-$H_2SO_4$ with fixed reaction temperature of $100\pm5°C$ for 2 h, the results show that the decolorization efficiency increase when increase bentonite clay to $H_2SO_4$ up to 1:2 then dropped because of clay structure destruction from excess acid effect on reduction specific surface area, which corresponds to the results in $N_2$ adsorption analysis area, resulting in reduction adsorption capacity. The best activated clay preparation conditions to obtain the highest decolorization efficiency are consist of bentonite clay to $H_2SO_4$ ratio of 1:2 and a soaking time of 30 min with achieved decolorization efficiency of 40.64%. It is summarized that both these bentonite clay to $H_2SO_4$ and soaking time are appropriated.

Table 4.15 Decolorization at 10 g of AC-$H_2SO_4$

| Activated clay | Decolorization at clay 10 g Absorbance | Decolorization efficiency % |
|---|---|---|
| AC-$H_2SO_4$ (1:1/30min) | 1.371 | 36.62 |
| AC-$H_2SO_4$ (1:1/60min) | 1.497 | 30.79 |
| AC-$H_2SO_4$ (1:1/120min) | 1.489 | 31.16 |
| AC-$H_2SO_4$ (1:2/30min) | 1.284 | 40.64 |
| AC-$H_2SO_4$ (1:2/60min) | 1.456 | 32.69 |
| AC-$H_2SO_4$ (1:2/120min) | 1.371 | 36.62 |
| AC-$H_2SO_4$ (1:3/30min) | 1.427 | 34.03 |
| AC-$H_2SO_4$ (1:3/60min) | 1.601 | 25.98 |
| AC-$H_2SO_4$ (1:3/120min) | 1.497 | 30.79 |
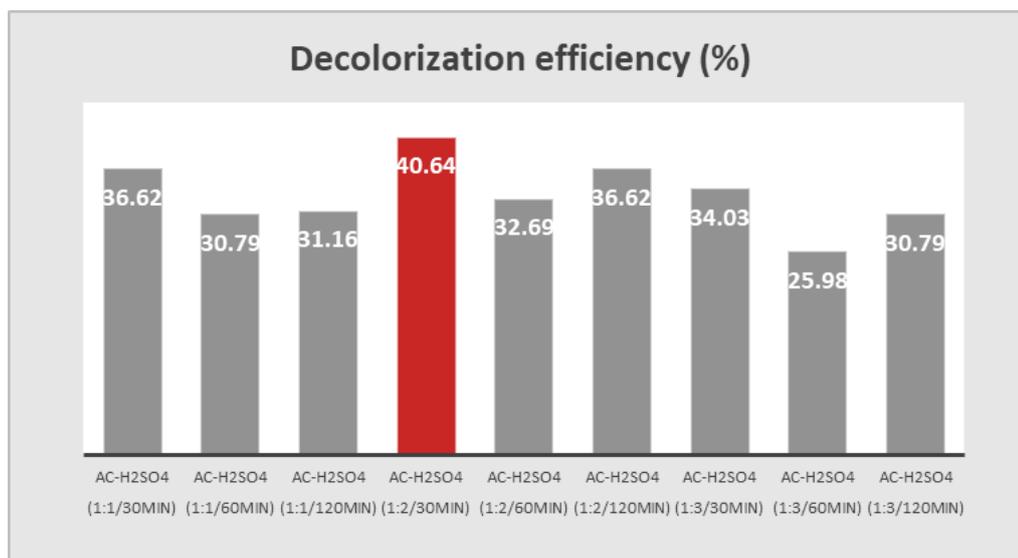
Figure 4.35 Decolorization efficiency with 10 gAC-H₂SO₄

Table 4.10 and Figure 4.14 show decolorization at 10 g of AC-HCl with fixed reaction temperature of $100\pm5°C$ for 2 h, the results show that the decolorization efficiency decrease when increase bentonite clay to HCl because of clay structure destruction from excess acid effect on reduction specific surface area, which corresponds to the results in $N_2$ adsorption analysis area, resulting in reduction adsorption capacity. The best activated clay preparation conditions to obtain the highest decolorization efficiency are consist of bentonite clay to HCl ratio of 1:1 and a soaking time of 30 min with achieved decolorization efficiency of 13.41%. It is summarized that both these bentonite clay to HCl and soaking time are appropriated.

Table 4.16 Decolorization at 10 g of AC-HCl

| Sample Name | Decolorization at clay 10 g Absorbance | Decolorization efficiency % |
|---|---|---|
| AC-HCl (1:1/30min) | 1.873 | 13.41 |
| AC-HCl (1:1/60min) | 1.896 | 12.34 |
| AC-HCl (1:1/120min) | 1.883 | 12.94 |
| AC-HCl (1:2/30min) | 1.889 | 12.67 |
| AC-HCl (1:2/60min) | 1.886 | 12.81 |
| AC-HCl (1:2/120min) | 1.898 | 12.25 |
| AC-HCl (1:3/30min) | 1.905 | 11.93 |
| AC-HCl (1:3/60min) | 1.922 | 11.14 |
| AC-HCl (1:3/120min) | 1.898 | 12.25 |
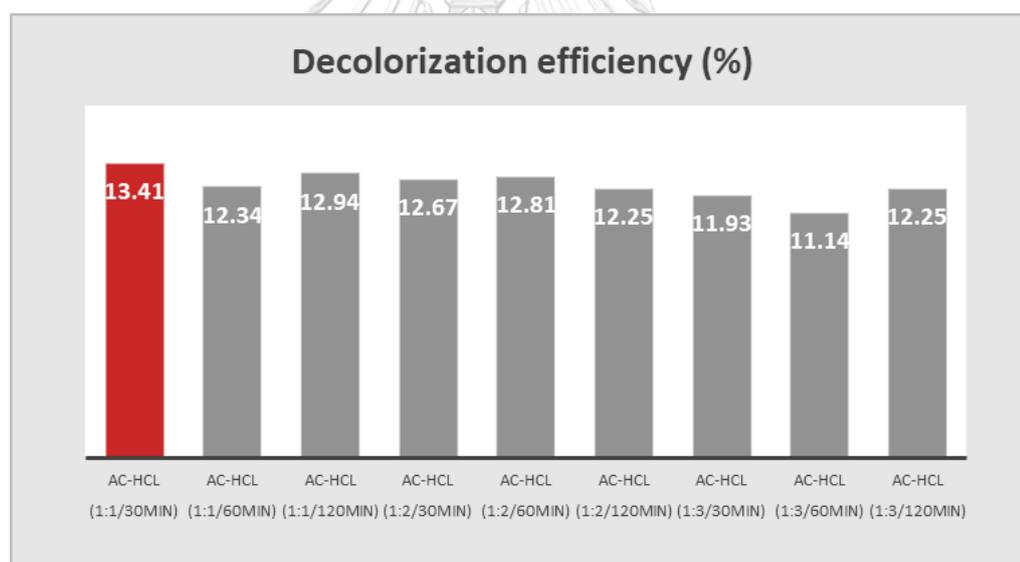


Figure 4.36 Decolorization efficiency with 10 g AC-HCl

Table 4.11 and Figure 4.15 show decolorization at 10 g of AC-NaOH with fixed reaction temperature of $100\pm5°C$ for 2 h, the results show that the decolorization efficiency decrease when increase bentonite clay to NaOH because of clay structure destruction from excess alkali and some part of sodium forming sodium-aluminum-silicate ($NaAlSiO_8$) effect on reduction specific surface area, which corresponds to the

results in N$_2$ adsorption analysis, resulting in reduction adsorption capacity. The best activated clay preparation conditions to obtain the highest decolorization efficiency are consist of bentonite clay to NaOH ratio of 1:1 and a soaking time of 30 min with achieved decolorization efficiency of 13.50%. It is summarized that both these bentonite clay to NaOH and soaking time are appropriated.

Table 4.17 Decolorization at 10 g of AC-NaOH

| Sample Name | Decolorization at clay 10 g Absorbance | Decolorization efficiency % |
|---|---|---|
| AC-NaOH (1:1/30min) | 1.871 | 13.50 |
| AC-NaOH (1:1/60min) | 1.993 | 7.86 |
| AC-NaOH (1:1/120min) | 1.972 | 8.83 |
| AC-NaOH (1:2/30min) | 1.932 | 10.68 |
| AC-NaOH (1:2/60min) | 1.994 | 7.81 |
| AC-NaOH (1:2/120min) | 1.981 | 8.41 |
| AC-NaOH (1:3/30min) | 2.000 | 7.54 |
| AC-NaOH (1:3/60min) | 1.986 | 8.18 |
| AC-NaOH (1:3/120min) | 1.952 | 9.75 |
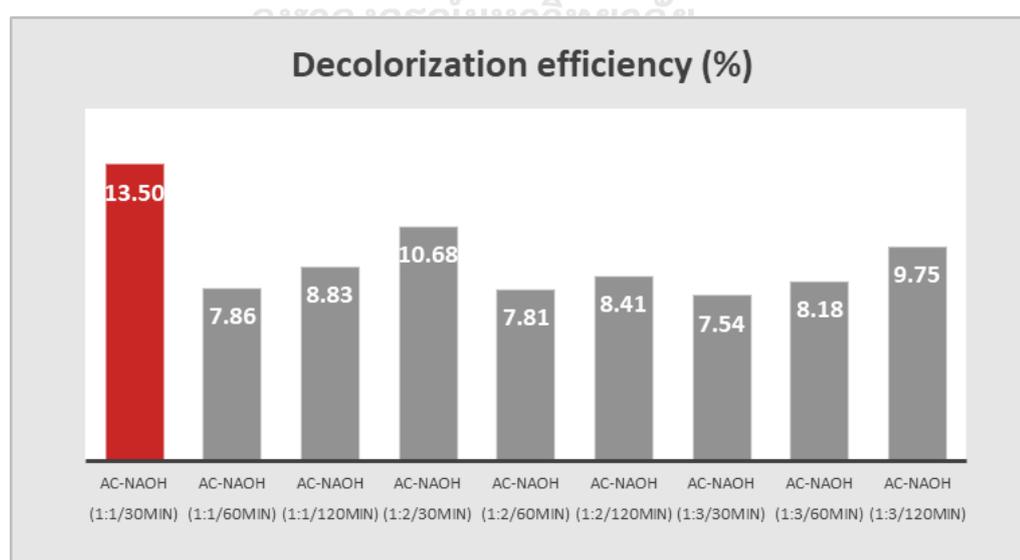


Figure 4.37 Decolorization efficiency with 10 g AC-NaOH

Table 4.12 and Figure 4.16 show decolorization at 10 g of AC-KOH with fixed reaction temperature of $100\pm5°C$ for 2 h, the results show that the decolorization efficiency increase when increase bentonite clay to KOH because of clay structure destruction from excess alkali effect on reduction specific surface area, which corresponds to the results in $N_2$ adsorption analysis. The best activated clay preparation conditions to obtain the highest decolorization efficiency are consist of bentonite clay to KOH ratio of 1:3 and a soaking time of 60 min with achieved decolorization efficiency of 20.80%. It is summarized that both these bentonite clay to KOH and soaking time are appropriated.

Table 4.18 Decolorization at 10 g of AC-KOH

| Sample Name | Decolorization at clay 10 g Absorbance | Decolorization efficiency % |
|---|---|---|
| AC-KOH (1:1/30min) | 2.014 | 6.89 |
| AC-KOH (1:1/60min) | 2.103 | 2.77 |
| AC-KOH (1:1/120min) | 1.996 | 7.72 |
| AC-KOH (1:2/30min) | 1.978 | 8.55 |
| AC-KOH (1:2/60min) | 1.813 | 16.18 |
| AC-KOH (1:2/120min) | 1.891 | 12.58 |
| AC-KOH (1:3/30min) | 1.778 | 17.80 |
| AC-KOH (1:3/60min) | 1.713 | 20.80 |
| AC-KOH (1:3/120min) | 1.889 | 12.67 |
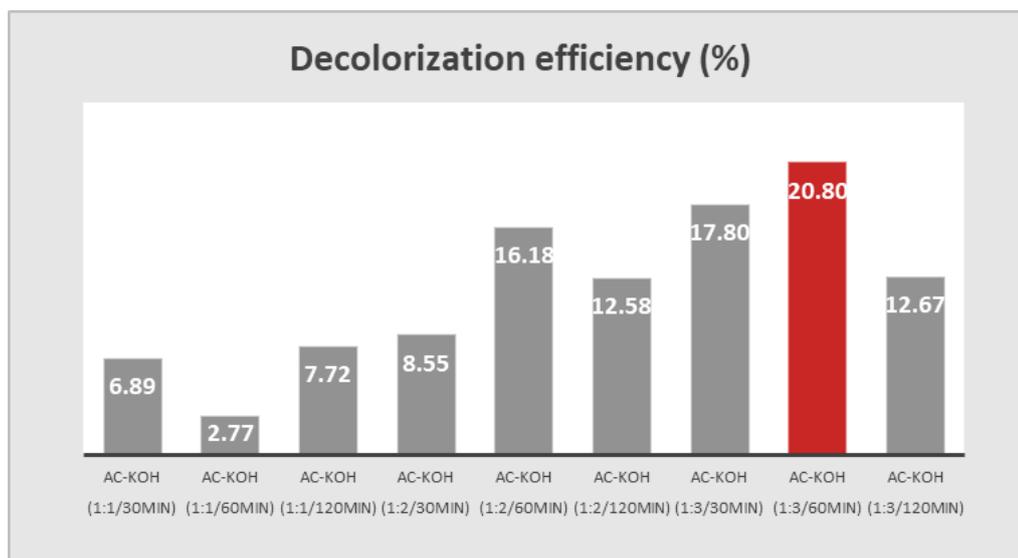
Figure 4.38 Decolorization efficiency with 10 g AC-KOH

### 4.3.2 Decolorization with various activated clay dosages

After achieving the activated clay preparation conditions from pyrolysis oil decolorization at 10 g of activated clay and subsequently varying the activated clay content at 30, 50 and 70 g with fixed reaction temperature of $100\pm5°C$ for 2 h. Table 4.13 and Figure 4.17 show the pyrolysis oil decolorization with various AC-$H_2SO_4$ dosages, the results present that the decolorization efficiency increase when increasing in AC-$H_2SO_4$ dosage due to the high amount of activated clay, which is an adsorbent, resulting in the ability to absorb color bodies is also increased. At the AC-$H_2SO_4$ dosage of 70 g is the best activated clay dosage for decolorization and unable to increase the activated clay volume further due to the rising in viscosity from the adsorption of activated clay absorbs more oil.

Table 4.19 Decolorization with various AC-$H_2SO_4$ dosages

| Descriptions | Absorbance | Decolorization efficiency % |
|---|---|---|
| Activated clay dosage 10 g | 1.284 | 40.64 |
| Activated clay dosage 30 g | 1.199 | 44.57 |
| Activated clay dosage 50 g | 0.566 | 73.83 |
| Activated clay dosage 70 g | 0.383 | 82.29 |
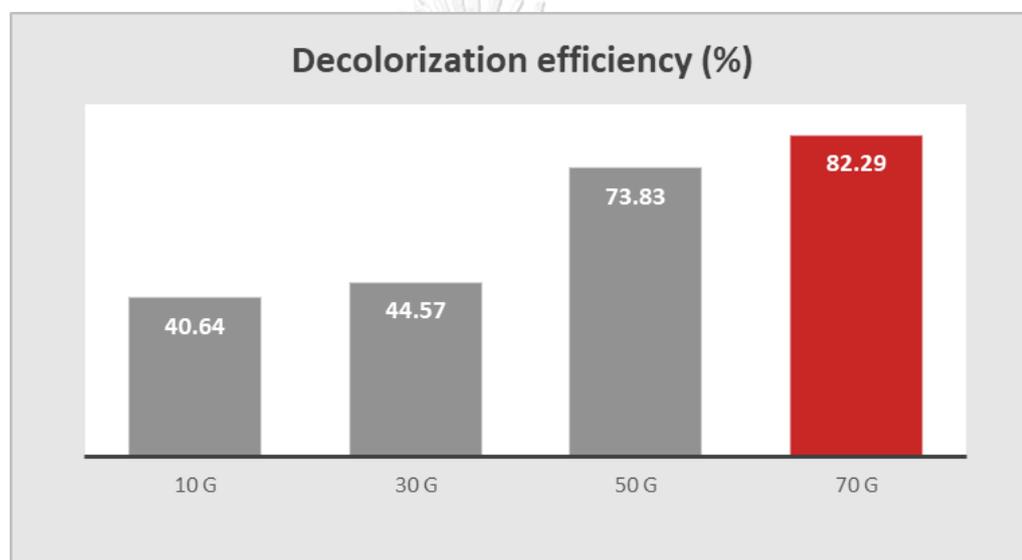


Figure 4.39 Variation of decolorization efficiency with AC-$H_2SO_4$ dosages

Table 4.14 and Figure 4.18 show the pyrolysis oil decolorization with various AC-HCl dosages with fixed reaction temperature of 100±5°C for 2 h, the results present that the decolorization efficiency increase when increasing in AC-HCl dosage due to the high amount of activated clay, which is an adsorbent, resulting in the ability to absorb color bodies is also increased. At the AC-HCl dosage of 70 g is the best activated clay dosage for decolorization and unable to increase the activated clay volume further due to the rising in viscosity from the adsorption of activated clay absorbs more oil.

Table 4.20 Decolorization with various AC-HCl dosages

| Descriptions | Absorbance | Decolorization efficiency % |
|---|---|---|
| Activated clay dosage 10 g | 1.873 | 13.41 |
| Activated clay dosage 30 g | 0.554 | 74.39 |
| Activated clay dosage 50 g | 0.391 | 81.92 |
| Activated clay dosage 70 g | 0.306 | 85.85 |
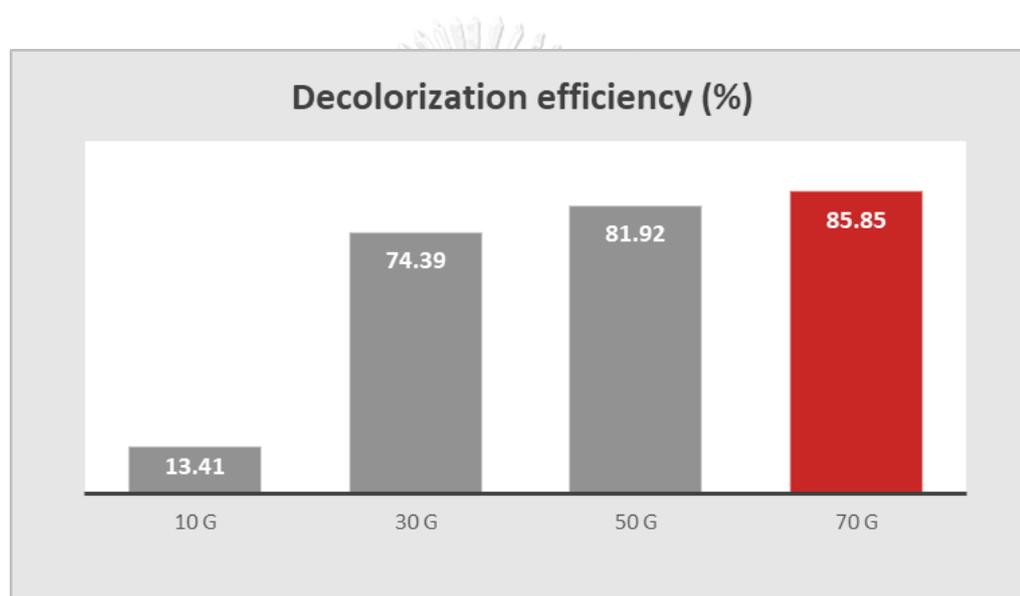


Figure 4.40 Variation of decolorization efficiency with AC-HCl dosages

Table 4.15 and Figure 4.19 show the pyrolysis oil decolorization with various AC-NaOH dosages with fixed reaction temperature of 100±5°C for 2 h, the results present that the decolorization efficiency increase when increasing in AC-NaOH dosage due to the high amount of activated clay, which is an adsorbent, resulting in the ability to absorb color bodies is also increased. At the AC-NaOH dosage of 70 g is the best activated clay dosage for decolorization and unable to increase the activated clay volume further due to the rising in viscosity from the adsorption of activated clay absorbs more oil.

Table 4.21 Decolorization with various AC-NaOH dosages

| Descriptions | Absorbance | Decolorization efficiency % |
|---|---|---|
| Activated clay dosage 10 g | 1.871 | 13.50 |
| Activated clay dosage 30 g | 1.469 | 32.09 |
| Activated clay dosage 50 g | 0.757 | 65.00 |
| Activated clay dosage 70 g | 0.713 | 67.04 |
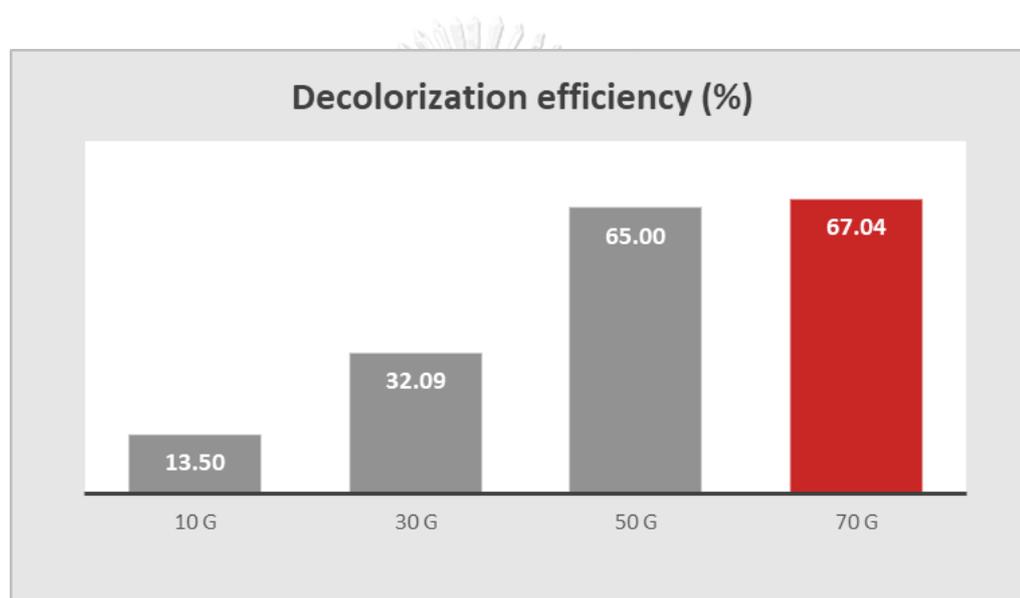


Figure 4.41 Variation of decolorization efficiency with AC-NaOH dosages

Table 4.16 and Figure 4.20 show the pyrolysis oil decolorization with various AC-KOH dosages with fixed reaction temperature of 100±5°C for 2 h, the results present that the decolorization efficiency increase when increasing in AC-KOH dosage due to the high amount of activated clay, which is an adsorbent, resulting in the ability to absorb color bodies is also increased. At the AC-KOH dosage of 70 g is the best activated clay dosage for decolorization and unable to increase the activated clay volume further due to the rising in viscosity from the adsorption of activated clay absorbs more oil.

Table 4.22 Decolorization with various AC-KOH dosages

| Descriptions | Absorbance | Decolorization efficiency % |
|---|---|---|
| Activated clay dosage 10 g | 1.713 | 20.80 |
| Activated clay dosage 30 g | 0.806 | 62.74 |
| Activated clay dosage 50 g | 0.523 | 75.82 |
| Activated clay dosage 70 g | 0.327 | 84.88 |
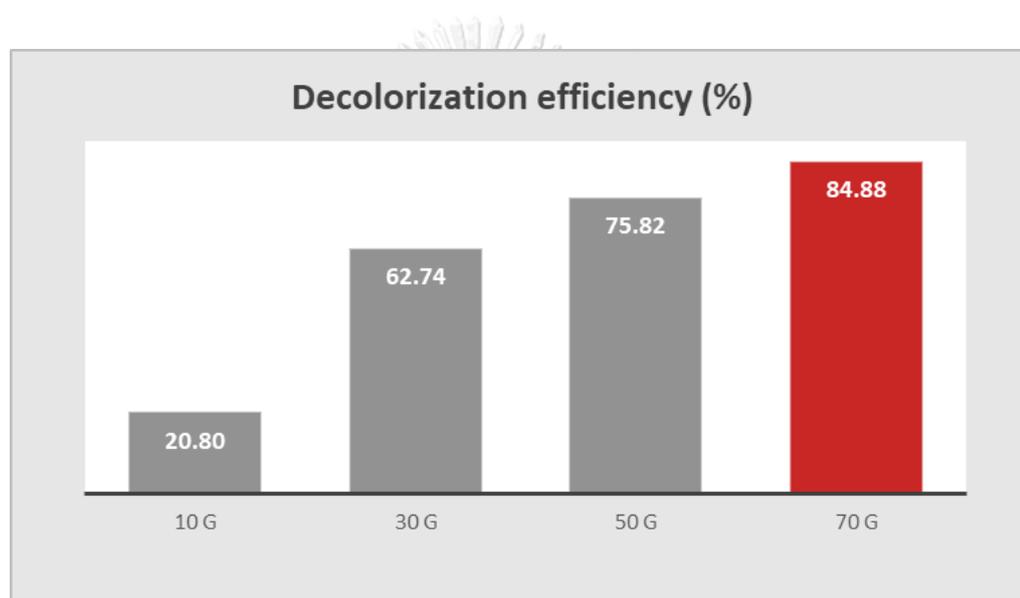


Figure 4.42 Variation of decolorization efficiency with AC-KOH dosages

Base on the results of decolorization efficiency which studied from pyrolysis oil decolorization at 10 g of activated clay dosages and decolorization with various activated clay dosages of 30, 50 and 70 g with fixed reaction temperature of 100±5°C for 2 h. The trend of decolorization efficiency increases when increasing in activated clay dosages due to a large amount of adsorbent to absorb color bodies and other impurities from the pyrolysis oil. It can be concluded that the color of the oil became clear at the reaction temperature of 100±5°C for 2 h obtained the activated clay dosage of 70 g for both acid-activated clay and alkali-activated clay by using AC-$H_2SO_4$ which produced at ratio 1:2 (bentonite/$H_2SO_4$) with soaking time of 30 min,

AC-HCl which produced at a ratio of 1:1 (bentonite/HCl) with soaking time of 30 min, AC-NaOH which produced at a ratio of 1:1 (bentonite/NaOH) with soaking time of 30 min and AC-KOH which produced at a ratio of 1:3 (bentonite/NaOH) with soaking time of 60 min these together with preparation temperature of $100\pm5°C$ which is the same preparation condition that obtains the highest specific surface area.

Figure 4.21 to Figure 4.24 show the appearance color of bleached pyrolysis oils with various AC-$H_2SO_4$, AC-HCl, AC-NaOH and AC-KOH dosages. The color of the oil became clear when the activated clay dosage was increased.
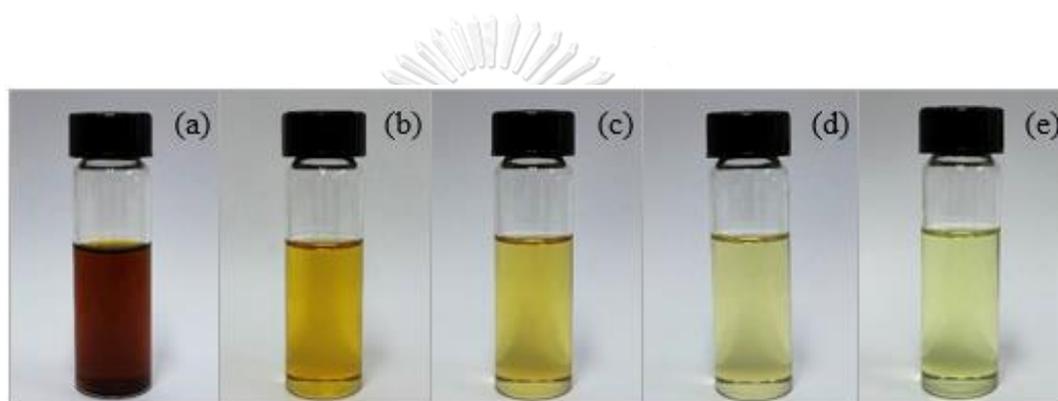


Figure 4.43 Variation of bleached pyrolysis oil with AC-$H_2SO_4$ dosages
(a) crude pyrolysis oil, (b) 10 g, (c) 30 g, (d) 50 g, (e) 70 g
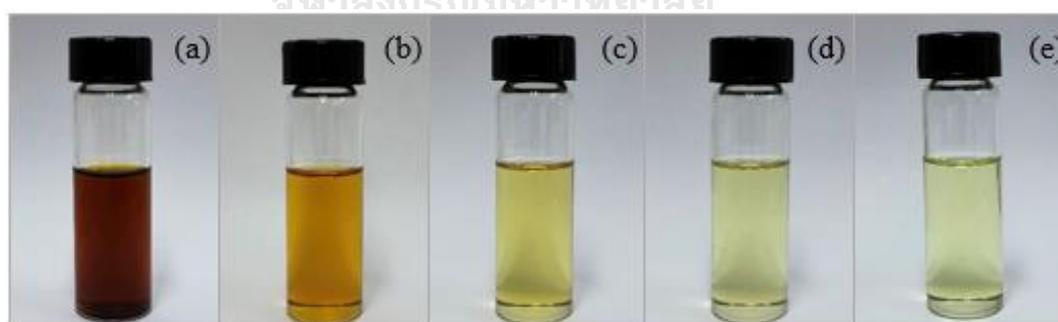


Figure 4.44 Variation of bleached pyrolysis oil with AC-HCl dosages
(a) crude pyrolysis oil, (b) 10 g, (c) 30 g, (d) 50 g, (e) 70 g
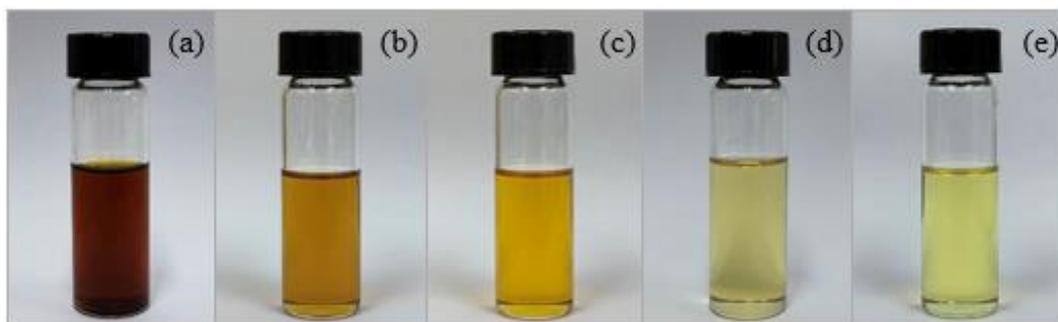
Figure 4.45 Variation of bleached pyrolysis oil with AC-NaOH dosages

(a) crude pyrolysis oil, (b) 10 g, (c) 30 g, (d) 50 g, (e) 70 g
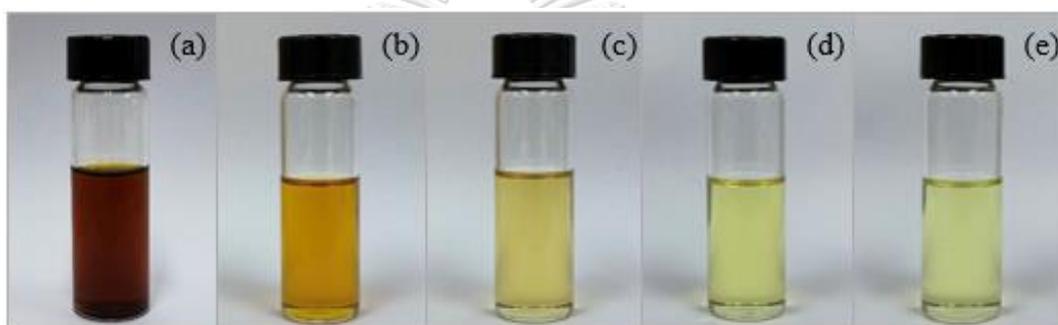


Figure 4.46 Variation of bleached pyrolysis oil with AC-KOH dosages

(a) crude pyrolysis oil, (b) 10 g, (c) 30 g, (d) 50 g, (e) 70 g

4.3.3 Decolorization with various temperatures

Furthermore, studying decolorization with various reaction temperatures of 30, 60, 80, 100 and 120±5°C with fixed reaction time of 2 h and activated clay dosage of 70 g. In Table 4.17 and Figure 4.25, it was found that the intensity of color bodies greatly decreased with decolorize using AC-H$_2$SO$_4$ at maximum temperatures of 80°C with decolorization efficiency of 88.53%. Similarly, the trend of decolorization efficiency is also increased when increasing in reaction temperatures until it reaches a maximum then it commences to drop.

Table 4.23 Decolorization of AC-H$_2$SO$_4$ with various temperatures

| Description | Absorbance | Decolorization efficiency % |
|---|---|---|
| Decolorization temperature 30°C | 0.730 | 66.25 |
| Decolorization temperature 60°C | 0.321 | 85.16 |
| Decolorization temperature 80°C | 0.248 | 88.53 |
| Decolorization temperature 100°C | 0.383 | 82.29 |
| Decolorization temperature 120°C | 0.483 | 77.67 |
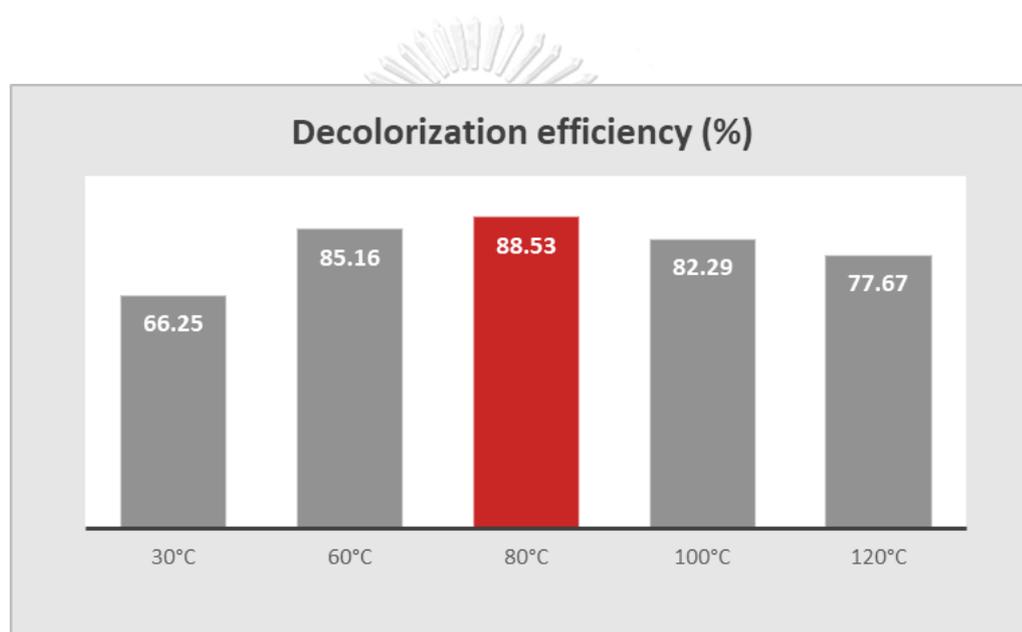


Figure 4.47 Variation of decolorization efficiency of AC-H$_2$SO$_4$ with different temperatures

Table 4.18 and Figure 4.26 show decolorization efficiency of AC-HCl with various temperatures, it was found that the intensity of color bodies greatly decreased with decolorize using AC-HCl at maximum temperatures of 80°C with decolorization efficiency of 89.55%. Similarly, the trend of decolorization efficiency is also increased when increasing in reaction temperatures until it reaches a maximum then it commences to drop.

Table 4.24 Decolorization of AC-HCl with various temperatures

| Description | Absorbance | Decolorization efficiency % |
|---|---|---|
| Decolorization temperature 30°C | 0.667 | 69.16 |
| Decolorization temperature 60°C | 0.257 | 88.12 |
| Decolorization temperature 80°C | 0.226 | 89.55 |
| Decolorization temperature 100°C | 0.306 | 85.85 |
| Decolorization temperature 120°C | 0.433 | 79.98 |
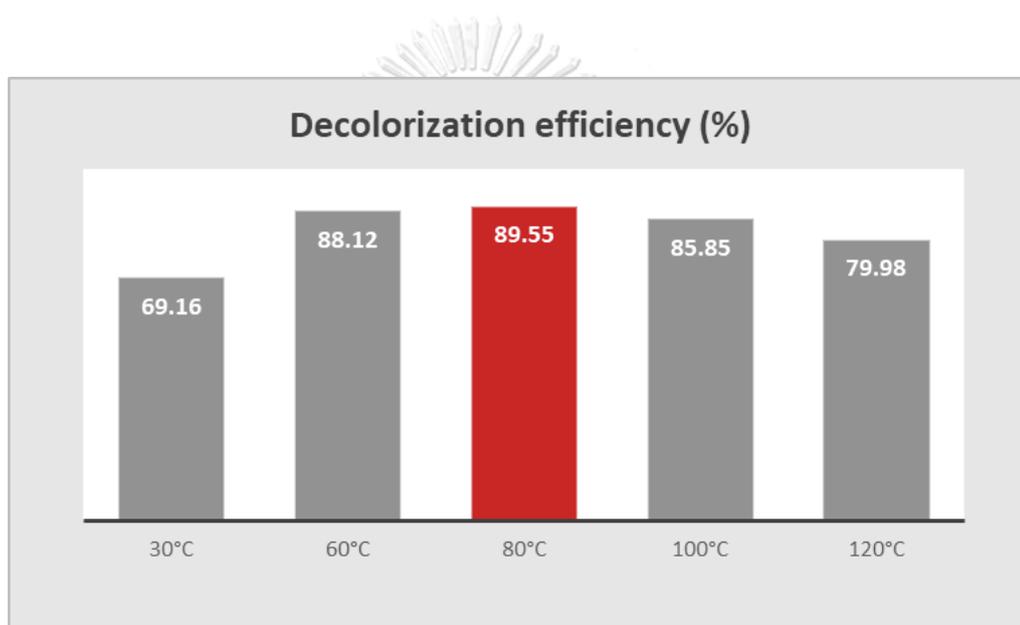


Figure 4.48 Variation of decolorization efficiency of AC-HCl with different temperatures

Table 4.19 and Figure 4.27 show decolorization efficiency of AC-NaOH with various temperatures, it was found that the intensity of color bodies greatly decreased with decolorize using AC-NaOH at maximum temperatures of 80°C with decolorization efficiency of 76.14%. Similarly, the trend of decolorization efficiency is also increased when increasing in reaction temperatures until it reaches a maximum then it commences to drop.

Table 4.25 Decolorization of AC-NaOH with various temperatures

| Description | Absorbance | Decolorization efficiency % |
|---|---|---|
| Decolorization temperature 30°C | 0.911 | 57.88 |
| Decolorization temperature 60°C | 0.765 | 64.63 |
| Decolorization temperature 80°C | 0.516 | 76.14 |
| Decolorization temperature 100°C | 0.713 | 67.04 |
| Decolorization temperature 120°C | 0.757 | 65.00 |
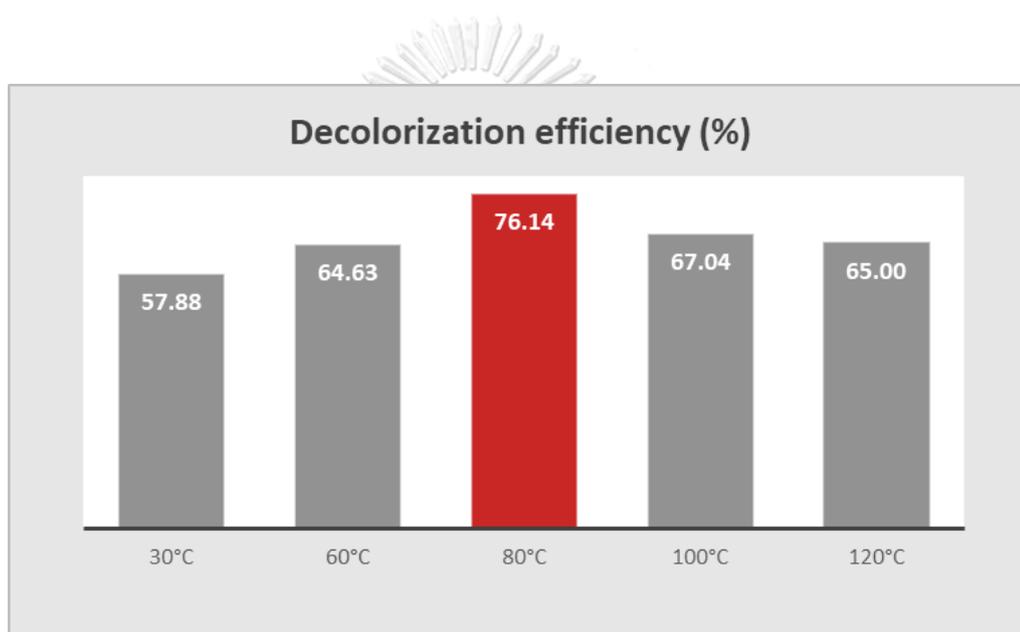


Figure 4.49 Variation of decolorization efficiency of AC-NaOH with different
temperatures

Table 4.20 and Figure 4.28 show decolorization efficiency of AC-KOH with various temperatures, it was found that the intensity of color bodies greatly decreased with decolorize using AC-KOH at maximum temperatures of 80°C with decolorization efficiency of 87.33%. Similarly, the trend of decolorization efficiency is also increased when increasing in reaction temperatures until it reaches a maximum then it commences to drop.

Table 4.26 Decolorization of AC-KOH with various temperatures

| Description | Absorbance | Decolorization efficiency % |
|---|---|---|
| Decolorization temperature 30°C | 0.757 | 65.00 |
| Decolorization temperature 60°C | 0.449 | 79.24 |
| Decolorization temperature 80°C | 0.274 | 87.33 |
| Decolorization temperature 100°C | 0.327 | 84.88 |
| Decolorization temperature 120°C | 0.331 | 84.70 |
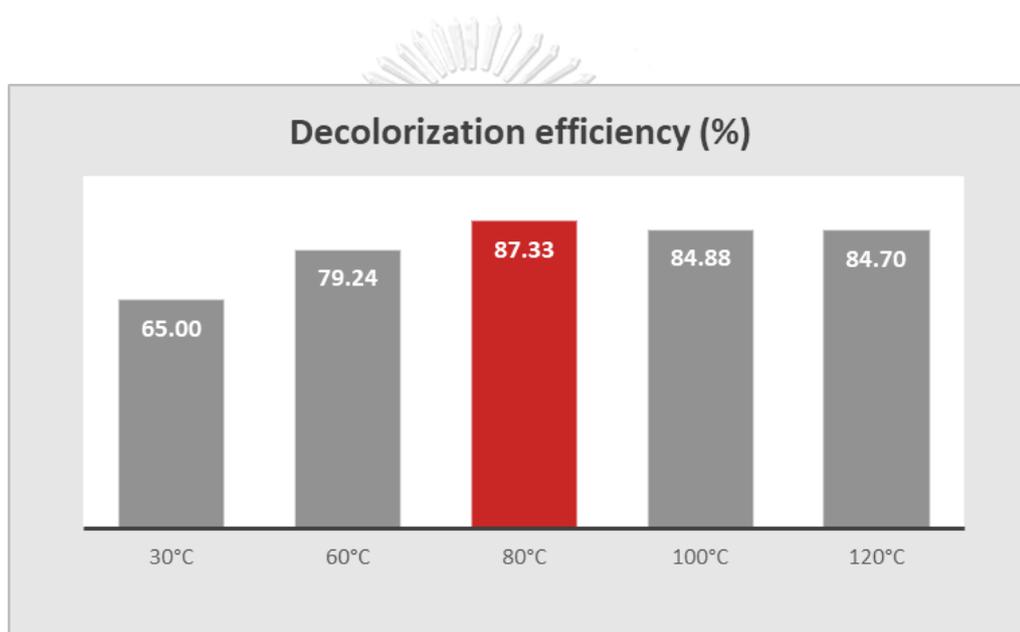


Figure 4.50 Variation of decolorization efficiency of AC-KOH with different temperatures

According to study in decolorization with various reaction temperatures, both acid-activated clays and alkali-activated clays can decolorize which attained highest decolorization efficiency at maximum temperature of 80°C then start to decrease. Likewise, it was also found that the decolorization efficiency trend is increase with increase in reaction temperature probably due to the increase of the velocity of molecules in solutions which increase contact between clay surface [9].

In summary, all previous experiments were carried out to determine the optimal conditions for the preparation of the activated clay from Ratchaburi bentonite and the pyrolysis oil decolorization of acid-activated clays and alkali-activated clays, it was found that the optimum condition for pyrolysis oil decolorization at 70 g of activated clay dosages and decolorization temperature of 80°C together with the reaction time of 2 h, which was achieved in all activated clays while the optimal conditions for the preparation of the activated clay were found at the bentonite clay to activation agent ratio of 1:2 (bentonite/$H_2SO_4$) with soaking time of 30 min, 1:1 (bentonite/HCl) with soaking time of 30 min, 1:1 (bentonite/NaOH) with soaking time of 30 min and 1:3 (bentonite/KOH) with soaking time of 60 min for AC-$H_2SO_4$, AC-HCl, AC-NaOH and AC-KOH respectively. The sample name of bleached pyrolysis oils with using the Ratchaburi bentonite and activated clays at optimum condition are shown in Table 4.21.

Table 4.27 The sample name of bleached pyrolysis oils

| Bleached pyrolysis oil | Sample name |
|---|---|
| Bleached pyrolysis oil using Ratchaburi bentonite | Oil/RCB |
| Bleached pyrolysis oil using AC-$H_2SO_4$ | Oil/AC-$H_2SO_4$ |
| Bleached pyrolysis oil using AC-HCl | Oil/AC-HCl |
| Bleached pyrolysis oil using AC-NaOH | Oil/AC-NaOH |
| Bleached pyrolysis oil using AC-KOH | Oil/AC-KOH |

For Table 4.22 is shown the oil retention values of activated clay, there are 23.99, 18.35, 24.60 and 22.53% for AC-$H_2SO_4$, AC-HCl, AC-NaOH and AC-KOH respectively that can be referred to loss of oil in activation process due to its retention in activated clay. The results present oil retention is in the specification of the Indian standard (IS 1965-1972), which is a maximum value of 35.00%.

Table 4.28 Oil retention of activated clays

| Activated clay | Oil retention % |
|----------------|-----------------|
| AC-$H_2SO_4$ | 23.99 |
| AC-HCl | 18.35 |
| AC-NaOH | 24.60 |
| AC-KOH | 22.53 |

4.3.4 Comparison in oil color with commercial diesel

Eventually, after success in optimizing conditions in activated clay preparation and pyrolysis oil decolorization that thereupon investigate double decolorizing pyrolysis oil and comparison in oil color with commercial diesel. Table 4.23 show that the absorbance of a variety of commercial diesel are values of 0.067, 0.081, 0.092 and 0.113 for Esso Hi Diesel, Supreme Plus Diesel, PTT Diesel B7 and Susco Diesel B7 respectively and bleached pyrolysis oils consist of Bleached 1 and Bleached 2, which are first bleaching and repeat bleaching respectively, it was found that the absorbance of Bleached 1 different from commercial diesel with values of 0.248, 0.226, 0.516 and 0.274 together with decolorization efficiency of 88.53, 89.55, 76.14 and 87.33% for AC-$H_2SO_4$, AC-HCl, AC-NaOH and AC-KOH respectively.

Furthermore, when the bleached pyrolysis oil was bleached again with fresh activated clay, the color of the pyrolysis oil is close to the color of commercial diesel as shown in the values of Bleached 2. The Bleached 2 is shown absorbance values, which were decreased continuously from Bleached 1 of 0.089, 0.086, 0.181 and 0.091 with sum up of decolorization efficiency of 95.89, 96.02, 91.63 and 95.79% for AC-$H_2SO_4$, AC-HCl, AC-NaOH and AC-KOH respectively, it can be seen that the absorbance of Bleached 2 is similar to commercial diesel.

Table 4.29 Benchmarking in oil color with commercial diesel

| Sample name | Absorbance | | | Decolorization efficiency (%) | |
|---|---|---|---|---|---|
| | Diesel | Bleached 1 | Bleached 2 | Bleached 1 | Bleached 2 |
| Esso Hi Diesel | 0.067 | - | - | - | - |
| Supreme Plus Diesel | 0.081 | - | - | - | - |
| PTT Diesel B7 | 0.092 | - | - | - | - |
| Susco Diesel B7 | 0.113 | - | - | - | - |
| Oil/RCB | - | 1.082 | 0.520 | 49.98 | 75.96 |
| Oil/AC-$H_2SO_4$ | - | 0.248 | 0.089 | 88.53 | 95.89 |
| Oil/AC-HCl | - | 0.226 | 0.086 | 89.55 | 96.02 |
| Oil/AC-NaOH | - | 0.516 | 0.181 | 76.14 | 91.63 |
| Oil/AC-KOH | - | 0.274 | 0.091 | 87.33 | 95.79 |

Although, when the first time of decolorization of pyrolysis oil, it will obtain a slightly different color from commercial diesel, while the decolorization efficiency is in the specification of the Indian standard (IS 1965-1972). The requirement for decolorization efficiency from classified by Indian standard is a minimum value of 85.00%. Excluding AC-NaOH that has the first time of decolorization efficiency less than 85.00%. In addition, when the bleached pyrolysis oil was decolorized again with fresh activated clay, the decolorization efficiency of all activated clay is more than specification which identified by Indian standard as shown in Figure 4.29. Overall decolorization efficiency indicates that the activated clay is a high performance in decolorizing more than original bentonite clay because activated clay has been modified to increase the specific surface area and porosity by chemical activation. When considering activated clay also found AC-$H_2SO_4$, AC-HCl, and AC-KOH provide similar decolorization efficiency while AC-NaOH shows the lowest decolorization efficiency as according to activating with NaOH shown the lowest specific surface area.
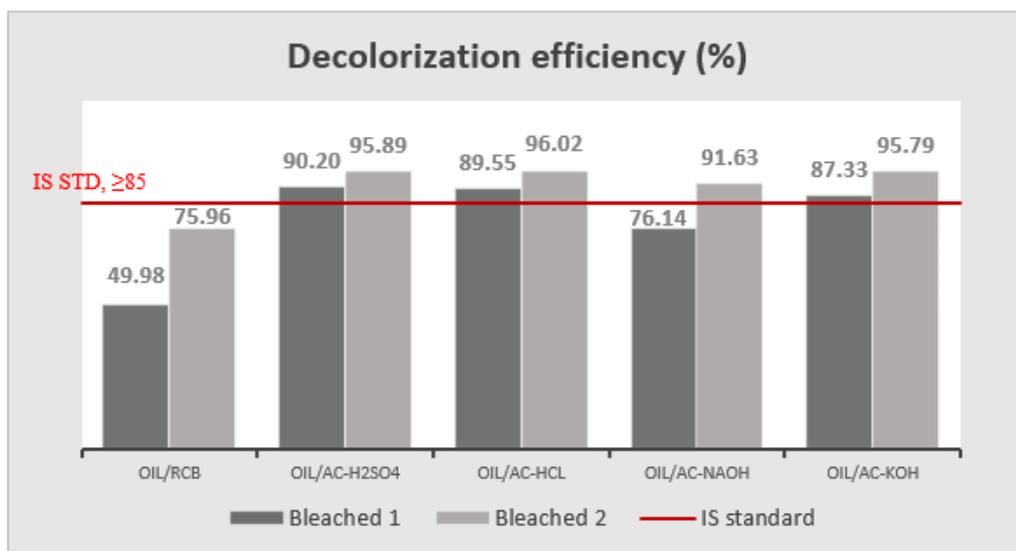
Figure 4.51 Comparison of decolorization efficiency with IS standard

Figure 4.30 shows the oil color of various commercial diesel consist of Esso Hi Diesel, Supreme Plus Diesel, PTT Diesel B7 and Susco Diesel B7 respectively, it can be observed that the color of all commercial diesel present in a light color. Figure 4.31 and Figure 4.32 are shown the color of the first bleached pyrolysis oil and second bleached pyrolysis oil respectively. It can be clearly seen that the color of all the first bleached pyrolysis oils is still slightly different from commercial diesel, while the color of the second bleached pyrolysis oils, which was re-bleaching, gives its color oil similar to diesel. To summarize, it can be indicated that the activated clays produced from Ratchaburi bentonite were achieved to decolorize the pyrolysis oil close to commercial diesel. However, activated clay activating with NaOH showed lower decolorization efficiency for the first bleaching. Because this activated clay has lowest surface area and highest CEC, which meant a lower exchange cation due to some part of sodium forming plagioclase (P peak) (Figure 4.11) as sodium-aluminum-silicate ($NaAlSiO_8$).
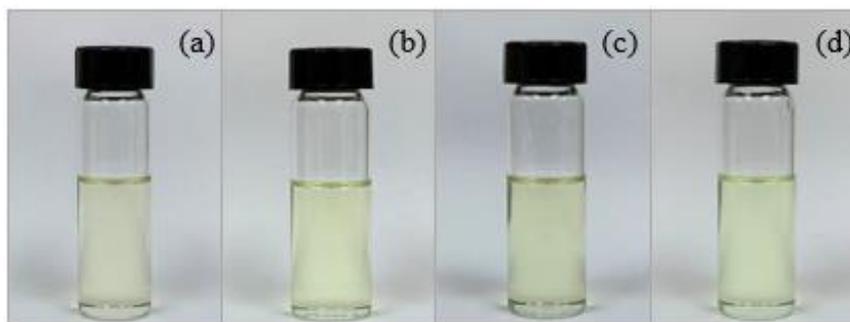
Figure 4.52 Commercial diesel

(a) Esso Hi Diesel, (b) Supreme Plus Diesel, (c) PTT Diesel B7, (d) Susco Diesel B7
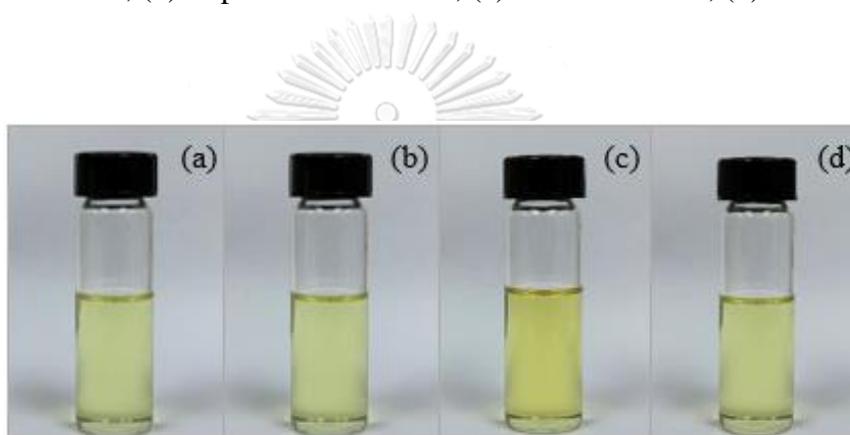


Figure 4.53 First bleached pyrolysis oil of activated clay

(a) Oil/AC-$H_2SO_4$, (b) Oil/AC-HCl, (c) Oil/AC-NaOH, (d) Oil/AC-KOH
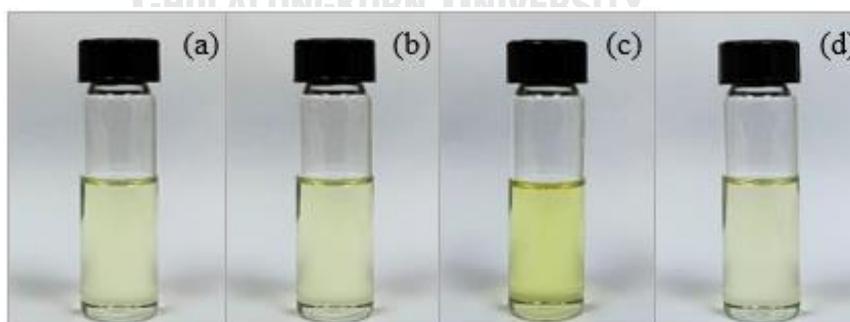


Figure 4.54 Second bleached pyrolysis oil of activated clay

(a) Oil/AC-$H_2SO_4$, (b) Oil/AC-HCl, (c) Oil/AC-NaOH, (d) Oil/AC-KOH

4.3.5 Adsorption isotherm

In this research, Langmuir isotherms and Freundlich isotherms were used to consider the adsorption characteristics of activated clays for pyrolysis oil decolorization. It is shown in Figure 4.33 to 4.36 that the activated clay adsorption isotherms correspond to both Langmuir isotherms and Freundlich isotherms, which achieved in both activated clays include acid-activated clays and alkali-activated clays. It can be identified from the coefficient of determination ($R^2$) value is closer to 1. From this studied, the $R^2$ of Langmuir isotherms and Freundlich isotherms for all activated clays there are 0.6652 and 0.8083 for AC-$H_2SO_4$, 0.9683 and 0.8786 for AC-HCl, 0.9909 and 0.9733 for AC-NaOH and 0.9898 and 0.9489 for AC-KOH.

Accordingly, the adsorption isotherm of activated clay, which is produced from Ratchaburi bentonite follows Langmuir isotherms for activated clay activated by HCl, NaOH and KOH. It was concluded that the exchange cation in clay and monoacid or alkali was formed in the monolayer during the development of the surface area. While activating with $H_2SO_4$ was consistent with Freundlich isotherm, which performs multilayer due to several exchange cations of diacid.
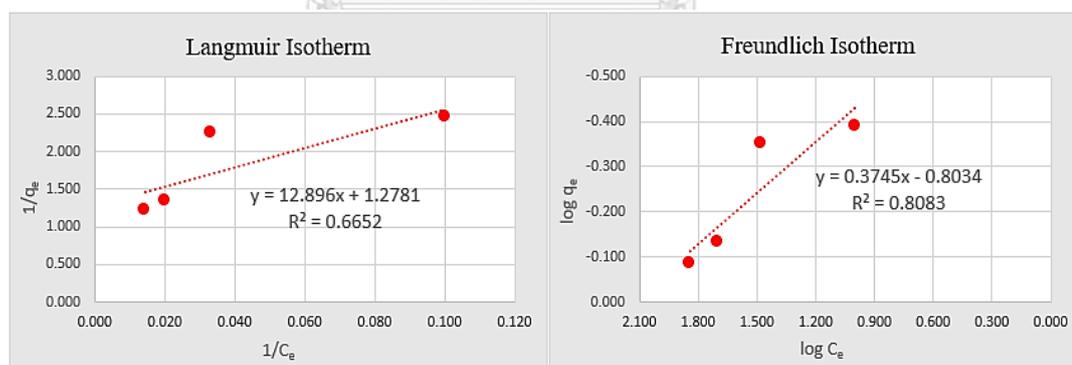


Figure 4.55 Adsorption isotherm of AC-$H_2SO_4$
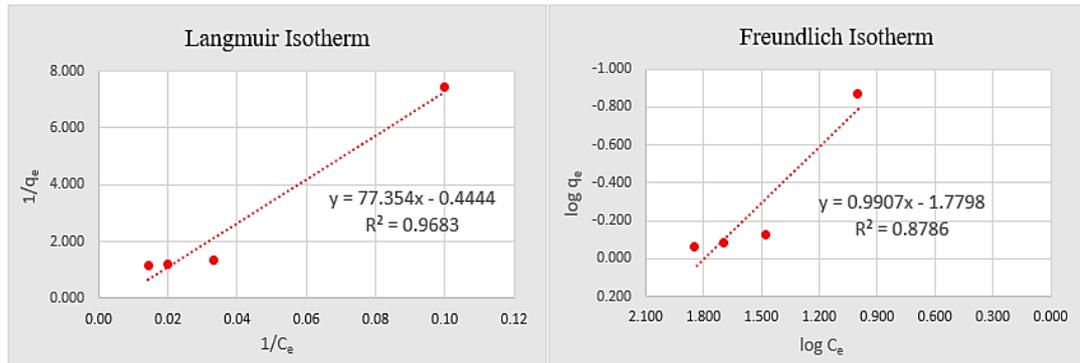
Figure 4.56 Adsorption isotherm of AC-HCl
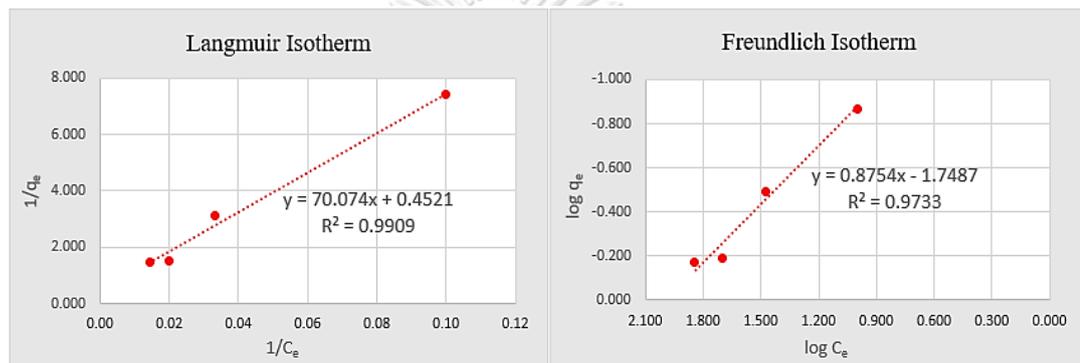


Figure 4.57 Adsorption isotherm of AC-NaOH
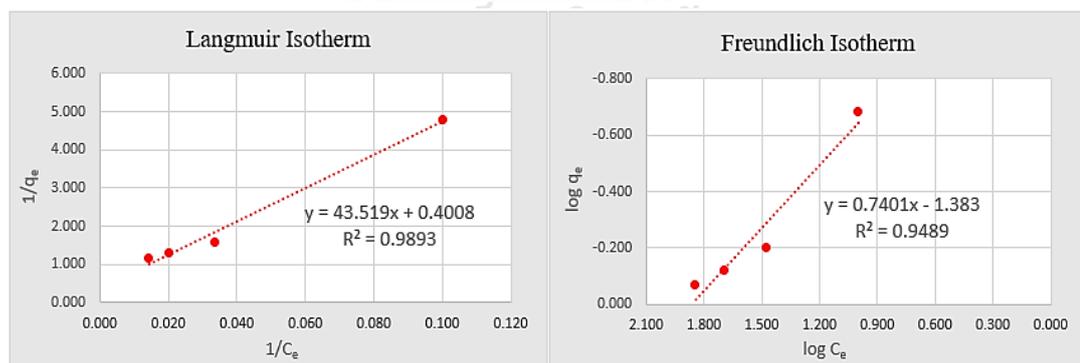


Figure 4.58 Adsorption isotherm of AC-KOH

**4.4 Regeneration of Spent Activated Clay**

4.4.1 Regenerated spent activated clay

In this section, the spent activated clays were obtained from pyrolysis oil decolorization by using acid-activated clays and alkali-activated clays include AC-$H_2SO_4$, AC-HCl, AC-NaOH and AC-KOH to decolorize pyrolysis oil. Spent activated clays were regenerated by the direct heat-treatment process with various temperatures of 400, 500 and 800°C. Figures 4.37 and 4.38 are shown spent activated clays and regenerated spent activated clays respectively, it shows that the appearance color of regenerated spent activated clays is completely different from initial spent activated clays and fresh activated clays because of organic compounds as the color bodies in pyrolysis oil that are absorbed in the spent activated clay structure turned into char and ash was produced.
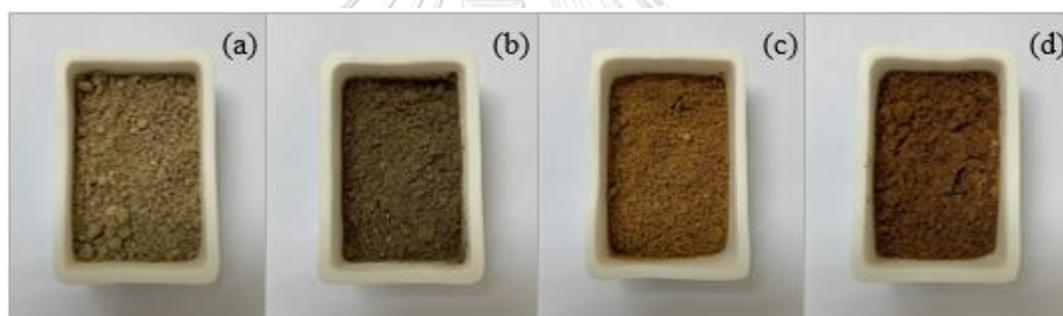


Figure 4.59 Spent activated clay

(a) SC-$H_2SO_4$, (b) SC-HCl, (c) SC-NaOH, (d) SC-KOH
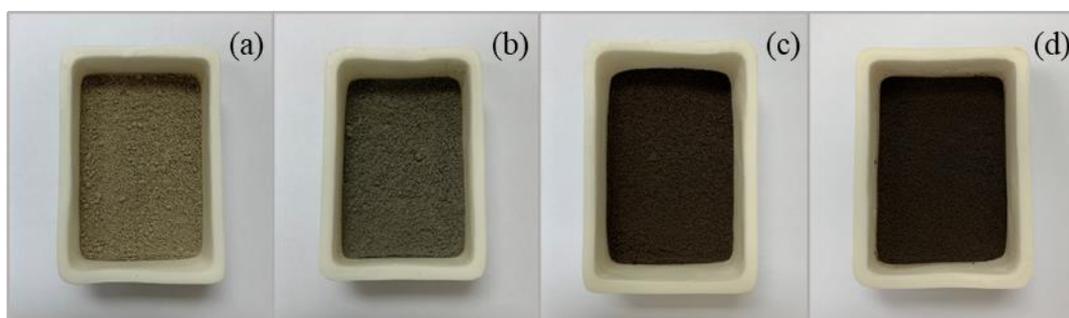


Figure 4.60 Regenerated spent activated clay

(a) RC-H2SO4, (b) RC-HCl, (c) RC-NaOH, (d) RC-KOH

The yield of regenerated spent activated clays which obtained from regeneration process are shown in Table 4.24 these indicate when increasing in regenerated temperature the yield is decreased, it clearly shows that yield of both acid-activated clays and alkali-activated clay is the lowest at high temperature caused by mass loss of decomposition and loss of volatile, there are loss of adsorbed water at temperatures of 100-200°C, loss of water molecules occupied interlamellar at temperatures of 475-525°C, de-hydroxylation of montmorillonite at temperatures of 600-700°C and temperatures of 875-950°C, there is resulting in structural change of montmorillonite minerals [1].

Table 4.30 Yield of regenerated spent activated clays

| Sample Name | Yield % |
|---|---|
| RC-$H_2SO_4$ (400°C) | 67.41 |
| RC-$H_2SO_4$ (500°C) | 65.02 |
| RC-$H_2SO_4$ (800°C) | 62.92 |
| RC-HCl (400°C) | 74.97 |
| RC-HCl (500°C) | 71.28 |
| RC-HCl (800°C) | 68.49 |
| RC-NaOH (400°C) | 70.49 |
| RC-NaOH (500°C) | 69.92 |
| RC-NaOH (800°C) | 60.38 |
| RC-KOH (400°C) | 60.38 |
| RC-KOH (500°C) | 58.82 |
| RC-KOH (800°C) | 57.27 |

4.4.2 $N_2$ physisorption analysis of regenerated spent activated clay

The results in Table 4.25 and Figures 4.39, after regeneration the BET specific surface area and total pore volume which were determined by $N_2$ physisorption analysis of all regenerated spent activated clays were increased up to 500°C and then dropped at a temperature of 800°C, it can be indicated that the suitable temperature

for regeneration of all spent activated clays is 500°C while the BET specific surface area and total pore volume were still lower than fresh activated clay, which was previous studied, with the values decreased from 182 to 120 $m^2/g$ and 0.423 to 0.348 $cm^3/g$ for RC-$H_2SO_4$ $cm^3/g$, 144 to 98 $m^2/g$ and 0.324 to 0.221 $cm^3/g$ for RC-HCl, 119 to 69 m2/g and 0.286 to 0.260 $cm^3/g$ for RC-NaOH and 150 to 111 $m^2/g$ and 0.397 to 0.350 $cm^3/g$ for RC-KOH. The decrease in BET specific surface area and total pore volume at high temperature is caused by pore collapse and thermal decomposition which damages the structure [h]. Besides activated clay prepares by using NaOH shows the lowest specific surface area due to lowest surface area of fresh prepared activated clay whereas $H_2SO_4$, HCl and KOH have similar results.

Table 4.31 $N_2$ physisorption analysis of regenerated spent activated clays

| Sample Name | BET | Pore Volume | Average Pore Size |
|---|---|---|---|
| | m2/g | cm³/g | nm |
| RC-$H_2SO_4$ (400°C) | 92 | 0.301 | 9.49 |
| RC-$H_2SO_4$ (500°C) | 120 | 0.348 | 9.54 |
| RC-$H_2SO_4$ (800°C) | 108 | 0.303 | 8.90 |
| RC-HCl (400°C) | 80 | 0.198 | 7.23 |
| RC-HCl (500°C) | 98 | 0.221 | 7.12 |
| RC-HCl (800°C) | 97 | 0.222 | 7.16 |
| RC-NaOH (400°C) | 30 | 0.151 | 16.38 |
| RC-NaOH (500°C) | 69 | 0.260 | 12.24 |
| RC-NaOH (800°C) | 50 | 0.179 | 12.31 |
| RC-KOH (400°C) | 104 | 0.313 | 12.03 |
| RC-KOH (500°C) | 111 | 0.350 | 9.55 |
| RC-KOH (800°C) | 101 | 0.322 | 12.69 |
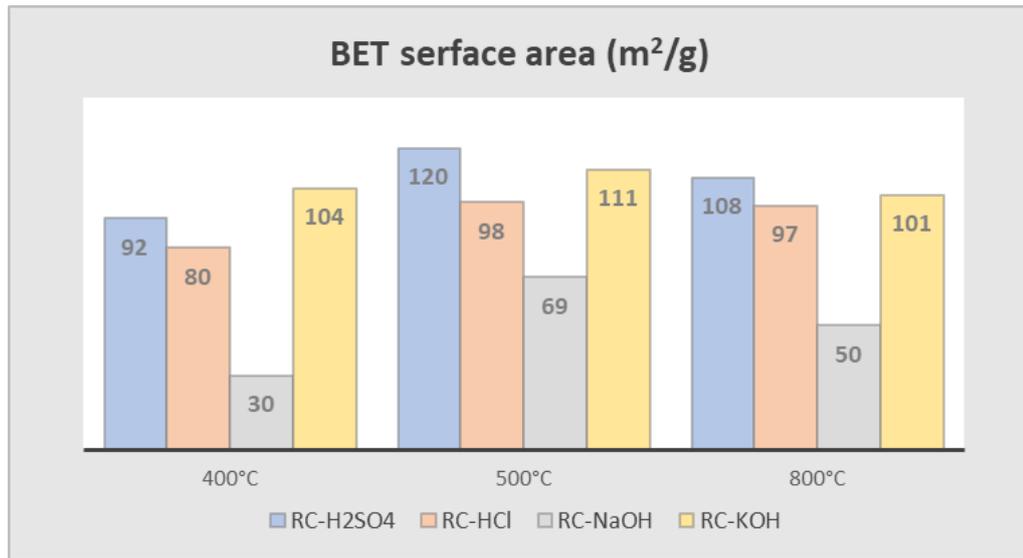
Figure 4.61 BET analysis of regenerated spent activated clays

The $N_2$ adsorption isotherm of regenerated spent activated clays as shown in Figures 4.40 was found in type IV with the hysteresis loop seems to combine between H1 and H3 for RC-$H_2SO_4$ and RC-HCl, it shows cylinder-shaped with wedge-shaped pore while RC-NaOH shows the hysteresis loop seems to H3, wedge-shaped pore AC-KOH was to be evident in hysteresis loop seem to type H1, it shows cylinder-shaped pore. This indicates that the adsorption isotherm and hysteresis loop are retained the same characteristics as fresh activated clay.
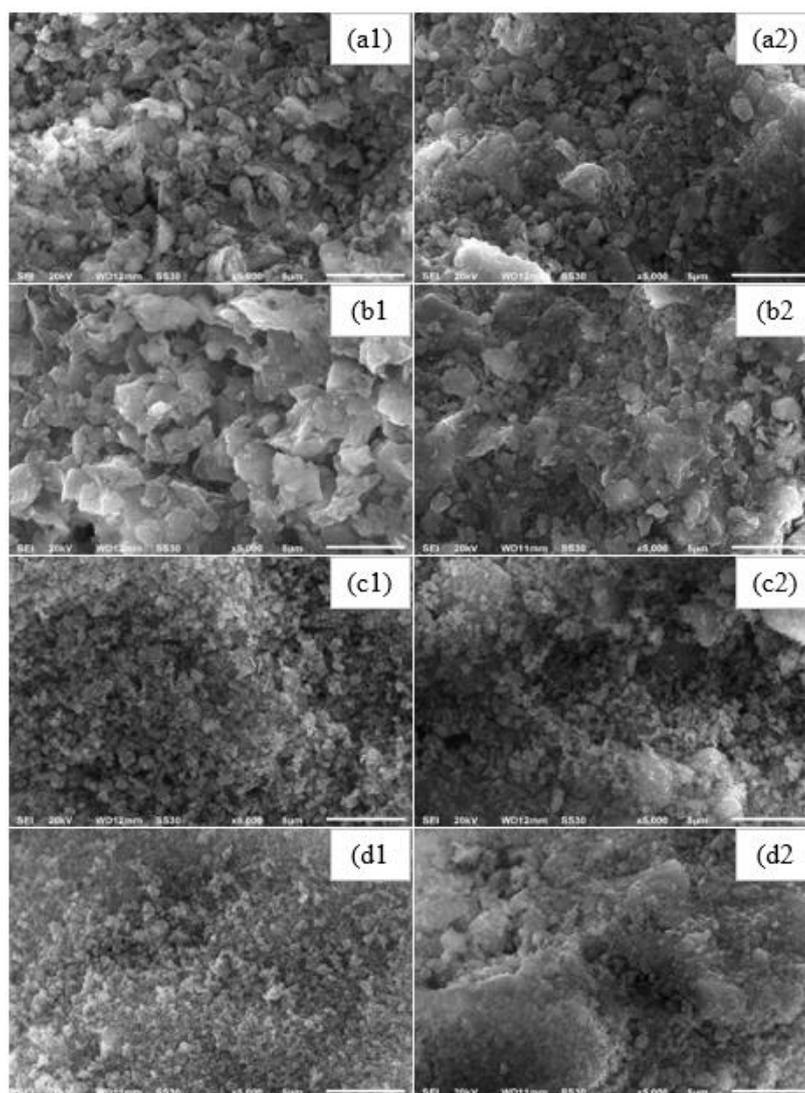
Figure 4.62 Scanning electron micrographs of regenerated spent activated
clays

(a1) AC-H$_2$SO$_4$, (a2) RC-H$_2$SO$_4$, (b1) AC-HCl, (b2) RC-HCl, (c1) AC-NaOH,
(c2) RC-NaOH, (d1) AC-KOH, (d2) RC-KOH

4.4.4 Pyrolysis oil decolorization of spent activated clay

Pyrolysis oil decolorization of regenerated spent activated clays were
investigated as following to activated clay, including the optimum condition for
pyrolysis oil decolorization at 70 g of activated clay dosages and decolorization
temperature of 80°C together with the reaction time of 2 h with various regenerated
spent activated clay that calcined at 400, 500 and 800°C as shown in Table 4.26 and

Figure 4.42. The results are achieved that the temperature of 500°C was found to be the highest decolorization efficiency meanwhile decreasing at high temperature is 800°C because of calcinating at high temperature resulting in structural destruction and pore collapse make the regenerated activated clay to low specific surface area as according in $N_2$ adsorption analysis, it indicated the temperature of 500°C is the optimum temperature for decolorize pyrolysis oil. Likewise, it was also found RC-NaOH provide the least decolorizing performance which is directly proportional to the specific surface area that show the lowest specific surface area in activating with NaOH.

Table 4.32 Pyrolysis oil decolorization of regenerated spent activated clays

| Sample Name | Absorbance | Decolorization efficiency % |
|---|---|---|
| RC-$H_2SO_4$ (400°C) | 1.471 | 31.99 |
| RC-$H_2SO_4$ (500°C) | 0.372 | 82.80 |
| RC-$H_2SO_4$ (800°C) | 0.478 | 77.90 |
| RC-HCl (400°C) | 1.687 | 22.01 |
| RC-HCl (500°C) | 0.426 | 80.31 |
| RC-HCl (800°C) | 0.694 | 67.91 |
| RC-NaOH (400°C) | 1.570 | 27.42 |
| RC-NaOH (500°C) | 1.233 | 43.00 |
| RC-NaOH (800°C) | 1.282 | 40.73 |
| RC-KOH (400°C) | 0.678 | 68.65 |
| RC-KOH (500°C) | 0.571 | 73.60 |
| RC-KOH (800°C) | 0.469 | 78.32 |
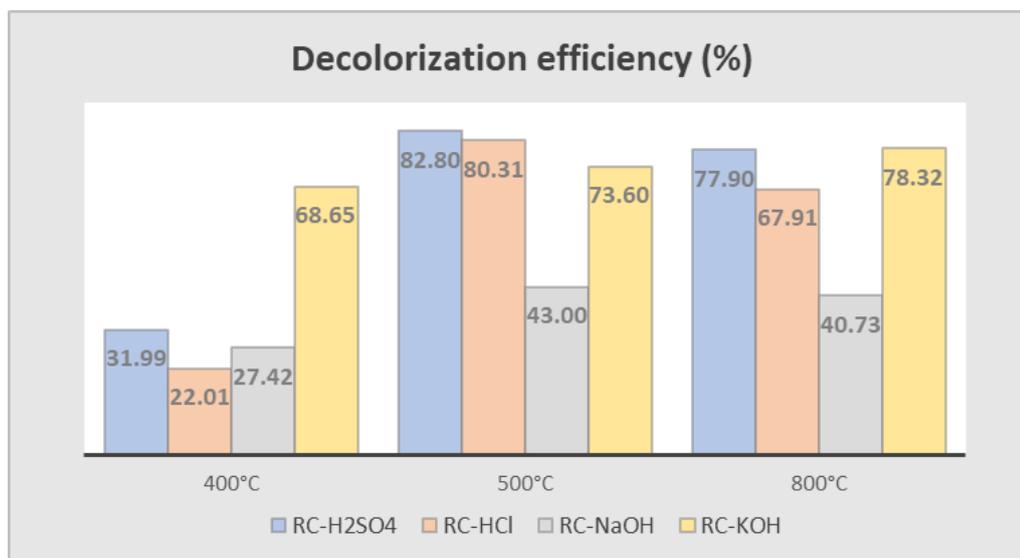
Figure 4.63 Variation of decolorization efficiency of regenerated clay with different temperatures

Table 4.27 and Figure 4.43, comparison of decolorization efficiency between non-regenerated spent activated clays and regenerated spent activated clay, it evidently to observed the regeneration process is precious to confirm that recycle the waste spent activated clays which low decolorization efficiency come into high decolorization efficiency because calcination is remove the oil and impurities that cover the pore. The decolorization efficiency that compared with non-regenerated spent activated clays was increased from 47.02 to 82.80% for RC-$H_2SO_4$, 56.73 to 80.31% for RC-HCl, 21.96 to 43.00% for RC-NaOH and 42.53 to 78.32% for RC-KOH.

Table 4.33 Decolorization efficiency of regenerated and non-regenerated clay

| Sample Name | Absorbance | Decolorization efficiency % |
|---|---|---|
| SC-$H_2SO_4$ | 1.146 | 47.02 |
| SC-HCl | 0.936 | 56.73 |
| SC-NaOH | 1.688 | 21.96 |
| SC-KOH | 1.243 | 42.53 |
| RC-$H_2SO_4$ (500°C) | 0.372 | 82.80 |
| RC-HCl (500°C) | 0.426 | 80.31 |
| RC-NaOH (500°C) | 1.233 | 43.00 |
| RC-KOH (500°C) | 0.469 | 78.32 |
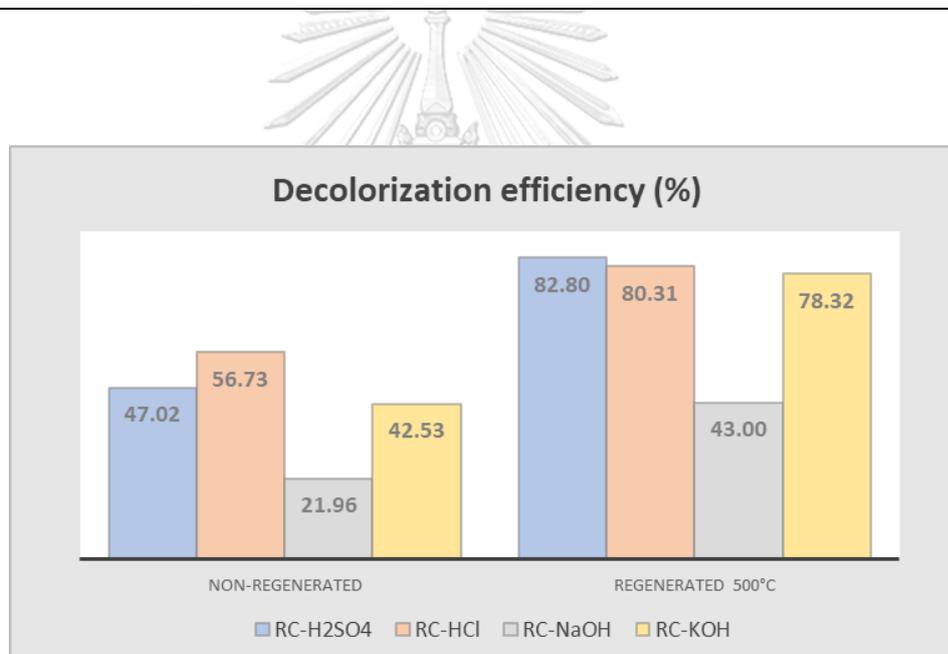


Figure 4.64 Comparison of decolorization efficiency with non-regenerated clay

Base on achieved in the study about optimum temperature for the regeneration process, the regeneration of spent activated clays from both acid-activated clay and alkali-activated clay were accomplished in regenerate by the direct heat-treatment process at a temperature of 500°C and its trend to decrease regeneration performance when increase temperature as a consequence of pore collapse and damage in the structure thus reducing specific surface area and porosity together with also reducing

decolorization efficiency. The sample name of bleached pyrolysis oil using the regenerated activated clays at optimum temperature, which was obtained at a temperature of 500°C is shown in Table 4.28.

Table 4.34 The sample name of bleached pyrolysis oils

| Bleached pyrolysis oil | Sample name |
|---|---|
| Bleached pyrolysis oils using RC-H$_2$SO$_4$ | Oil/RC-H$_2$SO$_4$ |
| Bleached pyrolysis oils using RC-HCl | Oil/RC-HCl |
| Bleached pyrolysis oils using RC-NaOH | Oil/RC-NaOH |
| Bleached pyrolysis oils using RC-KOH | Oil/RC-KOH |

Table 4.29 show that the bleached pyrolysis oils consist of Bleached 1 and Bleached 2, which are first bleaching and repeat bleaching respectively, it was found that the absorbance of Bleached 1 is shown values of 0.372, 0.426, 1.233 and 0.469 together with decolorization efficiency of 82.80, 80.31, 43.00 and 78.32% for RC-H$_2$SO$_4$, RC-HCl, RC-NaOH and RC-KOH respectively. Additionally, when the bleached pyrolysis oil was bleached again with fresh spent activated clay resulting in increased decolorization efficiency as shown in the values of Bleached 2 in Table 4.29. The Bleached 2 is shown sum up absorbance values of 0.198, 0.164, 0.658 and 0.285 with sum up of decolorization efficiency of 90.85, 92.42, 69.58 and 86.385% for RC-H$_2$SO$_4$, RC-HCl, RC-NaOH and RC-KOH respectively,

Table 4.35 Pyrolysis oil decolorization of regenerated spent activated clay

| Sample name | Absorbance | | Decolorization efficiency (%) | |
|---|---|---|---|---|
| | Bleached 1 | Bleached 2 | Bleached 1 | Bleached 2 |
| Oil/RC-H$_2$SO$_4$ | 0.372 | 0.198 | 82.80 | 90.85 |
| Oil/RC-HCl | 0.426 | 0.164 | 80.31 | 92.42 |
| Oil/RC-NaOH | 1.233 | 0.658 | 43.00 | 69.58 |
| Oil/RC-KOH | 0.469 | 0.285 | 78.32 | 86.85 |

However, when the comparison between the bleached pyrolysis oil was decolorized with fresh regenerated activated clay and Indian standard, it obtained the decolorization efficiency of regenerated spent activated clays in Bleached 2 is in the specification of the Indian standard (IS 1965-1972) as shown in Figure 4.44, excluding RC-NaOH that show a value is out of specification. Consequently, it can be demonstrated that the spent activated clays consist of SC-H$_2$SO$_4$, SC-HCl and SC-KOH achieved in regeneration to recovery for reuse in pyrolysis oil decolorization while SC-NaOH shows low performance to recovery in the regeneration process due to lowest specific surface area of fresh prepared activated clay.
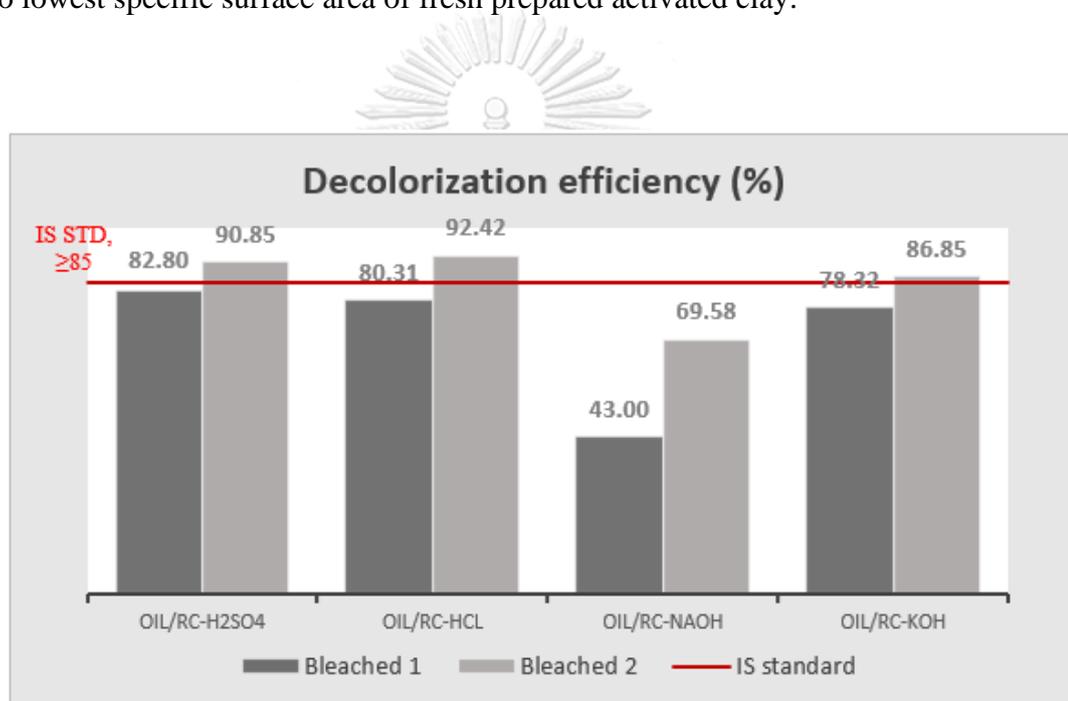


Figure 4.65 Comparison of decolorization efficiency with IS standard
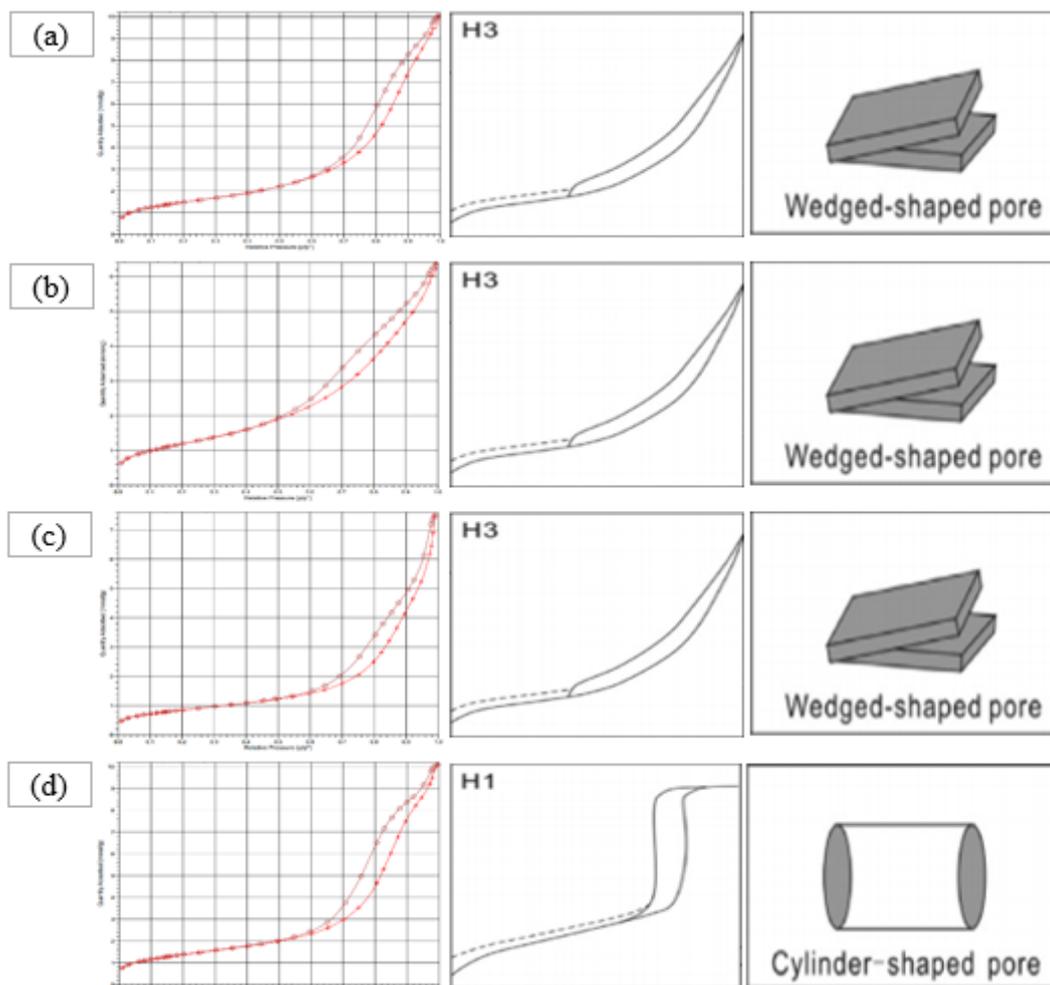
Figure 4.66 N$_2$ adsorption isotherm of regenerated spent activated clays
(a) RC-H$_2$SO$_4$, (b) RC-HCl, (c) RC-NaOH, (d) RC-KOH

### 4.4.3 Morphological characteristic of spent activated clay

The characteristics of the regenerated spent activated clays surface after calcined at a temperature of 500°C was investigated by using scanning electron microscopy as shown in Figure 4.41. The resulting images at a magnification of 5000 that comparison between activated clay and regenerated spent activated clays, it shows the regenerated spent activated clays surface remains rougher and porous but less than the fresh activated clay which corresponds to the pore collapse after calcination.
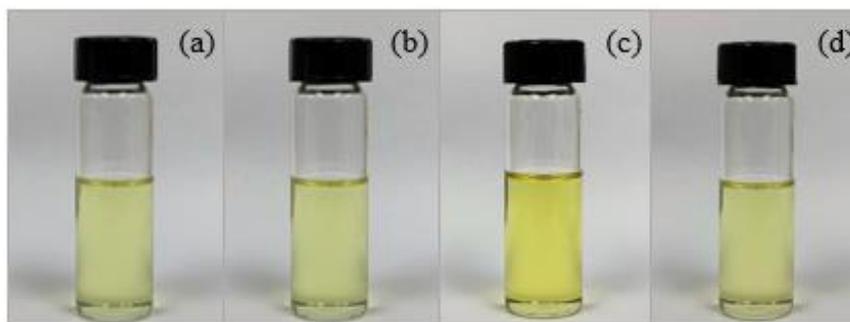
Figure 4.67 Second bleached pyrolysis oil of regenerated spent activated clay

(a) Oil/RC-H$_2$SO$_4$, (b) Oil/RC-HCl, (c) Oil/RC-NaOH, (d) Oil/RC-KOH

4.4.5 Repeated regeneration performance of spent activated clay

Furthermore, the regenerated spent activated clays at optimum regenerated condition, which was obtained at the optimum temperature of 500°C, were also investigated repetition in the regeneration process to study the number of times in regeneration for reuse in pyrolysis oil decolorization. In this study, the spent activated clays were recovery five times by calcinating at a temperature of 500°C and used as adsorbents in pyrolysis oil decolorization then take the spent activated clay this time to calcinating at a temperature of 500°C and apply to pyrolysis oil decolorization again, doing this for five times. The decolorization efficiency decreases when increase repeated recovery times caused by structural and pore more destruction as shown in Table 4.30.

Meanwhile, the first time of recovery of RC-H$_2$SO$_4$, RC-HCl and RC-KOH were found that decolorization efficiency is in the specification of the Indian standard (IS 1965-1972) but still have a slightly lower value than the fresh activated clay. Additionally, it can be demonstrated in decreasing in decolorization efficiency of the RC-NaOH show extremely decreased recovery performance as shown Figure 4.46.

Table 4.36 Decolorization efficiency with repeated regeneration

| Sample Name | Absorbance | | Decolorization efficiency (%) | |
|---|---|---|---|---|
| | Bleached 1 | Bleached 2 | Bleached 1 | Bleached 2 |
| RC-H$_2$SO$_4$ (500°C)_Re1 | 0.372 | 0.198 | 82.80 | 90.85 |
| RC-H$_2$SO$_4$ (500°C)_Re2 | 0.478 | 0.289 | 77.90 | 86.64 |
| RC-H$_2$SO$_4$ (500°C)_Re3 | 0.662 | 0.361 | 69.39 | 83.31 |
| RC-H$_2$SO$_4$ (500°C)_Re4 | 0.555 | 0.308 | 74.34 | 85.78 |
| RC-H$_2$SO$_4$ (500°C)_Re5 | 0.677 | 0.439 | 68.70 | 79.73 |
| RC-HCl (500°C)_Re1 | 0.426 | 0.164 | 80.31 | 92.42 |
| RC-HCl (500°C)_Re2 | 0.595 | 0.328 | 72.49 | 84.86 |
| RC-HCl (500°C)_Re3 | 0.782 | 0.441 | 63.85 | 79.61 |
| RC-HCl (500°C)_Re4 | 0.694 | 0.447 | 67.91 | 79.33 |
| RC-HCl (500°C)_Re5 | 0.690 | 0.375 | 68.10 | 82.66 |
| RC-NaOH (500°C)_Re1 | 1.233 | 0.658 | 43.00 | 69.58 |
| RC-NaOH (500°C)_Re2 | 1.309 | 0.755 | 39.48 | 65.12 |
| RC-NaOH (500°C)_Re3 | 1.432 | 0.916 | 33.80 | 57.65 |
| RC-NaOH (500°C)_Re4 | 1.409 | 0.905 | 34.86 | 58.18 |
| RC-NaOH (500°C)_Re5 | 1.579 | 0.890 | 27.00 | 58.88 |
| RC-KOH (500°C)_Re1 | 0.469 | 0.285 | 78.32 | 86.85 |
| RC-KOH (500°C)_Re2 | 0.575 | 0.318 | 73.42 | 85.32 |
| RC-KOH (500°C)_Re3 | 0.569 | 0.385 | 73.69 | 82.22 |
| RC-KOH (500°C)_Re4 | 0.678 | 0.439 | 68.65 | 79.70 |
| RC-KOH (500°C)_Re5 | 0.609 | 0.355 | 71.84 | 83.61 |
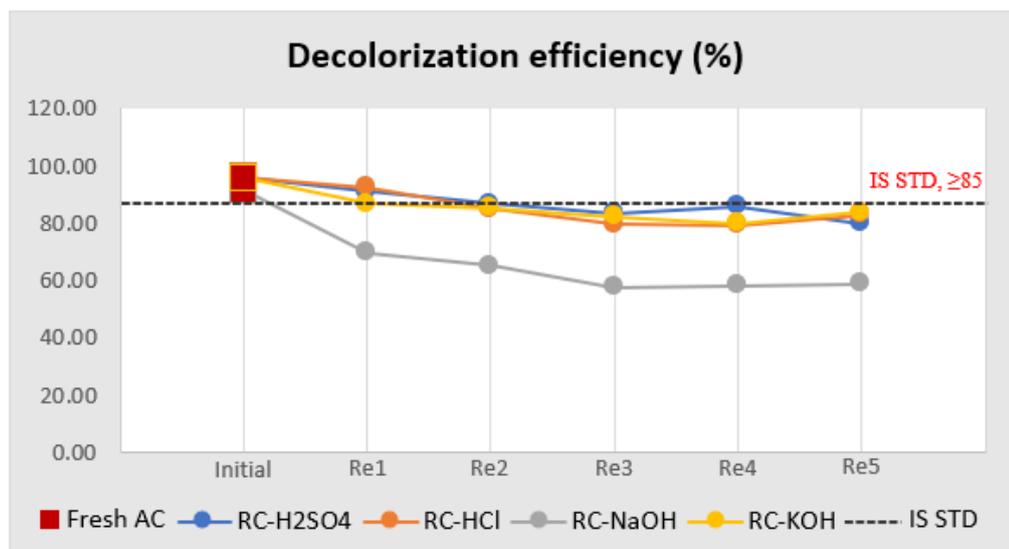
Figure 4.68 Variation of decolorization efficiency of regenerated clay with repeated recovery time

Overall study in this research about local bentonite clay, the Ratchaburi bentonite was particularly interesting to be activated to produce the activated clay by activated with both acid and alkali substances including $H_2SO_4$, HCl, NaOH and KOH as well as a study on its performance as an adsorbent in decolorization together with also study regeneration for recovery spent activated clay.

Eventually, achievement in this research found that the Ratchaburi bentonite can be activated with $H_2SO_4$, HCl, NaOH and KOH and also use as an adsorbent which provided the same excellent performance. After activation, it changed to higher specific surface area and higher decolorization efficiency. While in the part of regeneration, the activated clay prepares by using NaOH shows low regeneration performance due to lowest specific surface area of fresh prepared activated clay, whereas the activated clay prepared by using $H_2SO_4$, HCl and KOH can be regenerated twice.

**CHAPTER V**

**CONCLUSIONS**

**5.1    Conclusions**

Activated clays have been successfully prepared from the Ratchaburi bentonite by acid-activation process and alkali-activation process which were used $H_2SO_4$, HCl, NaOH and KOH solutions as an activation agent. The Ratchaburi bentonite can be converted into a potential adsorbent for the pyrolysis oil decolorization process. Both activations were modified bentonite structure and improved adsorption capacity with increasing in the specific surface area of activated clays to more than initial bentonite and can efficiently decolorize pyrolysis oil for removal color bodies and other impurities which were conducted to oil color benchmarking with commercial diesel together with attained in the color of pyrolysis oil similar to commercial diesel. The achieve in this research could be concluded are as follows;

1. The optimum condition for acid-activated clays preparation from the Ratchaburi bentonite were consisted of;
    a) AC-$H_2SO_4$ was obtained bentonite clay to activation agent ratio of 1:2 (bentonite/$H_2SO_4$), activation temperature of $100\pm5°C$ with soaking time of 30 min together with specific surface area and total pore volume of 182 m$^2$/g and 0.423 cm³/g, decolorization efficiency of 95.86%
    b) AC-HCl was obtained bentonite clay to activation agent ratio of 1:1 (bentonite/HCl), activation temperature of $100\pm5°C$ with soaking time of 30 min together with specific surface area and total pore volume of 144 m$^2$/g and 0.324 cm³/g, decolorization efficiency of 96.02%
2. The optimum condition for alkali-activated clays preparation from the Ratchaburi bentonite were consisted of;
    a) AC-NaOH was obtained bentonite clay to activation agent ratio of 1:1 (bentonite/NaOH), activation temperature of $100\pm5°C$ with soaking

time of 30 min together with specific surface area and total pore volume of 119 $m^2$/g and 0.286 $cm^3$/g, decolorization efficiency of 91.63%

b) AC-KOH was obtained bentonite clay to activation agent ratio of 1:3 (bentonite/KOH), activation temperature of 100±5°C with soaking time of 60 min together with specific surface area and total pore volume of 150 $m^2$/g and 0.397 $cm^3$/g, decolorization efficiency of 95.79%

3. The optimum condition for pyrolysis oil decolorization of acid-activated clays and alkali-activated clays together with success in oil color similar to commercial diesel was decolorized at 70 g oil of activated clay dosages per 100 ml and decolorization temperature of 80±5°C with decolorization time of 2 h.

4. The adsorption isotherm of activated clay, which is produced from Ratchaburi bentonite follows Langmuir isotherms for activated clay activated by HCl, NaOH and KOH with Langmuir coefficient of determination ($R^2$) of 0.9683, 0.9909 and 0.9898 respectively. While activating with $H_2SO_4$ was consistent with Freundlich isotherm include Freundlich coefficient of determination ($R^2$) of 0.8083.

5. Accomplished in the regeneration of spent activated clays by the direct heat-treatment process at the optimum temperature of 500°C. SC-$H_2SO_4$, SC-HCl and SC-KOH can be regenerated twice for pyrolysis oil decolorization with decolorization efficiency of 90.85, 92.42 and 86.85%, it is in the specification of IS standard (≥85.00%) while SC-NaOH obtained decolorization efficiency of 69.58, it unable to regenerate.

## 5.2 Recommendation for Future Research

According to the achievement in this research about activated clays preparation from the Ratchaburi bentonite. Therefore, it can be considered for further studies to improve the performance of local bentonite in the future as follows:

1. The raw bentonite clays should be purification to remove impurities and other contaminates before investigating activation in the future study for improving performance and increase the value of Ratchaburi bentonite.

2. X-ray diffraction analysis (XRD) and thermogravimetric analysis (TGA) should be analyzed in regenerated spent activated clay to determine the crystallographic structure and its fraction of volatile components of spent activated clay structures after calcination.

3. The commercial activated clay should be characterized to compare its performance with activated clay from Ratchaburi bentonite.

4. The acidity of bleached pyrolysis oil should be further analyzed to determine the effect of activated clay decolorizing on the acidity of the oil.

จุฬาลงกรณ์มหาวิทยาลัย

CHULALONGKORN UNIVERSITY

# REFERENCES

1.  Al-Ani, T. and O. Sarapaa, *Clay and clay mineralogy.* Physical-chemical properties and industrial uses, 2008.

2.  Kunimine.Co., L. *Bentonite*. Available from: https://www.kunimine.co.jp/english/bent/basic.html.

3.  Kutlic, A., G. Bedekovic, and I. Sobota, *Bentonite processing.* Rudarsko-geolosko-naftni zbornik, 2012. **24**(1): p. 61-65.

4.  Hoerudin, A.H. *How does Montmorillonite clay swell?* ; Available from: https://agushoe.wordpress.com/.

5.  Vorasith, N., *The use of Bentonite to Remove Dark Colour in Repeating Used Palm Oil*, in *Chemistry*. 2004, Kasetsart University. p. 112.

6.  Hussin, F., M.K. Aroua, and W.M.A.W. Daud, *Textural characteristics, surface chemistry and activation of bleaching earth: A review.* Chemical Engineering Journal, 2011. **170**(1): p. 90-106.

7.  Corp., M. *Acid Activated Clay Adsorption Properties*. Available from: https://www.911metallurgist.com/acid-activated-clays/.

8.  Okwara, C. and E. Osoka, *Caustic activation of local clays for palm oil bleaching.* Journal of Engineering and Applied Sciences, 2006. **1**(4): p. 526-529.

9.  Ujeneza, E., *Optimization of acid activation and bleaching performance of local bentonite clay*. 2014, University of Nairobi.

10. Sarikaya, Y.k., et al., *The effect of thermal treatment on some of the physicochemical properties of a bentonite.* Clays and Clay Minerals, 2000. **48**(5): p. 557-562.

11. วีรณรงค์กร, ก. and อ. อาภรณ์วิชานพ, *Pyrolysis*. Energy & Environmental, 2015. **42**(June-July 2015): p. 241.

12. Riedewald, F., et al., *Economic assessment of a 40,000 t/y mixed plastic waste pyrolysis plant using direct heat treatment with molten metal: A case study of a plant located in Belgium.* Waste Management, 2021. **120**: p. 698-707.

13. Laval, A. *Flexible bleaching solutions*. Available from: www.alfalaval.com.

14. Kennedy, K.K., K.J. Maseka, and M. Mbulo, *Selected adsorbents for removal of contaminants from wastewater: towards engineering clay minerals.* Open Journal of Applied Sciences, 2018. **8**(8): p. 355-369.

15. Sing, K.S. and R.T. Williams, *Physisorption hysteresis loops and the characterization of nanoporous materials.* Adsorption Science & Technology, 2004. **22**(10): p. 773-782.

16. Yang, C., et al., *Compositional controls on pore-size distribution by nitrogen adsorption technique in the Lower Permian Shanxi Shales, Ordos Basin.* Journal of Natural Gas Science and Engineering, 2016. **34**: p. 1369-1381.

17. Ayawei, N., A.N. Ebelegi, and D. Wankasi, *Modelling and interpretation of adsorption isotherms.* Journal of chemistry, 2017. **2017**.

18. Tang, J., et al., *One-step calcination of the spent bleaching earth for the efficient removal of heavy metal ions.* ACS Sustainable Chemistry & Engineering, 2015. **3**(6): p. 1125-1135.

19. Aziz, B.K., M.A. Abdullah, and K.J. Jubrael, *Acid activation and bleaching*

*capacity of some clays for decolourizing used oils.* Asian Journal of Chemistry, 2011. **23**(6): p. 2449.

20. Ajemba, R. and O. Onukwuli, *Studies of the effects of hydrochloric acid-leaching on the structural and adsorptive performance of NTEJE (Nigeria) Clay.* International Journal of Engineering Research and Technology, 2012. **1**(3).

21. Ajemba, R.O. and O.D. Onukwuli, *Assessing influence of hydrochloric acid leaching on structural changes and bleaching performance of Nigerian clay from Udi.* Physicochemical Problems of Mineral Processing, 2014. **50**.

22. Wu, Z., et al., *Characterization, acid activation and bleaching performance of bentonite from Xinjiang.* Chinese Journal of Chemical Engineering, 2006. **14**(2): p. 253-258.

23. Akinwande, B., et al., *A suitability assessment of alkali activated clay for application in vegetable oil refining.* International Journal of Engineering and Advanced Technology Studies, 2014. **2**(1): p. 1.

24. Abd Wafti, N.S., et al., *Regeneration and Characterization of Spent Bleaching Clay.* Journal of Oil Palm Research, 2011. **23**: p. 999-1004.

25. Abd Majid, R. and C.R.C. Mat, *Regenerated spent bleaching earth for the decolourisation and BOD reduction of palm oil mill effluent.* J. of Oil Palm Res, 2017.

26. BALCI, S., *Structural property improvements of bentonite with sulfuric acid activation.* Journal of The Turkish Chemical Society Section B: Chemical Engineering, 2016. **1**(2): p. 201-212.

27. Tsai, W., et al., *Regeneration of spent bleaching earth by pyrolysis in a rotary furnace.* Journal of Analytical and Applied Pyrolysis, 2002. **63**(1): p. 157-170.

28. Komadel, P. and J. Madejová, *Acid activation of clay minerals*, in *Developments in clay science*. 2013, Elsevier. p. 385-409.

29. Rich, A., *Major factors that influence bleaching performance.* Journal of the American Oil Chemists' Society, 1967. **44**(7): p. 298A-323A.

30. Mine, A.P., *BENTONITE, PYROPHYLLITE AND TALC IN THE REPUBLIC OF SOUTH AFRICA.*

31. Ajemba, R.O. and O.D. Onukwuli, *Adsorptive removal of colour pigment from palm oil using acid activated Nteje clay. Kinetics, equilibrium and thermodynamics.* Physicochemical Problems of Mineral Processing, 2013. **49**.

32. Rosário, J.A., et al. *Influence of Alkaline Activation Over Swelling and Cation Exchange Capacity on Bentonites*. in *Materials Science Forum*. 2010. Trans Tech Publ.

33. Wang, X., et al., *Pore characterization of different clay minerals and its impact on methane adsorption capacity.* Energy & Fuels, 2020. **34**(10): p. 12204-12214.

34. Yurdakal, S., et al., *(Photo) catalyst characterization techniques: adsorption isotherms and BET, SEM, FTIR, UV–Vis, photoluminescence, and electrochemical characterizations*, in *Heterogeneous photocatalysis*. 2019, Elsevier. p. 87-152.

35. Pawar, R.R., H.C. Bajaj, and S.-M. Lee, *Activated bentonite as a low-cost adsorbent for the removal of Cu (II) and Pb (II) from aqueous solutions: Batch and column studies.* Journal of Industrial and Engineering Chemistry, 2016. **34**: p. 213-223.

จุฬาลงกรณ์มหาวิทยาลัย
CHULALONGKORN UNIVERSITY

# APPENDIX

Table A-1 The Indian standard (IS 6186-1986) specification for bentonite

| Sl No. | Characteristic | Requirement for Type 1 | Requirement for Type 2 High | Requirement for Type 2 Off-shore | Method of Test, Ref to Cl No. in Appendix A |
|---|---|---|---|---|---|
| (1) | (2) | (3) | (4) | (5) | (6) |
| i) | Moisture, percent by mass | 5·0-12·0 | 12·0, Max | 12·0, Max | A-2 |
| ii) | pH | 9·0-10 5 | — | — | A-3 |
| iii) | Gel formation index | To pass test | To pass test | To pass test | A-4 |
| iv) | Swelling power | To pass test | — | — | A-5 |
| v) | Fineness: | | | | A-6 |
| | a) Dry: | | | | |
| | To pass through 150-micron IS Sieve, percent by mass, Min | — | 98 | 98 | |
| | To pass through 75-micron IS Sieve, percent by mass, Min | 95 | 90 | — | |
| | b) Wet: | | | | |
| | Retained on 150-micron IS Sieve, percent by mass, Max | 0·01 | — | — | |
| | To pass through 45-micron IS Sieve, percent by mass, Min | 90 | 93 | — | |
| vi) | Viscosity at 30°C, centipoise, Min: | | | | A-7 |
| | a) Apparent | — | 15 | — | |
| | b) Plastic | — | 6 | — | |
| vii) | Filtration loss, ml, Max | -- | 15 | 15 | A-8 |
| viii) | Sand content, percent by mass, Max | — | 2 | 2 | A-9 |

Table A-2 The Indian standard (IS 1965-1972) specification for bleaching earths

| Sl No. | Characteristic | Requirement Acidic | | Neutral | Method of Test (Ref to Cl No. of IS : 1035-1972*) |
| | | Grade 1 | Grade 2 | | |
| --- | --- | --- | --- | --- | --- |
| (1) | (2) | (3) | (4) | (5) | (6) |
| i) | Moisture, percent by mass, *Max* | 15·0 | 10·0 | 10·0 | 4 |
| ii) | Bulk density. grams per millilitre, *Max* | 0·9 | 0·9 | 1·2 | 5 |
| iii) | Screen analysis: | | | | 6 |
| | a) Retained on 125-micron IS Sieve, percent by mass, *Max* | 15·0 | 20·0 | 25·0 | |
| | b) Retained on 53-micron IS Sieve, percent by mass, *Max* | 40·0 | 40·0 | 40·0 | |
| iv) | Acidity, as $H_2SO_4$, percent by mass, *Max* | 0·2 | 0·2 | Nil | 7 |
| v) | Alkalinity, as NaOH, percent by mass, *Max* | Nil | Nil | 0·1 | 7 |
| vi) | Bleaching efficiency, percent, *Min* | 95 | 85 | 80 | 8 |
| vii) | Oil retention, percent by mass, *Max* | 40 | 35 | 30 | 9 |

*Methods of sampling and test for bleaching earths ( *second revision* ).

Table A-3 Determination Langmuir isotherm of AC-$H_2SO_4$

| Temp (°C) | m (g) | $A_0$ | At | $q_e$ | $C_e$ | $1/q_e$ | $1/C_e$ |
|---|---|---|---|---|---|---|---|
| 100 | 10 | 2.163 | 1.284 | 0.406 | 10.00 | 2.461 | 0.100 |
| 100 | 30 | 2.163 | 1.199 | 0.446 | 30.00 | 2.244 | 0.033 |
| 100 | 50 | 2.163 | 0.566 | 0.738 | 50.00 | 1.354 | 0.020 |
| 100 | 70 | 2.163 | 0.383 | 0.823 | 70.00 | 1.215 | 0.014 |

Table A-4 Determination Freundlich isotherm of AC-$H_2SO_4$

| Temp (°C) | m (g) | $A_0$ | At | $q_e$ | $C_e$ | $\log q_e$ | $\log C_e$ |
|---|---|---|---|---|---|---|---|
| 100 | 10 | 2.163 | 1.284 | 0.406 | 10.000 | -0.391 | 1.000 |
| 100 | 30 | 2.163 | 1.199 | 0.446 | 30.000 | -0.351 | 1.477 |
| 100 | 50 | 2.163 | 0.566 | 0.738 | 50.000 | -0.132 | 1.699 |
| 100 | 70 | 2.163 | 0.383 | 0.823 | 70.000 | -0.085 | 1.845 |

จุฬาลงกรณ์มหาวิทยาลัย

CHULALONGKORN UNIVERSITY

Table A-5 Determination Langmuir isotherm of AC-HCl

| Temp (°C) | m (g) | $A_0$ | At | qe | Ce | 1/qe | 1/Ce |
|-----------|-------|-------|-------|-------|-------|-------|-------|
| 100 | 10 | 2.163 | 1.873 | 0.134 | 10.00 | 7.459 | 0.100 |
| 100 | 30 | 2.163 | 0.554 | 0.744 | 30.00 | 1.344 | 0.033 |
| 100 | 50 | 2.163 | 0.391 | 0.819 | 50.00 | 1.221 | 0.020 |
| 100 | 70 | 2.163 | 0.306 | 0.859 | 70.00 | 1.165 | 0.014 |

Table A-6 Determination Freundlich isotherm of AC-HCl

| Temp (°C) | m (g) | $A_0$ | At | $q_e$ | $C_e$ | log $q_e$ | log $C_e$ |
|-----------|-------|-------|-------|-------|--------|-----------|-----------|
| 100 | 10 | 2.163 | 1.873 | 0.134 | 10.000 | -0.873 | 1.000 |
| 100 | 30 | 2.163 | 0.554 | 0.744 | 30.000 | -0.129 | 1.477 |
| 100 | 50 | 2.163 | 0.391 | 0.819 | 50.000 | -0.087 | 1.699 |
| 100 | 70 | 2.163 | 0.306 | 0.859 | 70.000 | -0.066 | 1.845 |

Table A-7 Determination Langmuir isotherm of AC-NaOH

| Temp (°C) | m (g) | $A_0$ | At | $q_e$ | $C_e$ | $1/q_e$ | $1/C_e$ |
|---|---|---|---|---|---|---|---|
| 100 | 10 | 2.163 | 1.871 | 0.135 | 10.00 | 7.408 | 0.100 |
| 100 | 30 | 2.163 | 1.469 | 0.321 | 30.00 | 3.117 | 0.033 |
| 100 | 50 | 2.163 | 0.757 | 0.650 | 50.00 | 1.538 | 0.020 |
| 100 | 70 | 2.163 | 0.713 | 0.670 | 70.00 | 1.492 | 0.014 |

Table A-8 Determination Freundlich isotherm of AC-NaOH

| Temp (°C) | m (g) | $A_0$ | At | $q_e$ | $C_e$ | $\log q_e$ | $\log C_e$ |
|---|---|---|---|---|---|---|---|
| 100 | 10 | 2.163 | 1.871 | 0.135 | 10.000 | -0.870 | 1.000 |
| 100 | 30 | 2.163 | 1.469 | 0.321 | 30.000 | -0.494 | 1.477 |
| 100 | 50 | 2.163 | 0.757 | 0.650 | 50.000 | -0.187 | 1.699 |
| 100 | 70 | 2.163 | 0.713 | 0.670 | 70.000 | -0.174 | 1.845 |

จุฬาลงกรณ์มหาวิทยาลัย

CHULALONGKORN UNIVERSITY

Table A-9 Determination Langmuir isotherm of AC-KOH

| Temp (°C) | m (g) | $A_0$ | At | $q_e$ | $C_e$ | $1/q_e$ | $1/C_e$ |
|-----------|-------|-------|-------|-------|-------|---------|---------|
| 100 | 10 | 2.163 | 1.713 | 0.208 | 10.00 | 4.807 | 0.100 |
| 100 | 30 | 2.163 | 0.806 | 0.627 | 30.00 | 1.594 | 0.033 |
| 100 | 50 | 2.163 | 0.523 | 0.758 | 50.00 | 1.319 | 0.020 |
| 100 | 70 | 2.163 | 0.327 | 0.849 | 70.00 | 1.178 | 0.014 |

Table A-10 Determination Freundlich isotherm of AC-KOH

| Temp (°C) | m (g) | $A_0$ | At | $q_e$ | $C_e$ | $\log q_e$ | $\log C_e$ |
|-----------|-------|-------|-------|-------|--------|------------|------------|
| 100 | 10 | 2.163 | 1.713 | 0.208 | 10.000 | -0.682 | 1.000 |
| 100 | 30 | 2.163 | 0.806 | 0.627 | 30.000 | -0.202 | 1.477 |
| 100 | 50 | 2.163 | 0.523 | 0.758 | 50.000 | -0.120 | 1.699 |
| 100 | 70 | 2.163 | 0.327 | 0.849 | 70.000 | -0.071 | 1.845 |

Table A-11 An acid dissociation constant ($K_a$)

| $K_a$ | Acid | |
| --- | --- | --- |
| | Name | Formula |
| Large | Perchloric acid | $HClO_4$ |
| $3.2 \times 10^9$ | Hydroiodic acid | HI |
| $1.0 \times 10^9$ | Hydrobromic acid | HBr |
| $1.3 \times 10^6$ | Hydrochloric acid | HCl |
| $1.0 \times 10^3$ | Sulfuric acid | $H_2SO_4$ |
| $2.4 \times 10^1$ | Nitric acid | $HNO_3$ |
| $5.4 \times 10^{-2}$ | Oxalic acid | $HO_2C_2O_2H$ |
| $1.3 \times 10^{-2}$ | Sulfurous acid | $H_2SO_3$ |
| $1.0 \times 10^{-2}$ | Hydrogen sulfate ion | $HSO_4^-$ |
| $7.1 \times 10^{-3}$ | Phosphoric acid | $H_3PO_4$ |
| $7.2 \times 10^{-4}$ | Nitrous acid | $HNO_2$ |
| $6.6 \times 10^{-4}$ | Hydrofluoric acid | HF |
| $1.8 \times 10^{-4}$ | Methanoic acid | $HCO_2H$ |
| $6.3 \times 10^{-5}$ | Benzoic acid | $C_6H_5COOH$ |
| $5.4 \times 10^{-5}$ | Hydrogen oxalate ion | $HO_2C_2O^{2-}$ |
| $1.8 \times 10^{-5}$ | Ethanoic acid | $CH_3COOH$ |
| $4.4 \times 10^{-7}$ | Carbonic acid | $CO_3^{2-}$ |
| $1.1 \times 10^{-7}$ | Hydrosulfuric acid | $H_2S$ |
| $6.3 \times 10^{-8}$ | Dihydrogen phosphate ion | $H_2PO_4^-$ |
| $6.2 \times 10^{-8}$ | Hydrogen sulfite ion | $HS^-$ |
| $2.9 \times 10^{-8}$ | Hypochlorous acid | HClO |
| $6.2 \times 10^{-10}$ | Hydrocyanic acid | HCN |
| $5.8 \times 10^{-10}$ | Ammonium ion | $NH_4^+$ |
| $5.8 \times 10^{-10}$ | Boric acid | $H_3BO_3$ |
| $4.7 \times 10^{-11}$ | Hydrogen carbonate ion | $HCO_3^-$ |
| $4.2 \times 10^{-13}$ | Hydrogen phosphate ion | $HPO_4^{2-}$ |
| $1.8 \times 10^{-13}$ | Dihydrogen borate ion | $H_2BO_3^-$ |
| $1.3 \times 10^{-13}$ | Hydrogen sulfide ion | HS- |
| $1.6 \times 10^{-14}$ | Hydrogen borate ion | $HBO_3^{2-}$ |

# VITA

**NAME**                    Woranan Koedsang

**DATE OF BIRTH**           18 April 1988

**PLACE OF BIRTH**          Kanchanadit District, Surat Thani Province

**INSTITUTIONS**            Bachelor's degree of Science (Industrial Chemistry) at
**ATTENDED**                Department of chemistry, Faculty of Science, King
                            Mongkut's Institute of Technology Ladkrabang in 2013